

# **Cellular maturation of mitochondrial molybdoenzymes**

Inaugural-Dissertation

zur

Erlangung des Doktorgrades

der Mathematisch-Naturwissenschaftlichen Fakultät

der Universität zu Köln

vorgelegt von

**Julian Klein**

aus Köln

Berichterstatter: Prof. Dr. G. Schwarz

(Gutachter) Prof. Dr. T. Langer

Tag der mündlichen Prüfung: 6. November 2012

## Publications

published:

**Klein JM**, and Schwarz G. Cofactor-dependent maturation of mammalian sulfite oxidase links two mitochondrial import pathways.  
**Journal of Cell Science (2012)**

submitted:

**Klein JM**, Busch JD, Potting C, Baker MJ, Langer T, and Schwarz G. The mitochondrial amidoxime-reducing component (mARC1) is a novel signal-anchored protein of the outer mitochondrial membrane.  
**Journal of Biological Chemistry (2012)**

## Conference contributions

2012:

**Klein JM**, and Schwarz G. Mitochondrial maturation of sulfite oxidase. Gordon Research Conference "Protein Transport Across Cell Membranes"; Galveston, USA.  
(Poster presentation)

2011:

**Klein JM**, and Schwarz G. Assembly and maturation of sulfite oxidase. "Molybdenum and Tungsten Enzyme Conference"; Edmonton, Canada  
(Oral presentation)

2010:

**Klein JM**, and Schwarz G. Assembly and maturation of sulfite oxidase. Gordon Research Conference "Mitochondria and Chloroplasts"; Barga, Italy.  
(Poster presentation)

**Table of contents**

<b>1 Introduction</b>	<b>1</b>
1.1 Molybdenum and Moco	1
1.2 Moco synthesis	2
1.3 Moco dependent enzymes	4
1.3.1 Mammalian cytosolic Moco enzymes	4
1.3.2 Mammalian mitochondrial Moco enzymes	5
1.3.2.1 Sulfite oxidase	5
1.3.2.2 Sulfite oxidase- and Moco-deficiency	8
1.3.2.3 Mitochondrial amidoxime reducing components	10
1.4 Mitochondrial architecture and function	12
1.5 Mitochondrial protein import	13
1.5.1 Import of proteins containing cleavable pre-sequences	14
1.5.2 Import of proteins lacking cleavable pre-sequences	16
1.5.2.1 Insertion of proteins into the inner membrane	16
1.5.2.2 Import of small IMS proteins	17
1.5.2.3 Integration of $\beta$ -barrel proteins into the outer membrane	17
1.5.2.4 Integration of $\alpha$ -helical proteins into the outer membrane	18
1.6 Cofactors and metabolites in mitochondria	20
1.6.1 Heme synthesis and transport	21
1.7 Aims of the current study	23
<b>2 Results</b>	<b>24</b>
2.1 Assembly and maturation of mammalian SO	24
2.1.1 Amplification, purification and characterization of mouse SO	24
2.1.2 Moco dependent mitochondrial localization of SO	27
2.1.3 Mitochondrial import of SO	32
2.1.4 Retrograde translocation of SO to the cytosol in absence of Moco	35
2.1.5 The role of heme in the mitochondrial maturation of SO	40
2.1.6 The impact of homodimerization on the mitochondrial maturation of SO	43
2.1.7 SO-independent population of Moco in mitochondria	46
2.2 Mitochondrial maturation of mARC1	48
2.2.1 Sub-cellular localization of mARC1	48
2.2.2 Localization of mARC1 within the mitochondrial compartments	50
2.2.3 Mitochondrial targeting of mARC1	53
2.2.4 Mechanisms of mitochondrial mARC1 import	57
<b>3 Discussion</b>	<b>61</b>
3.1 Maturation of mammalian SO	61
3.1.1 Moco dependent mitochondrial localization of SO	61
3.1.2 The SO import vs. other proteins with bipartite targeting signals	64
3.1.3 The role of heme and dimerization in the mitochondrial maturation of SO	66
3.1.4 Processing of SO in the IMS	68
3.1.5 Moco stabilization	69
3.1.6 Assembly and maturation of SO	70
3.2 Subcellular localization and sorting of human mARC1	71
3.2.1 Localization of mARC1 to the outer mitochondrial membrane	71
3.2.2 Targeting of mARC1 to the outer mitochondrial membrane	73

3.2.3 Outer membrane targeting of mARC1 vs inner membrane sorting of SO	76
3.2.4 <i>In vitro</i> import of mARC1	79
3.2.5 Assembly and maturation of mARC1	80
<b>4 Material and methods</b>	<b>82</b>
4.1 Material	82
4.1.1 Organisms	82
4.1.2 Plasmids	83
4.1.3 Enzymes and chemicals	83
4.1.4 Antibodies	84
4.2 Methods	85
4.2.1 Biochemical methods	85
4.2.1.1 Expression of recombinant SO variants in <i>E. coli</i>	85
4.2.1.2 <i>E. coli</i> cell disruption	85
4.2.1.3 Purification of recombinantly expressed SO variants	85
4.2.1.4 Concentration of purified proteins	86
4.2.1.5 Analytical size exclusion chromatography	86
4.2.1.6 Buffer exchange	86
4.2.1.7 Determination of protein concentration	86
4.2.1.8 SDS-PAGE	87
4.2.1.9 Western blot	87
4.2.1.10 Blue Native-PAGE	87
4.2.1.11 Sulfite:Cytochrome <i>c</i> assay	88
4.2.1.12 HPLC Form A analysis	88
4.2.1.13 <i>Nit-1</i> assay	89
4.2.1.14 TCA precipitation	90
4.2.2 Molecular biological methods	90
4.2.2.1 Cloning	90
4.2.2.2 Plasmid amplification and purification	90
4.2.2.3 Site directed mutagenesis	90
4.2.2.4 Fusion PCR	90
4.2.3 Cell biological methods	91
4.2.3.1 Cultivation of mammalian cells	91
4.2.3.2 Transfection of mammalian cells	91
4.2.3.3 shRNA mediated knockdown of gene products	91
4.2.3.4 Harvesting and disruption of mammalian cultured cells	92
4.2.3.5 Microscopic preparations	92
4.2.3.6 Staining of mitochondria	92
4.2.3.7 Confocal laser microscopy	92
4.2.3.8 Determination of the Pearson Correlation Coefficient	93
4.2.4 Methods to study mitochondrial localization and import of proteins	93
4.2.4.1 Enrichment of mitochondria	93
4.2.4.2 Purification of mitochondria	93
4.2.4.3 Na <sub>2</sub> CO <sub>3</sub> extraction of mitochondrial proteins	94
4.2.4.4 Protease treatment of mitochondria	94
4.2.4.5 Hypotonic swelling of mitochondria	94
4.2.4.6 <i>In vitro</i> translation	95
4.2.4.7 Mitochondrial <i>in vitro</i> import studies	95

<b>5 Appendix</b>	<b>97</b>
5.1 Primers	97
5.2 Constructs	98
5.3 Sequences	99
5.3.1 Mouse SO	99
5.3.2 Human mARC1	100
<b>6 References</b>	<b>101</b>

## **Figures and tables**

### **Figures**

Figure 1.1 Structures of two eukaryotic types of Moco	2
Figure 1.2 Human Moco biosynthesis	3
Figure 1.3 Reaction mechanism and crystal structure of animal SO	6
Figure 1.4 Severe neurological symptoms of SO deficiency	9
Figure 1.5 Composition and electron transfer in the N-reductive system	11
Figure 1.6 Mitochondrial import of pre-sequence containing precursors	15
Figure 1.7 Possible import pathways of signal-anchored proteins	20
Figure 1.8 Mammalian heme biosynthesis	21
Figure 2.1 Multiple sequence alignment of mammalian SO variants	25
Figure 2.2 Purification and characterization of MSO expressed in <i>E. coli</i>	26
Figure 2.3 Moco dependent localization of SO	28
Figure 2.4 Characterization of a Moco-deficient mutant variant of SO	29
Figure 2.5 Cellular distribution of Moco-deficient SO	30
Figure 2.6 Western blot analysis of Moco dependent distribution of SO	32
Figure 2.7 SO contains an N-terminal mitochondrial targeting signal	33
Figure 2.8 Moco independent mitochondrial processing of SO	34
Figure 2.9 Processing of SO by the IMP complex	35
Figure 2.10 Design of an unprocessed SO-TIM50 chimera	36
Figure 2.11 Similar enzymatic activities of WT-SO and SO-TIM50	37
Figure 2.12 Moco independent mitochondrial localization of SO-TIM50	38
Figure 2.13 Moco “pulls” SO across the outer mitochondrial membrane	39
Figure 2.14 Characterization of a heme deficient mutant variant of SO	41
Figure 2.15 Heme independent mitochondrial localization of SO	42
Figure 2.16 Heme mediated trapping of the SO heme domain	43
Figure 2.17 Characterization of a monomeric mutant variant of SO	44
Figure 2.18 Dimerization independent mitochondrial localization of SO	45
Figure 2.19 Mitochondria contain an SO independent population of Moco	47
Figure 2.20 Alignment of human mARC1 and mARC2	48
Figure 2.21 Analysis and prediction of mARC1 sequence and structural motifs	49
Figure 2.22 Mitochondrial localization of mARC1-GFP	50
Figure 2.23 Association of mARC1 with mitochondrial membranes	51
Figure 2.24 mARC1 localizes to the outer mitochondrial membrane	52
Figure 2.25 Mitochondrial targeting motifs of mARC1	55
Figure 2.26 Moco independent mitochondrial targeting of mARC1	56
Figure 2.27 <i>In vitro</i> translation of mARC1	57
Figure 2.28 mARC1 is not processed	58
Figure 2.29 Mitochondrial <i>in vitro</i> import of mARC1	59
Figure 3.1 Assembly and maturation of mammalian SO	71
Figure 3.2 Assembly and maturation of human mARC1	80

**Tables**

Table 3.1 Comparison of IMS proteins with bipartite N-terminal targeting signals	65
Table 3.2 Analysis of matrix-targeting capability of different protein N-termini	74
Table 3.3 TM domain comparison between signal-anchored proteins and inner membrane/IMS proteins with bipartite targeting signals	76
Table 4.1 <i>E. coli</i> cells used in this study	82
Table 4.2 Mammalian cells used in this study	82
Table 4.3 <i>N. crassa</i> cells used in this study	83
Table 4.4 Plasmids used in this study	83
Table 4.5 Primary antibodies used in this study	84
Table 4.6 Secondary antibodies used in this study	84
Tab. 5.1 Primers used in this study	97
Tab. 5.2 Constructs used in this study	98



**Abbreviations**

A	absorption
aa	amino acid
ADP	adenosine diphosphate
AMP	adenosine monophosphate
AO	aldehyde oxidase
ATP	adenosine triphosphate
AU	absorption units
BN-PAGE	Blue Native-polyacrylamide gel electrophoresis
BSA	bovine serum albumin
cDNA	complementary DNA
CDS	coding sequence
CMV	cytomegalovirus
cPMP	cyclic pyranopterin monophosphate
Da	Dalton
DMSO	dimethyl sulfoxide
DNA	deoxyribonucleic acid
DTT	dithiothreitol
ECL	enhanced chemiluminescence
EDTA	ethylenediaminetetraacetic acid
ELISA	enzyme-linked immunosorbent assay
ER	endoplasmic reticulum
ERMES	ER-mitochondria encounter structure
FAD	flavin adenine dinucleotide
FPLC	fast performance liquid chromatography
g, mg, µg, ng	gram, milligram, microgram, nanogram
GFP	green fluorescent protein
GSH	glutathione
GTP	guanosine triphosphate
h	hours
Hepes	2-[4-(2-hydroxyethyl) piperazin-1-yl] ethanesulfonic acid
His-tag	histidine-tag
HPLC	high performance liquid chromatography
HRP	horseradish peroxidase
IBM	inner boundary membrane
IM	mitochondrial inner membrane
IMP	inner membrane peptidase
IMS	mitochondrial intermembrane space
IPTG	isopropyl-β-D-1-thiogalactopyranoside
kbar	kilo bar
kDa	kilo Dalton
l, ml, µl	liter, milliliter, microliter
LB	lysogeny broth
M, mM, µM	molar, millimolar, micromolar
mARC	mitochondrial amidoxime reducing component
min	minutes
MINOS	mitochondrial inner membrane organizing system

---

mm, $\mu\text{m}$ , nm	millimeter, micrometer, nanometer
Mo	molybdenum
MoCD	molybdenum cofactor deficiency
Moco	molybdenum cofactor
mol, mmol, $\mu\text{mol}$ , pmol	mole, millimole, micromole, picomole
MPP	matrix processing peptidase
MPT	molybdopterin
MPT-AMP	molybdopterin-adenosine monophosphate
MRI	magnetic resonance imaging
mRNA	messenger RNA
MSO	mouse sulfite oxidase
mt	mitochondrial
MTS	mitochondrial targeting signal
NAD/NADH	nicotinamide adenine dinucleotide
NADPH	nicotinamide adenine dinucleotide phosphate
NED	N-(1-Naphtyl)-ethylendiamine-dihydrochloride
Ni-NTA	nickel-nitrilotriacetic acid
NO	nitric oxide
NOHA	N-hydroxy-arginine
NR	nitrate reductase
OM	mitochondrial outer membrane
P	pellet
PAGE	polyacrylamide gel electrophoresis
PAM	pre-sequence associated motor complex
PBS	phosphate buffered saline
PCC	Pearson Correlation Coefficient
PCR	polymerase chain reaction
PEI	polyethylenimine
PK	proteinase k
PMSF	phenylmethanesulfonylfluoride
PSO	plant sulfite oxidase
PVDF	polyvinylidenfluorid
RNA	ribonucleic acid
ROS	reactive oxygen species
rpm	revolutions per minute
RT	room temperature
SA	sulfanilamide
SAM	sorting and assembly machinery
SDS	sodium dodecyl sulfate
sec	second
shRNA	small hairpin ribonucleic acid
SN	supernatant
SO	sulfite oxidase
TBS	tris buffered saline
TBST	tris buffered saline tween
TCA	trichloroacetic acid
TIM	translocase of the inner membrane
TOM	translocase of the outer membrane
Tris	tris(hydroxymethyl)aminomethane

VDAC	voltage dependent anion channel
WT	wildtype
XDH	xanthine dehydrogenase
XO	xanthine oxidase
XOR	xanthine oxidoreductase

## **Abbreviations of species**

<i>E. coli</i>	<i>Escherichia Coli</i>
<i>M. musculus</i>	<i>Mus musculus</i>
<i>N. crassa</i>	<i>Neurospora crassa</i>
<i>S. cerevisiae</i>	<i>Saccharomyces cerevisiae</i>

## Abstract

The molybdenum cofactor (Moco) is an essential component present in nearly all domains of life. In mammals, Moco is part of four currently known enzymes and constitutes a crucial redox-active center involved in a number of fundamental cellular reactions. Moco-dependent enzymes are present in the cytosol but also in or at mitochondria, where Moco is integrated into sulfite oxidase (SO) and the mitochondrial amidoxime-reducing component (mARC), respectively. The family of mitochondrial Moco-enzymes is of particular interest considering the cytosolic synthesis of enzymes and cofactor, which requires a coordinated mitochondrial transport and assembly process. In the current study, the mitochondrial maturation of SO and mARC1 were thus analyzed to obtain a mechanistic understanding of the processes starting with the cytosolic syntheses of apo-proteins all the way to the formation of the mature mitochondrial enzymes.

The first part of this work uncovered the cellular assembly of SO, a soluble protein of the mitochondrial intermembrane space, and revealed a Moco-dependent mitochondrial targeting mechanism. In spite of its functional bipartite N-terminal targeting signal, about 70% of SO mislocalized to the cytosol if Moco was not present. Following the identification of SO processing by the inner membrane peptidase (IMP) complex, prevention of this cleavage and thus anchoring of SO in the inner mitochondrial membrane resulted in an efficient mitochondrial targeting even in absence of Moco. SO was thereby identified to undergo a reverse translocation to the cytosol in absence of Moco, which is required to trap SO in the intermembrane space and to constitute in addition a vectorial driving force for completion of SO translocation across the TOM complex. The integration of Moco is not only essential for correct sub-mitochondrial localization, but also a prerequisite for *in vivo* heme integration and homodimerization of SO. In conclusion, the identified molecular hierarchy of SO maturation represents a novel link between the canonical pre-sequence pathway and folding-trap mechanisms of mitochondrial import.

The other mitochondrial Moco-enzyme mARC1 was recently discovered and its sub-mitochondrial localization had remained unclear. In the second part of this study, mARC1 was shown to be localized to the outer mitochondrial membrane. As a result of the translocation process, the C-terminal catalytic core of the protein remains exposed to the cytosol and confers an  $N_{(in)}-C_{(out)}$  membrane orientation of mARC1. This localization is mediated by the N-terminal domain of the enzyme, being composed of a classical but weak N-terminal targeting signal and a downstream transmembrane domain. Thereby, the transmembrane domain of mARC1 is sufficient for mitochondrial targeting, while the N-terminal targeting signal seems to function as a supportive receptor for the outer mitochondrial membrane. According to its localization and targeting mechanism, mARC1 is classified as a novel signal-anchored protein. Considering the membrane integration of mARC1, an SO-similar demand of Moco for mitochondrial retention of mARC1 is not required and its N-terminal targeting motifs are sufficient for adequate mitochondrial localization. During mitochondrial import, mARC1 is not processed and membrane integration proceeds membrane potential independently but requires external ATP, which finally results in the assembly of mARC1 into high-oligomeric protein complexes.

## Zusammenfassung

Der Molybdän-Cofaktor (Moco) ist ein essentieller Bestandteil in allen Organismenreichen. In Säugetieren bildet Moco ein wichtiges redox-aktives Zentrum von bisher vier bekannten Enzymen und ist dadurch an einer Vielzahl fundamentaler, zellulärer Reaktionen beteiligt. Moco-abhängige Enzyme liegen sowohl im Zytosol als auch in Mitochondrien vor, wobei Moco hier in die Sulfitoxidase (SO) und in die mitochondriale Amidoxim-reduzierende Komponente (mARC) eingebaut ist. Unter Berücksichtigung der zytosolischen Synthese von Moco, SO und mARC ist die Familie der mitochondrialen Moco-Enzyme dabei von besonderem Interesse, da diese einen koordinierten mitochondrialen Transport und einen entsprechend regulierten Reifungsprozess der beiden Enzyme verlangt. In dieser Arbeit wurden die mitochondrialen Reifungsprozesse von SO und mARC analysiert, um ein mechanistisches Verständnis dieser Prozesse zu erlangen.

Im ersten Teil wurden dabei hierarchische Stufen zur zellulären Reifung der SO aufgedeckt. SO ist ein lösliches Protein des mitochondrialen Intermembranraums und zeigt dabei eine Moco-abhängige mitochondriale Lokalisierung. Ungeachtet der zweigeteilten N-terminalen mitochondrialen Zielsequenz wurden in Abwesenheit von Moco etwa 70% des Enzyms im Zytosol detektiert. Nachdem die Innere-Membran-Peptidase (IMP) als SO-prozessierende Protease identifiziert wurde, konnte eine über Mutationen verhinderte Prozessierung und damit eine Verankerung der SO in der inneren Membran eine vollständige mitochondriale Lokalisation auch in Abwesenheit von Moco erreichen. Dieses Experiment belegte, dass die SO einer reversen Translokation in Richtung Zytosol unterliegt, wenn Moco nicht eingebaut werden kann. Moco ist dabei für die Initiierung der SO-Faltung verantwortlich und verhindert dadurch zum einen den Rücktransport ins Zytoplasma und greift dadurch zum anderen auch aktiv in die Translokation der SO ein, indem die Faltung eine zusätzliche vektoriell getriebene Kraft für die vollständige Translokation in den Intermembranraum darstellt. Der Einbau des Moco ist nicht nur für die Lokalisation der SO essentiell, sondern auch eine Voraussetzung für den Einbau des Häm-Cofaktors und die Homodimerisierung der SO. Insgesamt stellt die dargestellte molekulare Hierarchie der SO-Reifung eine neue Verbindung zwischen dem kanonischen Prä-Sequenz Importweg und faltungsabhängigen Importmechanismen dar.

Das mitochondriale Moco-Enzym mARC1 wurde erst kürzlich entdeckt, wobei seine sub-mitochondriale Lokalisation unklar blieb. Im zweiten Teil dieser Arbeit konnte nun die Assoziation von mARC1 mit der mitochondrialen Außenmembran demonstriert werden. Als Resultat des Translokationsprozesses bleibt die C-terminale katalytische Domäne dem Zytosol exponiert und verleiht mARC1 eine  $N_{(\text{innen})}-C_{(\text{außen})}$  Membrankonformation. Diese Lokalisation wird über die N-terminale Domäne des Enzyms gesteuert, welche aus einem klassischen aber schwachen N-terminalen Ziel-Signal und einer folgenden Transmembrandomäne besteht. Die Transmembrandomäne ist dabei hinreichend für die Lokalisation, wobei das Ziel-Signal als unterstützender Rezeptor für die mitochondriale Außenmembran zu dienen scheint. Sowohl die Lokalisation als auch der Transportmechanismus klassifizieren mARC1 dabei als ein neues Signal-verankertes Protein. Aufgrund der Membranverankerung von mARC1 ist der Einbau des Moco kein essentieller Bestandteil des Translokationsprozesses, welcher ausschließlich von den beiden N-terminalen Motiven gesteuert wird. Während des Importprozesses wird mARC1 nicht prozessiert und der Membraneinbau erfolgt unabhängig vom Membranpotential, erfordert jedoch die externe Zufuhr von ATP. Dies führt final zur Integration von mARC1 in hoch-oligomere Proteinkomplexe in der Außenmembran.

# **1 Introduction**

## **1.1 Molybdenum and Moco**

Molybdenum (Mo) belongs to the group of transition metals and constitutes an essential trace element for animals, plants and microorganisms. In nature, Mo occurs in different chemical compounds and exhibits a rich coordination and redox chemistry, as illustrated by its extended spectrum of oxidation states ranging from  $-II$  to  $+VI$ . Therefore, Mo depicts a potent catalyst of a large variety of redox reactions in biological systems. Although Mo is of very low abundance in the cell, its uptake requires an adequate and efficient mechanism to guarantee a constant supply of Mo. Amongst different forms and oxidation states of Mo occurring in nature, the molybdate anion ( $MoO_4^{2-}$ ) constitutes the only Mo compound that organisms can acquire from their environment (Llamas et al., 2011). While bacteria mediate uptake of molybdate by means of a high-affinity ATP-binding-cassette transporter (Maupin-Furlow et al., 1995), a homologous system has not been found in eukaryotes, yet. Instead, plants contain two different molybdate transporters referred to as MOT1 and MOT2, showing distant relations to sulfate transporters of the SULTR family (Tejada-Jimenez et al., 2007). Animals lack MOT1, while recently, MOT2 was identified as the first molybdate transporter in animals (Tejada-Jimenez et al., 2011).

Upon its successful uptake from the environment, Mo is complexed by a pterin compound to build the biologically active molybdenum cofactor (Moco). Moco is composed of a tricyclic pterin coordinating Mo via a dithiol group within the third pyrano ring. With the exception of bacterial nitrogenase, in which a unique iron-molybdenum cofactor confers catalytic activity, all other Mo-dependent enzymes contain a pterin type cofactor (Hille, 1996). Eukaryotic Moco occurs in two different forms that share a common backbone but differ in the coordination of Mo. In one variant, Mo is covalently bound to a conserved cysteine residue of the Moco binding domain (Figure 1.1 A), while in the other variant instead a third terminal sulfur ligand is bound to Mo with the cofactor remaining non-covalently bound to the respective protein (Figure 1.1 B) (Schwarz and Mendel, 2006). Integration of Mo into both types of Moco permits the positioning of Mo within the protein active site, thus controlling its redox behavior on the one hand and aligning the pterin ring system for electron transfer from or to Mo on the other hand (Mendel, 2007). In respect to its involvement in electron transfer, the pterin moiety is fully reduced and thus believed to be prone to oxidation. In addition, the isolated coordination of Mo by means of the dithiol group is fragile, finally resulting in destabilization of Moco in protein free environments (Rajagopalan and Johnson, 1992). Consequently, Moco was assumed not to occur free in the cell but rather to be associated rapidly with its respective target-enzymes.

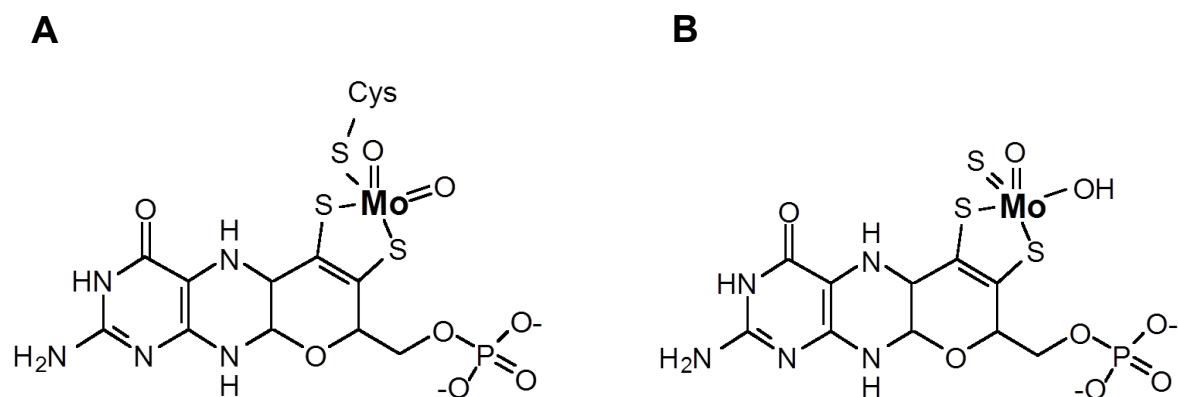


**Figure 1.1 Structures of two eukaryotic types of Moco.** Within eukaryotic enzymes, Mo is either (A) covalently connected to a conserved cysteine or (B) non-covalently bound to the protein and instead exposing a third terminal sulfur ligand. Figure modified from (Mendel and Bittner, 2006).

## 1.2 Moco synthesis

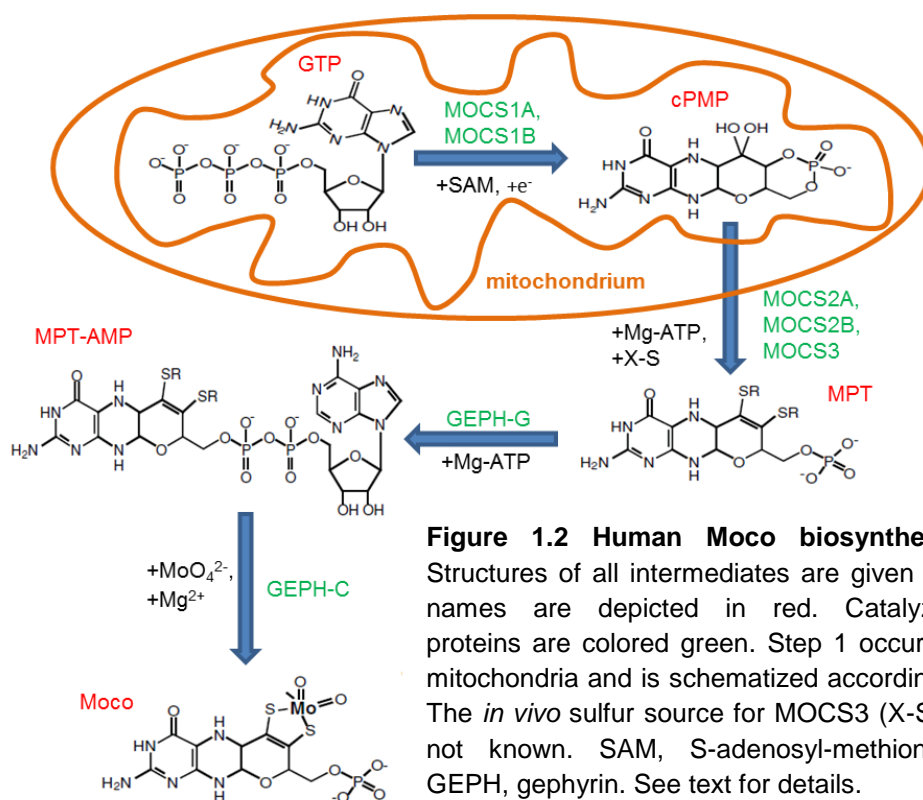
The biosynthesis of Moco is highly conserved from bacteria to eukaryotes and is composed of four enzymatic steps (Figure 1.2), which are catalyzed by six gene products in eukaryotes.

The first step of the Moco synthesis cascade starts out from GTP, which is converted to cyclic pteranopterin monophosphate (cPMP) by two proteins (MOCS1A and MOCS1B in humans) in a complex reaction mechanism. MOCS1A contains two [4Fe-4S] clusters and belongs to the group of S-adenosyl-methionine dependent radical enzymes (Hanzelmann et al., 2004). Although the overall mechanism of cPMP synthesis is not fully understood, MOCS1A and MOCS1B are believed to build a complex with S-adenosyl-methionine and GTP (Hanzelmann et al., 2002) to generate cPMP as a fully reduced tetrahydropteranopterin backbone (Santamaria-Araujo et al., 2012). The subcellular localization of both MOCS proteins have remained uncharacterized in mammals, their N-terminal mitochondrial targeting signals however strongly suggest the synthesis of cPMP to take place in mitochondria. Moreover, the plant homologues Cnx2 and Cnx3 have been exclusively detected in mitochondria (Teschner et al., 2010).

The second step of Moco synthesis occurs in the cytosol, suggesting that cPMP is exported from mitochondria to become converted to the next intermediate. In plants, the inner mitochondrial membrane transporter Atm3 has been shown to be involved in the export of cPMP to the cytosol (Teschner et al., 2010). Following its mitochondrial export, two sulfur atoms are transferred to cPMP to build molybdopterin (MPT) dithiolate. This reaction is

catalyzed by MPT-synthase, a hetero-tetrameric complex consisting of two large (MOCS2A in humans) and two small (MOCS2B in humans) subunits. While the large subunits mediate oligomerization, the small subunits each carry a single sulfur atom as thiocarboxylates being sequentially transferred to cPMP (Gutzke et al., 2001). Following the completion of a reaction cycle, the small subunits dissociate from the MPT-synthase and transiently bind to the MOCS3 protein, where they are re-sulfurated in an ATP-dependent reaction (Matthies et al., 2004).

The third and fourth steps of the Moco synthesis pathway are catalyzed by gephyrin in humans. Gephyrin is composed of an N-terminal G-domain and a C-terminal E-domain, which are both involved in separate reactions during the last steps of Moco synthesis (Schwarz and Mendel, 2006). First, the G-domain binds and adenylates MPT in an  $Mg^{2+}$  and ATP dependent manner, yielding MPT-AMP as the last intermediate of the Moco synthesis pathway. The reaction mechanism was uncovered in plants and revealed the binding of MPT to the homologous Cnx1G protein and the subsequent transfer of AMP to the terminal phosphate of MPT (Llamas et al., 2004). In the last step of Moco synthesis, Mo is attached to the dithiolate of the MPT backbone by the gephyrin E-domain. As again first discovered for the plant protein, MPT-AMP is hydrolyzed by the homologous Cnx1E protein and Mo is simultaneously transferred to the MPT dithiolate, finally resulting in the formation of Moco (Llamas et al., 2006).





### 1.3 Moco dependent enzymes

Following the completion of its synthesis, Moco becomes incorporated into a multitude of different Mo-enzymes to fulfill its biological function. More than 50 Moco-dependent enzymes were described so far, most of them catalyzing redox reactions that are important for the global cycles of nitrogen, carbon and sulfur (Schwarz et al., 2009). The majority of these proteins exclusively occur in prokaryotes, while to date five Moco-dependent enzymes are known in eukaryotes.

One of these enzymes, nitrate reductase (NR), is solely present in plants and fungi and plays a key role during nitrogen assimilation by catalyzing the reduction of nitrate to nitrite. Moco is covalently bound by a conserved cysteine as depicted in figure 1.1 A. Apart from Moco, NR requires the integration of a cytochrome *b<sub>5</sub>* type heme and a FAD-cofactor as well as homodimerization to achieve catalytic activity. Thereby, electrons are transferred from NAD(P)H to FAD and via heme to the Moco domain, which harbors the active site where nitrate is reduced.

Animals do not have a NR, while they comprise a subset of four other Moco enzymes, which can be classified into two groups according to their active site structure as well as sub-cellular distributions. The first group is composed of the cytosolic proteins aldehyde oxidase (AO) and xanthine oxidoreductase (XOR), both sharing the terminal sulfide group, while mitochondria constitute the second site of Moco-activity and harbor sulfite oxidase (SO) as well as the mitochondrial amidoxime reducing component (mARC 1+2), each having a cysteine linked Moco in their active site (Chamizo-Ampudia et al., 2011, Rajapakshe et al., 2011).

#### 1.3.1 Mammalian cytosolic Moco enzymes

AO and XOR can be grouped according to their cytosolic localizations, but they also share significant structural and functional similarities. Both proteins contain Moco within their C-terminal domains, which also mediate homodimerization in each case. In contrast to NR and mitochondrial molybdoenzymes, Moco is not covalently bound by a protein derived conserved cysteine, but instead contains a third terminal sulfido group as illustrated in figure 1.1 B. This sulfur atom is added to the cofactor by the enzyme Moco sulfurase in a final maturation step (Hille et al., 2011). As additional redox active domains, AO and XOR contain N-terminal [2Fe-2S] clusters and a central FAD domain to build the conserved tripartite structure of the AO/XOR enzyme family.

AO acts on a large array of substrates, but the general types of reactions imply hydroxylation of heterocycles and oxidation of aldehydes to the corresponding carboxylic acids (Garattini et al., 2008). Mechanistically, substrates are oxidized in the substrate binding pocket at the Mo-center. Electrons are transferred from Moco via the [2Fe-2S] clusters to FAD. During electron transfer, the [2Fe-2S] clusters act as electron sinks to store reducing equivalents during catalysis (Hille, 2002). While the human genome harbors a single AO gene, other vertebrates contain several different AO isoforms. Physiological functions of AO are poorly understood, an AO knockout mouse however revealed a function in the biosynthesis of retinoic acid (Terao et al., 2009). Furthermore, mammalian AOs represent an import drug-metabolizing system in the cytoplasm of hepatic cells. Thereby, AOs are proposed to act in concert with the microsomal cytochrome P450 system and to activate or inactivate various types of drugs and toxic compounds (Garattini et al., 2008).

XOR resembles AO in respect to structure and reaction mechanism, but catalyzes the hydroxylation of a different subset of substrates, which is much better defined as for AO. XOR mediates the oxidation of hypoxanthine to xanthine and the downstream reaction of xanthine to uric acid (Hille and Nishino, 1995). XOR exists in two forms, as xanthine dehydrogenase (XDH), constituting the primary gene product, and as xanthine oxidase (XO), arising from XDH by formation of internal disulfide bonds. While XD favors  $\text{NAD}^+$  as a primary electron acceptor, XO does not bind  $\text{NAD}^+$  and instead transfers electrons to  $\text{O}_2$ . Therefore, numerous reactive oxygen species (ROS) are formed, that are proposed to function in the innate immune response (Vorbach et al., 2003) and together with the antioxidant uric acid act in the regulation of the cellular redox potential (Droge, 2002). While no isolated forms of AO-deficiency are known, inactive XOR, either occurring in response to mutations in the *XOR* gene (Ichida et al., 1997) or secondary caused by the loss of Moco-sulfurase (Ichida et al., 2001), results in xanthinuria. The symptoms of the disease are not lethal, but affected patients suffer from xanthine stones due to elevated levels of xanthine.

## 1.3.2 Mammalian mitochondrial Moco enzymes

### 1.3.2.1 Sulfite oxidase

Sulfite oxidase (SO) is generally referred to as the most important eukaryotic Moco enzyme, as its depletion results in a severe neurodegenerative phenotype (see chapter 1.3.2.2 for details). SO catalyzes the essential oxidation of toxic sulfite to nonhazardous sulfate and thereby mediates the final step in the oxidative degradation of the sulfur-containing amino acids methionine and cysteine (Figure 1.3 A).

In contrast to AO and XOR, SO covalently binds Moco by a conserved cysteine in the central domain of the protein. Furthermore, Moco is deeply buried within the protein, forming numerous stabilizing hydrogen bonds to several residues of the central Moco-binding domain, as illustrated by the chicken SO crystal structure (Figure 1.3 B) (Kisker et al., 1997). To become catalytically active, SO requires the integration of a cytochrome  $b_5$  type heme as a second metal containing cofactor. Although not covalently attached to the protein, heme is stably integrated into the N-terminal domain of SO with two conserved histidines symmetrically coordinating the heme iron (Kisker et al., 1997). In analogy to structurally related plant NR and also both cytosolic Moco enzymes, SO undergoes homodimerization mediated by a large interface of the C-terminal domain. Upon the integration of both cofactors and homodimerization, SO is catalytically active and ready for sulfite oxidation.

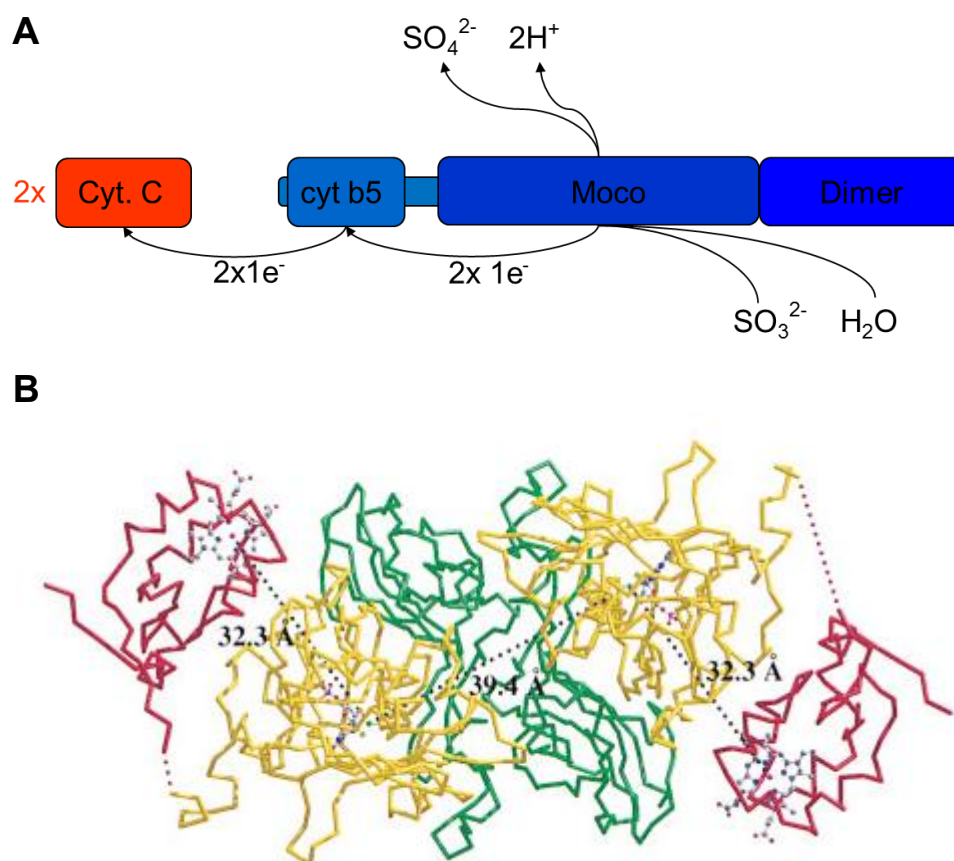


**Figure 1.3 Reaction mechanism and crystal structure of animal SO.** (A) Sulfite is oxidized at the Mo-active site of SO (depicted in blue with all three domains) and sulfate is released. The two electrons are sequentially transferred to the  $b_5$  heme and cytochrome  $c$  as the final electron acceptor. Monomeric SO is depicted for simplicity. (B) Crystal structure of mature chicken liver SO. The N-terminal heme domain is depicted in red, the central Moco domain in yellow and the C-terminal dimerization domain in green. Moco and heme are shown in ball-stick representations. The gray dotted lines connect the metal centers of the cofactors, the red dotted lines indicate a loop region, which is weakly defined in the electron density. Figure modified from (Kisker et al., 1997).

Sulfite oxidation takes place in the mitochondrial intermembrane space (IMS) in mammals, where cytochrome *c* is reduced as the physiological and final electron acceptor. The catalytic mechanism of mammalian SO starts with the oxidation of sulfite at the Mo-active site to generate a two-electron reduced Mo(IV) state (Hille, 1994). In a one-electron transfer reaction, *b<sub>5</sub>* heme is reduced to generate the EPR visible Mo(V)/Fe(II) intermediate of SO (Astashkin et al., 2002). This part is referred to as the reductive half reaction, resulting in the release of sulfate and the formation of fully reduced SO. In the oxidative half reaction, the electron is passed to cytochrome *c* to build a one electron reduced Mo(V)/Fe(III) form of the enzyme. In analogy to the first electron transfer reaction from the Mo center to cytochrome *c*, the second electron is transferred to a second equivalent of cytochrome *c* to regenerate the fully oxidized Mo(VI)/Fe(III) form of SO (Feng et al., 2007). As a multi-redox center enzyme, SO performs rapid electron transfer between Mo- and heme-domain to achieve an efficient oxidation of sulfite (Pacheco et al., 1999). However, the crystal structure of chicken SO revealed a comparatively large distance of ~32Å between both domains (Kisker et al., 1997). This conflict has led to the proposal of domain movements prior to electron transfer in order to bring Mo- and heme-domain in closer proximity. Consistently, the electron transfer rate of SO was shown to be dependent on solution viscosity and dropped in the presence of increasing concentrations of sucrose or polyethylene-glycol (Feng et al., 2002).

SO is mainly present in the liver as the predominant site of methionine and cysteine catabolism, but it is also abundant heart, kidney and to a lesser extent in brain to ensure comprehensive protection from sulfite accumulation (Moriwaki et al., 1997). Using cytochrome *c* as the final electron acceptor of the sulfite oxidation, SO is localized in the IMS of mitochondria as a soluble enzyme (Ito, 1971). As most mitochondrial proteins, SO is synthesized in the cytosol and imported into mitochondria. The mechanism of mitochondrial translocation of SO was investigated by pioneer work of Ono and Ito in the early 1980's. While the presence of ribosomes on the surface of mitochondria suggested a co-translational import of some precursors (Kellems et al., 1975, Ades and Butow, 1980), the translation of SO was demonstrated to take place on free ribosomes in the cytosol, indicating a post-translational import of SO (Ono et al., 1982). Following its translation, SO was shown to enter mitochondria ATP- and membrane potential-dependently and the inner mitochondrial membrane was found to be involved in the translocation process (Ono and Ito, 1982b). Import of SO is accompanied by processing, as illustrated by a truncated mature enzyme compared to the precursor during *in vitro* mitochondrial import experiments (Ono and Ito, 1984). Upon completion of import, the half-life of SO was measured to last between three and four days (Ono and Ito, 1982a).

The significance of sulfite oxidation is not restricted to animals, but also an important reaction in plants and bacteria. In plants, a protein homologous to animal SO was discovered (Eilers et al., 2001). Its primary and crystal structure however revealed a number of differences to animal SO, as plant SO (PSO) lacks a heme cofactor and Moco thus constitutes the only redox center of the enzyme (Schrader et al., 2003). Accordingly, PSO does not use cytochrome *c* but instead molecular oxygen as a physiological electron acceptor with the corresponding reaction taking place in peroxisomes. Bacteria oxidize sulfite by means of a sulfite dehydrogenase, a heterodimer of a large Mo-binding subunit and a small heme *c*-containing subunit (Kappler et al., 2000). While the sulfite dehydrogenase sequence is not related to mammalian SO, the heme *c* containing subunit revealed structural similarities to the *b*<sub>5</sub> heme domain of mammalian SO (Kappler and Bailey, 2005).

#### 1.3.2.2 Sulfite oxidase- and Moco-deficiency

The physiological relevance of SO is displayed by a severe neurodegenerative disorder termed isolated SO-deficiency, rapidly evolving in absence of functional SO. Affected patients suffer from neurological abnormalities such as microcephaly, mental retardation and seizures, usually accompanied by death in early infancy (Figure 1.4). The disease follows an autosomal recessive trait and is very rare, with less than 30 described cases in the literature (Johnson et al., 2002, Tan et al., 2005). SO-deficiency either occurs in response to mutations in the SO gene or based on a secondary loss of activity caused by mutations in one of the four genes involved in Moco biosynthesis. The latter causes a simultaneous loss of all five mammalian Moco enzymes with the corresponding disease termed Moco-deficiency (Schwarz, 2005). The clinical symptoms of Moco-deficiency are however hardly distinguishable from those of isolated SO-deficiency, demonstrating the loss of SO to be the predominant cause of the pathophysiology in Moco-deficiency and SO to be the most important Moco enzyme in humans.

In absence of functional SO, sulfite initially accumulates in the liver as the main site of methionine and cysteine catabolism and subsequently spreads out the entire body via the blood circulation and finally reaches the brain. The pathogenesis of SO- and Moco-deficiency is not completely understood and may derive from sulfite toxicity, a lack of sulfate or the accumulation of sulfur-containing compounds that are formed in response to excessive sulfite accumulation. Sulfite is a strong nucleophile breaking disulfide bridges and thereby affecting numerous proteins and cellular functions. In addition, sulfite exposure to mouse neuronal cells was shown to increase reactive oxygen species (ROS) and to simultaneously decrease intracellular ATP production. The concomitant inhibition of glutamate dehydrogenase by sulfite led to the proposal of a general neuronal energy deficit during SO

deficiency, resulting in neuronal ischemia followed by brain lesions, as seen in most patients (Zhang et al., 2004).

Accumulation of sulfite within the cells also leads to the excess formation of sulfur compounds like s-sulfocysteine, a structural analog of glutamate potentially contributing to neuronal death by hyperactivating NMDA-receptors (Olney et al., 1975, Salman et al., 2002).

Finally, inactive SO causes a cellular deficit of sulfate, which is required for the synthesis of myelin stabilizing sulfatides in the brain. A lack of sulfate was thus proposed to result in myelin destabilization and the following neurologic dysfunctions observed upon SO-deficiency. Characterizations of neuropathological changes in isolated SO-deficiency however revealed normal sulfatide levels, contradicting a deficiency of sulfate to be the primary cause of the SO-deficiency symptoms (Rosenblum, 1968).

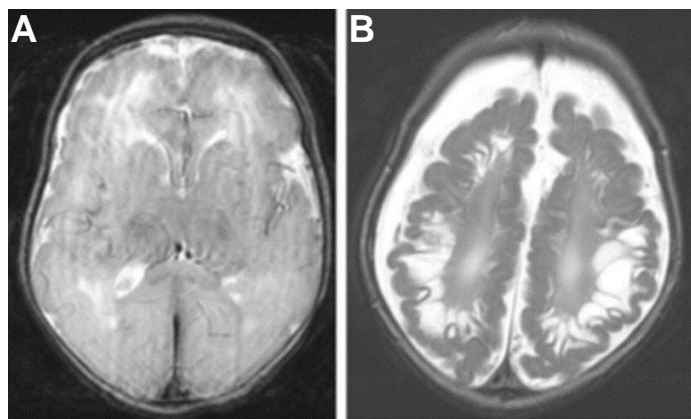


**Figure 1.4 Severe neurological symptoms of SO deficiency.** Axial magnetic resonance imaging (MRI) scan of an isolated SO deficiency patient brain. (A) MRI scan 11 days after birth revealed a diffuse loss of gray-white distinction and (B) severe encephalomalacia and increasing neurodegeneration after 3.5 months. Figure modified from (Tan et al., 2005).

Efficient therapeutic treatments of isolated SO-deficiency are not available so far, given that a cellular enzyme replacement therapy as the most obvious and promising solution would fail due to inefficient cellular uptake of externally applied SO. The mitochondrial localization of SO increases this problem and would interfere with successful sub-cellular sorting of cofactor loaded and folded SO upon a hypothetical cellular uptake. Therefore, mostly unsuccessful attempts to attenuate the symptoms of isolated SO-deficiency have been reported. Low protein diets aiming in a decrease of sulfite production (Touati et al., 2000) or inhibition of NMDA-receptor channels to circumvent their potential hyperactivation during disease progression (Kurlemann et al., 1996) did however not sustainably improve the symptoms.

In contrast to isolated SO-deficiency, an efficient therapy is available for a group of patients suffering from Moco-deficiency. Treatment of patients with externally applied Moco could theoretically cure all types of Moco-deficiency, but is less likely due to the high

instability of protein-free cofactor (Deistung and Bray, 1989). However, cPMP as the first and most stable precursor of the Moco synthesis pathway turned out to be able to significantly improve the phenotypes of patients suffering from mutations affecting the first step of Moco synthesis (Veldman et al., 2010).

### 1.3.2.3 Mitochondrial amidoxime reducing components

Numerous drugs and drug candidates contain strongly basic functional groups like amidines, which interfere with efficient absorption by the gastrointestinal tract in response to their protonation under physiological conditions. Therefore, a so-called prodrug principle was developed to enhance oral bioavailability of such molecules (Ettmayer et al., 2004). By N-hydroxylation of certain functional groups, the latter become less basic and unprotonated under physiological conditions, thus increasing intestinal uptake by diffusion. These N-hydroxylated prodrugs must then be converted to the active drug upon cellular assimilation by reduction and reformation of the basic functional groups. The functionality of this principle and its application on a wide range of different drugs implied the presence of a cellular N-reductive system catalyzing the reduction and activation of N-hydroxylated prodrugs (Clement, 2002).

In mammals, outer mitochondrial membrane proteins cytochrome *b<sub>5</sub>* and its reductase as well as a third unidentified component were shown to be involved in these prodrug activating reductions (Kadlubar and Ziegler, 1974, Clement et al., 1997). In a screen for the missing third component of the N-reductive system, Havemeyer et al. (2006) identified a novel mitochondrial protein annotated as *MOSC2* (Moco-sulfurase C-terminal domain) according to its similarities to the C-terminal domain of the Moco-sulfurase, which sulfurates Moco in XO and AO. Due to its involvement in the reductive activation of N-hydroxylated prodrugs, the enzyme was termed the mitochondrial amidoxime reducing component 2 (mARC2). The human chromosome 1 harbors a second gene in tandem orientation to *MOSC2*, revealing striking sequence similarities and being annotated as *MOSC1*. The corresponding protein was shown to have similar functions in the reduction of N-hydroxylated prodrugs and was hence termed mARC1 (Gruenewald et al., 2008).

Considering the structural analogies of both mARC proteins to Moco sulfurase, their potential Moco incorporation was tested and thereby indeed revealed mARC1 and mARC2 to be novel mammalian Moco enzymes. In contrast to cytosolic animal Moco enzymes, Moco of both mARC proteins was shown not to contain a third terminal sulfido group (Wahl et al., 2010). Instead, pulsed EPR spectroscopy suggested a protein derived equatorial Moco ligand and both mARC proteins to join the SO/NR family covalently binding Moco by a conserved cysteine (Rajapakshe et al., 2011). This was confirmed and extended by

characterizations of the *Chlamydomonas reinhardtii* homologue crARC, which revealed cysteine 252 to be essential for Moco binding and catalysis (Chamizo-Ampudia et al., 2011).

The mARC proteins confer a number of unique traits that distinguish it from all other eukaryotic Moco enzymes. First, purification and oligomerization analyses revealed both mARC proteins to be monomeric (Wahl et al., 2010), while most other eukaryotic Moco enzymes require homodimerization for catalytic activity. Moreover, mARC proteins contain Moco as a single redox active center and do not contain any further cofactors, qualifying mARC as the simplest animal Moco enzyme. Instead, mARC is integrated into a three component enzyme system with the overall cofactor composition mirroring eukaryotic NR proteins (FAD, heme, Moco). Interestingly, the electrons pass from NADH to FAD containing cytochrome  $b_5$  reductase and via heme containing cytochrome  $b_5$  to Moco within the mARC subunit, which harbors the active site for substrate reduction (Figure 1.5). Thereby, not only cofactor composition, but also cofactor arrangement and electron flow of the N-reductive system are similar to NR.

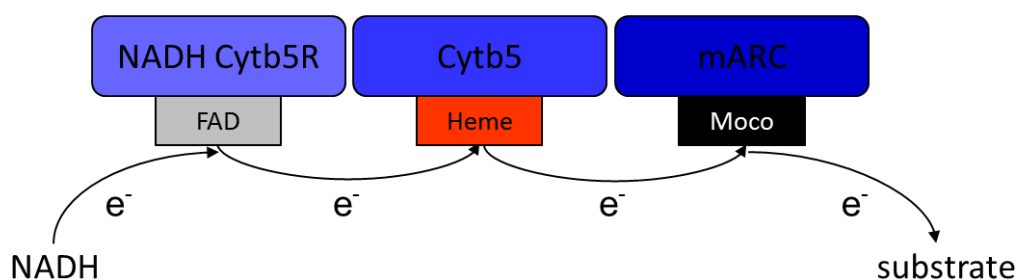


**Figure 1.5 Composition and electron transfer in the N-reductive system.** NADH is oxidized by FAD containing NADH cytochrome  $b_5$  reductase (NADH Cytb5R) and electrons are passed to heme integrating cytochrome  $b_5$  (Cytb5). Moco binding mARC receives electrons from Cytb5 and reduces the substrate within the active site.

While many N-hydroxylated compounds were identified as substrates for native and recombinant mARC proteins, the physiological functions of mARC remain poorly understood. So far, the only known physiological role of both mARC proteins accounts for their involvement in the regulation of nitric oxide (NO) synthesis (Kotthaus et al., 2011). NO synthases catalyze the oxidation of arginine to citrulline and NO via the intermediate N-hydroxy-arginine (NOHA). NO is an essential cellular signaling molecule with versatile functions in vascular homeostasis and innate immune response. However, overproduction of NO can cause severe diseases like ischemia or septic shocks, thus requiring a balanced regulation of NO synthesis (Moncada et al., 1991). Both mARC proteins were shown to be involved in one of those regulative mechanisms and to catalyze the reduction of NOHA to arginine in cooperation with cytochrome  $b_5$  and its reductase (Kotthaus et al., 2011).



## 1.4 Mitochondrial architecture and function

Mitochondria harbor SO and mARC and thereby exert crucial cellular functions in sulfite detoxification and NO synthesis regulation. These reactions however only represent a small fraction of the multitude of essential cellular processes and functions mitochondria are involved in. In addition to their central role in ATP production by oxidative phosphorylation, they play key roles in the metabolism of amino acids and lipids as well as in iron-sulfur cluster biogenesis (Lill, 2009, Osman et al., 2011). Further, mitochondria are fundamental for the regulation of programmed cell death and mitochondrial dysfunction is hallmark of many neurodegenerative diseases (Zeviani, 2004, Wang and Youle, 2009).

The cellular functions of mitochondria are tightly linked to its architecture, which is characterized by two membranes of distinct structure. The outer mitochondrial membrane builds the border to the cytosol and harbors voltage dependent anion channels (VDAC), which permit passive exchange of small molecules and metabolites between the cytosol and the mitochondrial IMS. The outer membrane also contains the translocase of the outer membrane (TOM) complex as the main entry gate for proteins, the sorting and assembly machinery (SAM) as well as mitofusins being involved in fusion of mitochondria.

The inner mitochondrial membrane constitutes a significantly larger surface area than the outer membrane and can be divided into two main regions. The inner boundary membrane (IBM) is juxtaposed to the outer membrane with the diameter of the IMS not exceeding 2-3 nm (Neupert, 2012). The IBM is rich in proteins involved in transport of other proteins as well as metabolites and harbors the translocase of the inner membrane (TIM) complex. Invaginations of the IBM, termed cristae, form a multitude of shapes from tubular to lamellar structures and comprise the second compartment of the inner mitochondrial membrane. Cristae membranes mainly contain components of the respiratory chain and the F<sub>1</sub>F<sub>0</sub>-ATP-synthase. IBM and cristae membranes are connected by narrow tubular openings called cristae junctions, which are believed to limit diffusion between both membranes and between intracristae space and the remainder of the IMS (van der Laan et al., 2012). The mechanisms controlling the ultrastructural organization of mitochondria had remained largely unknown, until the mitochondrial inner-membrane organizing system (MINOS) was recently discovered in *Saccharomyces cerevisiae* (*S. cerevisiae*) as the first protein scaffold regulating mitochondrial architecture (Harner et al., 2011, Hoppins et al., 2011, von der Malsburg et al., 2011). This large complex is composed of at least six subunits and is involved in the maintenance of inner membrane organization by regulation of cristae morphogenesis and controlling the lateral diffusion of membrane components between IBM and cristae. The MINOS complex further interacts with the TOM and SAM complex of the

outer mitochondrial membrane and thus permits contact sites between inner and outer mitochondrial membranes (Neupert, 2012). Mitochondria do not only require organization and regulation of their internal ultrastructures, but they also build physical links to the endoplasmic reticulum (ER). A protein complex tethering ER and mitochondria was recently identified and termed ERMES (ER-mitochondria encounter structure) (Kornmann et al., 2009). This complex is composed of transmembrane proteins residing in the ER and mitochondria, with proposed functions in interorganellar  $\text{Ca}^{2+}$  and phospholipid exchange, regulation of mitochondrial protein import and mitochondrial DNA maintenance (Kornmann and Walter, 2010).

Mitochondria form extended and dynamic networks within the cell continually undergoing fusion and fission events. While mitochondrial fusion is regulated by the large dynamin-like GTPases MFN1 and MFN2 in the outer membrane and OPA1 in the inner membrane, mitochondrial fission is exerted by the dynamin related GTPase DRP1 and the outer membrane proteins MFF and FIS1 (Chan, 2006, Zhao et al., 2012). Balanced fusion and fission permit interaction of mitochondria and are fundamental to maintain their shape and function.

## **1.5 Mitochondrial protein import**

The spectrum of mitochondrial functions as well as regulation of mitochondrial architecture depends on 1000-1500 different mitochondrial proteins present within the organelle (Baker et al., 2007). Although mitochondria have retained their own genome during endosymbiotic evolution, the majority of genes have been lost over the period of evolving from an endosymbiont to an organelle. Today, only ~1% of mitochondrial proteins are encoded by mitochondrial DNA. The remaining proteins are encoded by nuclear genes and become synthesized by cytosolic ribosomes. The cell has therefore developed sophisticated mechanisms to enable transport of proteins to and within mitochondria.

In spite of partial co-translational protein import to mitochondria (Kellems et al., 1975, Ades and Butow, 1980, Knox et al., 1998), the vast majority of mitochondrial proteins are synthesized as cytosolic precursors and imported by post-translational mechanisms. Chaperons are thereby required to guide the precursor proteins to receptors at the outer mitochondrial membrane and to keep them in an unfolded and import competent state (Wiedemann et al., 2004a). Considering the complex two-membrane architecture of mitochondria, several protein import pathways have evolved to ensure routing towards the correct mitochondrial sub-compartment.

Mitochondrial precursor proteins can be divided into two main classes. Pre-proteins designated for the mitochondrial matrix and a number of proteins residing in the inner membrane or the IMS carry cleavable N-terminal extensions of 10-30 residues in length (Wiedemann et al., 2004a). These pre-sequences form amphipathic  $\alpha$ -helices and direct the protein across both the TOM and TIM complexes. The second class of mitochondrial proteins is synthesized as non-cleavable precursors and contains internal motifs triggering translocation.

Almost all mitochondrial precursors enter mitochondria via the TOM complex as the universal protein entry gate of the outer membrane. It consists of seven different subunits, which can be subdivided into three groups according to their individual functions during the translocation process. TOM20, TOM22 and TOM70 expose cytosolic domains and serve as receptors initially binding different types of precursors (Ahting et al., 1999). The general import channel is formed by the beta-barrel protein TOM40 (Hill et al., 1998), while the small proteins TOM5, TOM6 and TOM7 have TOM complex stabilizing functions and may also participate in the transfer of precursor proteins (Honlinger et al., 1996, Dietmeier et al., 1997, Kato and Mihara, 2008). Following their mitochondrial entry via the TOM complex, precursors diverge into different pathways in order to reach their destined mitochondrial sub-compartment.

### **1.5.1 Import of proteins containing cleavable pre-sequences**

Almost half of all mitochondrial precursors contain cleavable N-terminal extensions, which are also called matrix sequences, as they transport the N-terminus of a given protein across the inner membrane into the matrix (Neupert and Herrmann, 2007). After cytosolic synthesis, precursors are initially recognized by the outer membrane surface receptor TOM20, based on the hydrophobic surface of their amphipathic helix (Abe et al., 2000). Interactions to the negatively charged carboxy-terminus of TOM22, mediated by the positively charged helix-surface, and binding to TOM5 trigger the subsequent transfer to the import pore TOM40 (Brix et al., 1997). According to the so-called binding chain hypothesis, the process of outer membrane translocation is driven by gradually increasing affinities between precursors and the mentioned TOM components (Milenkovic et al., 2007). After translocation via TOM40, the pre-sequence binds to the IMS domain of TOM22 (Komiya et al., 1998).

Following translocation through the TOM complex, pre-sequence containing precursors are transferred to the pre-sequence translocase of the inner membrane, the TIM23 complex. TIM23 constitutes the channel-forming protein and together with TIM17

builds the membrane embedded core of the complex. Pre-sequences leaving the TOM complex are recognized by the IMS domains of TIM23 and TIM50 as the primary pre-sequence receptor at the inner membrane (Schulz et al., 2011). Insertion of precursors into the TIM23 channel depends on an intact membrane potential across the inner membrane, which constitutes an electrophoretic driving force towards the mitochondrial matrix.

Two main classes of proteins enter the TIM23 complex based on their cleavable pre-sequences. The first group of proteins is destined to reach the mitochondrial matrix. The second class of proteins contains bipartite targeting signals with a transmembrane domain downstream of the pre-sequence serving as a stop-transfer signal, thus resulting in an arrest of translocation in the inner mitochondrial membrane. Accordingly, two different forms of the TIM23 complexes exist, either mediating membrane potential dependent translocation towards the matrix or insertion into the inner mitochondrial membrane (Figure 1.6).

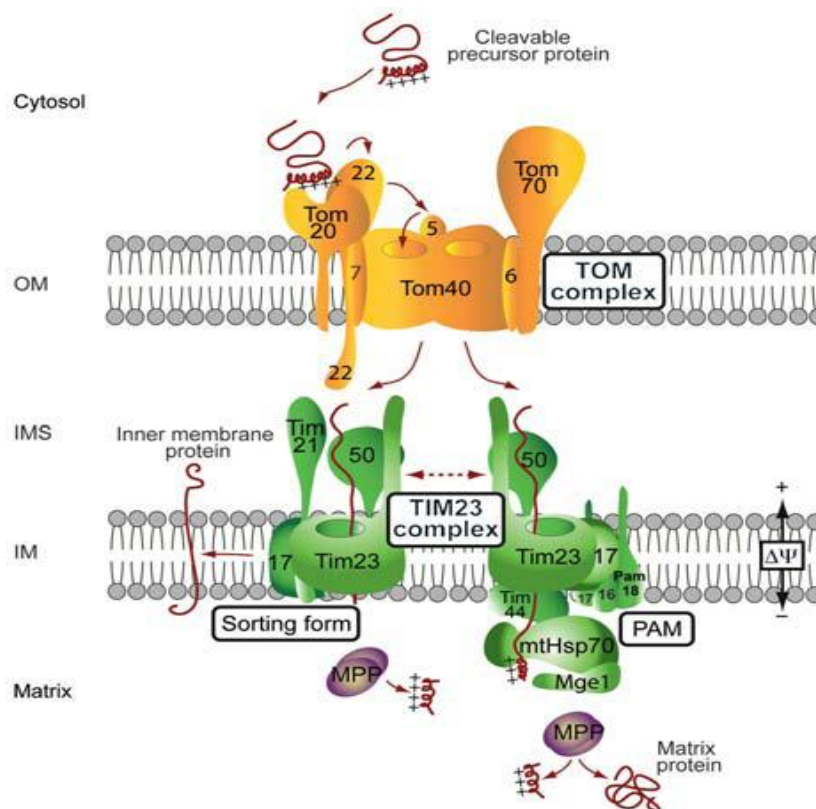


**Figure 1.6 Mitochondrial import of pre-sequence containing precursors.** Proteins containing a cleavable pre-sequence are imported by TOM and two forms of TIM23 complexes. Inner membrane or IMS proteins contain a hydrophobic stop transfer signal downstream of the matrix targeting peptide and are membrane potential dependently imported. Matrix proteins lack transmembrane domains and require the ATP dependent PAM complex as an additional driving force for complete import into the matrix. Figure modified from (Milenkovic et al., 2007).

Both types share TIM23, TIM17 and TIM50 as essential core subunits of the complex. TIM21 is a unique subunit of the so-called sorting form of the TIM23 complex, which allows lateral integration of precursors into the inner membrane (Milenkovic et al., 2007). The function of TIM21 is not completely understood, but it was shown to interact with the IMS domain of TOM22, suggesting a role in the interactions between TIM and TOM complexes (Chacinska et al., 2005). Proteins with bipartite targeting signals either remain anchored within the inner membrane, or they become proteolytically cleaved downstream of the transmembrane domain to generate a soluble IMS protein.

Mitochondrial matrix proteins lack transmembrane domains and therefore completely cross the TIM23 complex. This is mediated by a different type of TIM23 complex, which does not contain TIM21, but instead binds the pre-sequence translocase-associated motor (PAM) within the mitochondrial matrix. The PAM complex consists of mitochondrial HSP70 (mtHSP70), the nucleotide exchange factor GRPE (Mge1 in *S.cerevisiae*), TIM44, linking mtHSP70 to the TIM23 complex, and the three co-chaperons PAM16, PAM17 and PAM18. HSP70 thereby exerts a crucial function as a motor protein, ATP-dependently pulling the incoming precursor entirely towards the mitochondrial matrix. The translocation of pre-sequence containing precursors is completed by cleavage of the matrix targeting signal by the mitochondrial processing peptidase (MPP) (Neupert and Herrmann, 2007).

### **1.5.2 Import of proteins lacking cleavable pre-sequences**

Mitochondrial proteins lacking a cleavable pre-sequence retain their primary structure during mitochondrial transport and are targeted to the organelle by internal motifs. According to their designated sub-compartments and import mechanisms, these proteins can be subdivided into four main classes.

#### **1.5.2.1 Insertion of proteins into the inner membrane**

While inner membrane proteins containing a single transmembrane domain usually become imported based on cleavable pre-sequences as described above, multi-membrane-spanning, mostly carrier proteins of the inner membrane as well as membrane embedded components of the TIM complex are imported by the alternative TIM22 import pathway (Milenkovic et al., 2007).

Following their synthesis, these precursors are bound by cytosolic chaperons owing to their hydrophobicity and targeted to TOM70 as the primary import receptor of solute carrier proteins (Young et al., 2003). Upon translocation through the TOM complex, precursors are

bound by hexameric complexes composed of TIM9 and TIM10 and are chaperone assisted through their way to the soluble IMS (Curran et al., 2002, Vial et al., 2002, Baker et al., 2009). With the help of TIM12, the precursors dock onto the carrier translocase of the inner membrane (TIM22 complex), which is composed of TIM22 as the essential core of the complex, mediating the membrane insertion of carrier proteins. In addition, TIM54 as a non-essential accessory component and TIM18, only found in fungal mitochondria so far, assemble into the TIM22 complex (Milenkovic et al., 2007). Yeast succinate dehydrogenase subunit 3 (Sdh3) was further recently identified as a novel subunit of the TIM22 complex and was proposed to be involved in complex biogenesis (Gebert et al., 2011). The carrier proteins are inserted into the two channels of the TIM22 complex in a loop conformation, with the membrane potential activating TIM22 and constituting the driving force of the insertion (Rehling et al., 2003). Carrier proteins finally dimerize into their native state upon their membrane release from the TIM22 complex (Neupert and Herrmann, 2007).

#### 1.5.2.2 Import of small IMS proteins

Many proteins of the mitochondrial IMS are imported based on bipartite targeting signals followed by downstream proteolytic cleavages as described above. However, the majority of IMS proteins is small and becomes imported by alternative mechanisms. These proteins are translocated through the TOM complex and, in respect to their size of less than 20 kDa, tend to bi-directionally cross the TOM complex if not folded, which also includes their reverse translocations to the cytosol (Lutz et al., 2003). Folding of these proteins prevents retrograde movements and converts the bi-directional diffusion into a vectorial process. This so-called folding-trap mechanism of IMS protein import is based on cofactor mediated folding (Dumont et al., 1988, Field et al., 2003) or the formation of intramolecular disulfide bonds. Proteins undergoing internal disulfide-bond formations contain conserved Cys-X<sub>3</sub>-Cys or Cys-X<sub>9</sub>-Cys motifs and require the MIA40 import machinery for the formation of internal disulfide bonds (Chacinska et al., 2004). MIA40 is an oxidoreductase and serves as a receptor for small IMS precursors upon their import into the IMS. Substrates and MIA40 initially form intermediate mixed disulfide bonds, while formation of intramolecular disulfide bonds leads to the release of the folded and trapped precursors in a final maturation step. This disulfide-relay system is accomplished by reoxidation of MIA40 mediated by the sulfhydryl oxidase ERV1 (Bottinger et al., 2012).

#### 1.5.2.3 Integration of $\beta$ -barrel proteins into the outer membrane

The outer mitochondrial membrane contains two distinct classes of integral membrane proteins, which are either inserted by  $\alpha$ -helical transmembrane segments or based on multiple  $\beta$ -strands. Apart from outer mitochondrial membranes, the corresponding  $\beta$ -barrel

proteins are only present in outer membranes of chloroplasts and gram-negative bacteria, thus presumably reflecting the evolutionary origin of eukaryotic organelles (Walther and Rapaport, 2009).

After their cytosolic synthesis,  $\beta$ -barrel proteins are guided to the TOM complex, where they become recognized by TOM20 as well as TOM22 and transported into the IMS via the TOM40 import channel (Walther and Rapaport, 2009). Following their translocation into the IMS, a number of  $\beta$ -barrel proteins have been shown to associate with the chaperone like small proteins TIM8-TIM13 or TIM9-TIM10, respectively (Hoppins and Nargang, 2004, Wiedemann et al., 2004b). Integration of  $\beta$ -barrel proteins into the outer membrane is mediated by the SAM (sorting and assembly machinery) / TOB (topogenesis of  $\beta$ -barrel proteins) complex of the outer mitochondrial membrane (Paschen et al., 2003, Wiedemann et al., 2003). In yeast, the SAM machinery is composed of three core subunits, with the  $\beta$ -barrel protein Sam50 constituting the main component and the peripherally associated components Sam35 and Sam37 being located at the cytosolic surface of the SAM complex. While Sam50 (Humphries et al., 2005) and Sam37 (Armstrong et al., 1997) have clear homologues in mammals, metaxin2 is proposed to be the functional homologue of Sam35, although direct sequence homology is lacking (Neupert and Herrmann, 2007). Furthermore, Mdm12 and Mmm1 were identified as yeast SAM complex subunits (Meisinger et al., 2007) and Mdm10 has been identified as an additional SAM subunit being specific for the assembly of Tom40 (Meisinger et al., 2004). The mechanisms by which the SAM complex mediates membrane insertion of  $\beta$ -barrel proteins are poorly defined. Sam50 is however suggested to build a huge pore and to assist in folding of incoming  $\beta$ -barrel proteins, finally releasing them laterally into the outer membrane (Paschen et al., 2003). The MINOS complex, which interacts with both the TOM and the SAM complex, was recently shown to be also involved in  $\beta$ -barrel protein biogenesis, since depletion of mitofilin as the large core subunit of MINOS resulted in impaired  $\beta$ -barrel protein membrane assembly (Bohnert et al., 2012).

#### 1.5.2.4 Integration of $\alpha$ -helical proteins into the outer membrane

The insertion of proteins containing single  $\alpha$ -helical transmembrane segments into the outer mitochondrial membrane is only partially understood and seems to be divergent. These proteins either contain N- or C-terminal transmembrane segments flanked by positively charged residues, with the soluble core of the protein being exposed to the cytosol.

Outer membrane proteins comprising N-terminal  $\alpha$ -helical transmembrane domains are termed signal-anchored proteins according to the dual function of the hydrophobic segment in membrane anchoring and sorting signal. The few known members of this family,

including TOM20 and TOM70, lack obvious primary sequence similarities in their N-terminal region, suggesting that the sorting information is delivered by a conserved structural feature. This was confirmed by mutagenesis studies of the N-terminal domains of signal-anchored proteins, indicating that a moderate degree of hydrophobicity rather than the length of the transmembrane segment is fundamental for correct sorting (Waizenegger et al., 2003). The mechanisms of outer membrane integration are not completely understood and seem not to follow a common principle of targeting. The import however seems to be independent on the primary receptors of the TOM complex and blocking of the translocation pore does not affect membrane insertion of the known signal-anchored proteins (Ahting et al., 2005, Meineke et al., 2008). Still, TOM40 was shown to play a role in the membrane integration of TOM20 and TOM70, which may however represent a specific requirement of these proteins as TOM complex subunits (Dukanovic and Rapaport, 2011). Another signal anchored protein that is not part of the TOM complex, the yeast signal-anchored protein OM45, has been shown to be inserted into the membrane independently of TOM complex subunits and other proteinaceous factors involved in membrane protein insertion. Instead, OM45 displayed the ability to acquire a transmembrane topology within artificial lipid bilayers. The specific lipid composition of outer mitochondrial membranes and the achieved thermodynamic gain upon membrane integration was therefore recently proposed to constitute the targeting information and driving force for insertion of this signal-anchored protein into the correct membrane (Merklinger et al., 2012). The proposed mechanisms of outer membrane targeting of signal-anchored proteins are summarized in figure 1.7.

In addition to signal-anchored proteins, the outer mitochondrial membrane contains proteins with a C-terminal transmembrane segment, termed tail-anchored proteins, and multi-spanning proteins including more than one  $\alpha$ -helical transmembrane segment. The membrane insertions of tail-anchored proteins seem to be related to those of signal-anchored proteins, with some components requiring the presence of the TOM core complex (Horie et al., 2003) and others being incorporated independently of the TOM components (Ross et al., 2009). The schematic proposals of figure 1.7 are therefore also transferable to tail-anchored proteins. However, the SAM complex was also suggested to be required for membrane insertion of TOM components with single C-terminal membrane anchors (Stojanovski et al., 2007). Integrations of outer membrane proteins containing multiple transmembrane segments were shown to require the small outer membrane protein Mim1 (Becker et al., 2011, Papic et al., 2011). These findings were recently extended by the identification of Mim2, which interacts with Mim1 to build the MIM complex required for the insertion of multispanning outer membrane proteins (Dimmer et al., 2012).



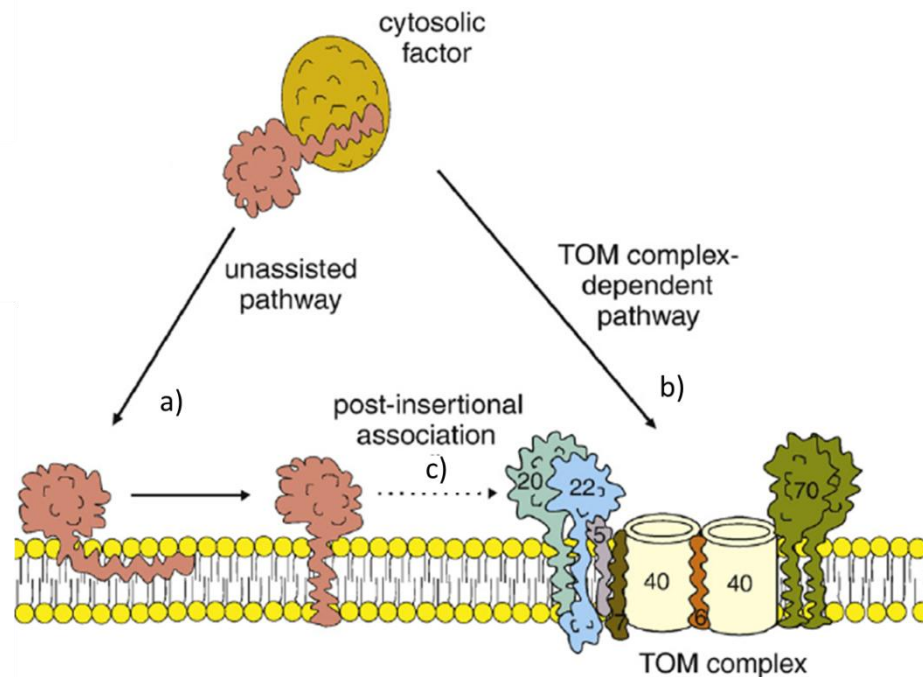


**Figure 1.7 Possible import pathways of signal-anchored proteins.** The transmembrane domains of signal-anchored proteins are presumably engaged by cytosolic factors. Insertion into the outer membrane can occur (a) without assistance of any other proteins or (b) mediated by a pre-existing TOM complex in case of TOM20 and TOM70. The TOM complex may be involved in the initial steps of membrane insertion or (c) TOM complex mediated assembly could occur after membrane insertion of the precursor. Figure modified from (Dukanovic and Rapaport, 2011).

## 1.6 Cofactors and metabolites in mitochondria

Mitochondrial function does not only require targeted import of proteins, but also a continued and diversified flux of cofactors, metabolites and nucleotides into and out of mitochondria. The outer mitochondrial membrane contains voltage dependent anion channels (VDAC), which permit passive, bi-directional diffusion of molecules up to ~ 5kDa in size (Lemasters and Holmuhamedov, 2006). All metabolites and cofactors can hence non-specifically cross the outer mitochondrial membrane. In contrast, the inner mitochondrial membrane does not contain porins and is rich in cardiolipin, rendering the inner membrane virtually impermeable. The transport of solutes is instead specifically coordinated by a family of more than 50 nuclear encoded and inner membrane embedded proteins called mitochondrial carriers. All of these proteins share a tripartite structure of three homologous repeats of approximately 100 amino acids, each containing two  $\alpha$ -helical transmembrane stretches. Mitochondrial carrier proteins are homodimers, with each monomer traversing the inner membrane six

times, being connected by hydrophilic loops or domains with the N- and C-termini remaining exposed to the IMS. The driving force of the transport is mediated by a concentration gradient of the solute and/or the electrochemical  $H^+$  gradient across the inner mitochondrial membrane (Palmieri, 2008). Prominent examples for inner membrane carriers transport ADP/ATP (Aquila et al., 1982), phosphate (Kolbe et al., 1984), aspartate/glutamate (Bisaccia et al., 1992) or ornithine (Indiveri et al., 1992).

### 1.6.1 Heme synthesis and transport

Mitochondria and cytosol cooperate in a large number of metabolic processes and thus strictly depend on inner membrane carrier proteins to ensure efficient metabolite exchanges. One example is depicted by the synthesis of heme cofactors, which partially occurs in the cytosol but is completed in mitochondria. Furthermore, heme is not only incorporated into mitochondrial proteins, but also an essential component of a number of non-mitochondrial enzymes. Therefore, the heme synthesis pathway including export of the final heme cofactor is subject to repeated exchange of intermediates between mitochondria and cytosol.

The synthesis of heme (figure 1.8) initiates in mitochondria by 5-aminolevulinate-synthase mediated condensation of glycine and succinyl CoA to form 5-aminolevulinate.

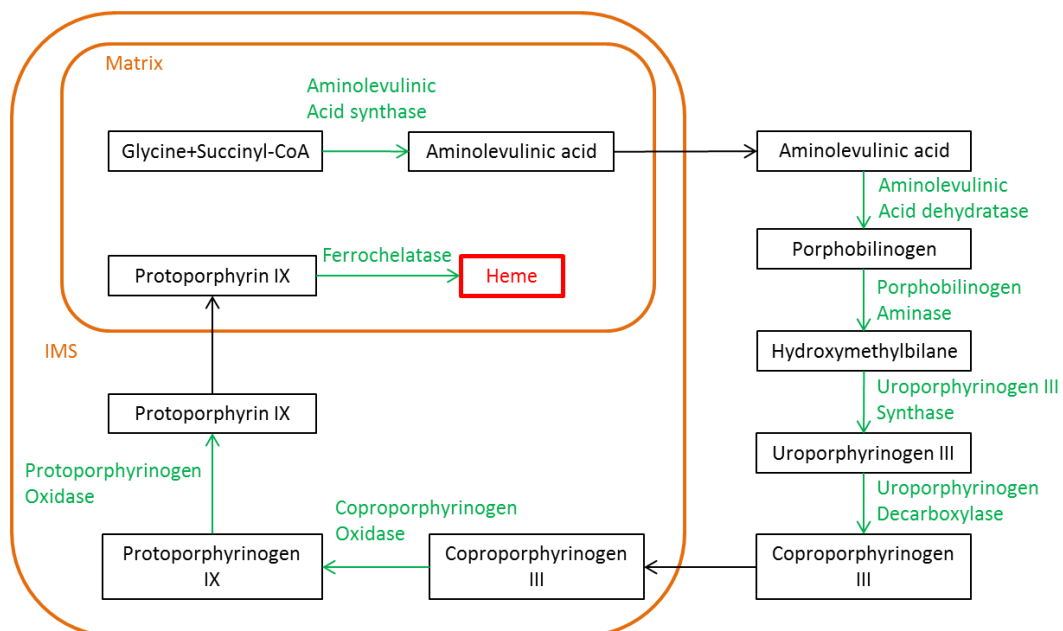


**Figure 1.8 Mammalian heme biosynthesis.** All heme precursors are depicted in black boxes, heme as the final product is highlighted red. Green arrows indicate enzymatic reactions and names of catalyzing enzymes are given. Black arrows illustrate transport of intermediates across mitochondrial membranes. Mitochondrion is schematized in orange, matrix and IMS are shown.

The subsequent four steps of heme biogenesis take place in the cytosol, thus requiring mitochondrial export of 5-aminolevulinate by a currently unknown carrier. Coproporphyrinogen III as the final cytosolic product is re-imported into mitochondria, where it is first converted to protoporphyrinogen IX and further modified to protoporphyrin IX in the IMS. The final step of heme synthesis occurs on the matrix side of the inner mitochondrial membrane, where iron is inserted into protoporphyrin IX by ferrochelatase (Ajioka et al., 2006). The carrier exporting heme to the cytosol remains unknown, while the heme-binding protein 1 (Taketani et al., 1998) and the ATP-binding cassette transporter M-ABC2 (Shirihai et al., 2000) were proposed to be involved in mitochondrial export of heme or one of its intermediates.

## **1.7 Aims of the current study**

The overall aim of the current study was to unravel the mechanisms underlying the cellular maturation of the mitochondrial Moco-enzymes SO and mARC. Considering the intrinsic instability of Moco and its cytosolic synthesis, the group of mitochondrial Moco-enzymes was of particular interest to gain insights into the open questions of cellular Moco transport and stabilization.

The first part of this thesis focused on the dissection of SO maturation and the impact and stabilization of Moco. This was supposed to answer the following questions:

- 1) How is the complex assembly of SO coordinated on the cellular level?
- 2) Are the individual steps of SO maturation subject to a molecular hierarchy?
- 3) What is the role of Moco during the maturation of SO and where do Moco and SO associate?
- 4) Which factors trigger mitochondrial localization of SO?
- 5) Which peptidase mediates processing of SO in the mitochondrial IMS?

In the second part of this study, the cellular maturation of mARC1 was investigated. Considering its recent discovery, a number of fundamental questions have remained unexplored so far:

- 1) Which mitochondrial sub-compartment is mARC1 residing in?
- 2) How is mARC1 targeted to mitochondria and which of the five import pathways does it follow?
- 3) What is the role of Moco for the mitochondrial localization of mARC1?
- 4) What are the characteristics and requirements of the mitochondrial import of mARC1?
- 5) What are similarities and differences between the mitochondrial maturation of SO and mARC1?

## **2 Results**

### **2.1 Assembly and maturation of mammalian SO**

The cellular assembly of SO starting with the cytosolic synthesis of the polypeptide chain all the way to the fully functional mitochondrial enzyme implies a complex network of several maturation steps. To fulfill its enzymatic activity, SO requires the integration of a cytochrome *b<sub>5</sub>* type heme cofactor into the N-terminal part of the protein, the integration of Moco into the central domain, homodimerization mediated by the C-termini and the translocation from the cytosol to the mitochondrial IMS, accompanied by processing of the first 80 residues (Kisker et al., 1997). All these processes have to be precisely regulated and spatially as well as temporally coordinated in order to ensure an efficient maturation of the enzyme. In particular, the stabilization of Moco upon its cytosolic synthesis until its integration into SO remained ambiguous, as Moco is known to be a very unstable molecule in a protein-free environment (Schwarz and Mendel, 2006). In this respect, Moco was expected to require an immediate association with the respective apo-proteins to achieve its stabilization (Schwarz et al., 2009). However, cytosolic folding of SO after Moco integration would interfere with the properties of the so far known mitochondrial import machinery. Thus, the first part of this study was supposed to uncover the cellular organization of the overall SO assembly process with a particular focus on the integration of Moco into SO and the mitochondrial transport of both components.

#### **2.1.1 Amplification, purification and characterization of mouse SO**

SO variants from different mammalian species are well conserved but slightly differ in their N-terminal domains (Figure 2.1), which represent the mitochondrial targeting sequence of the proteins. As confirmed by *in silico* prediction tools (Claros and Vincens, 1996, Kall et al., 2004), these differences in the primary structure do however not significantly influence the chemical properties of this domain, suggesting similar mechanisms for the cellular maturation and mitochondrial transport of all mammalian SO variants. Therefore, mouse SO was exemplarily chosen as a representative for mammalian SO in the current study.

After successful amplification of the SO coding sequence from a mouse cDNA library, SO was first characterized *in vitro* prior to the *in vivo* analysis of the SO maturation process. For this purpose, the SO coding sequence was cloned into the pQE80 expression vector for heterologous expression of the protein in *Escherichia coli* (*E. coli*). The full-length SO protein

contains a hydrophobic stretch of about 20 residues in the N-terminal part of the protein, which revealed to interfere with an efficient expression and purification from *E. coli*.

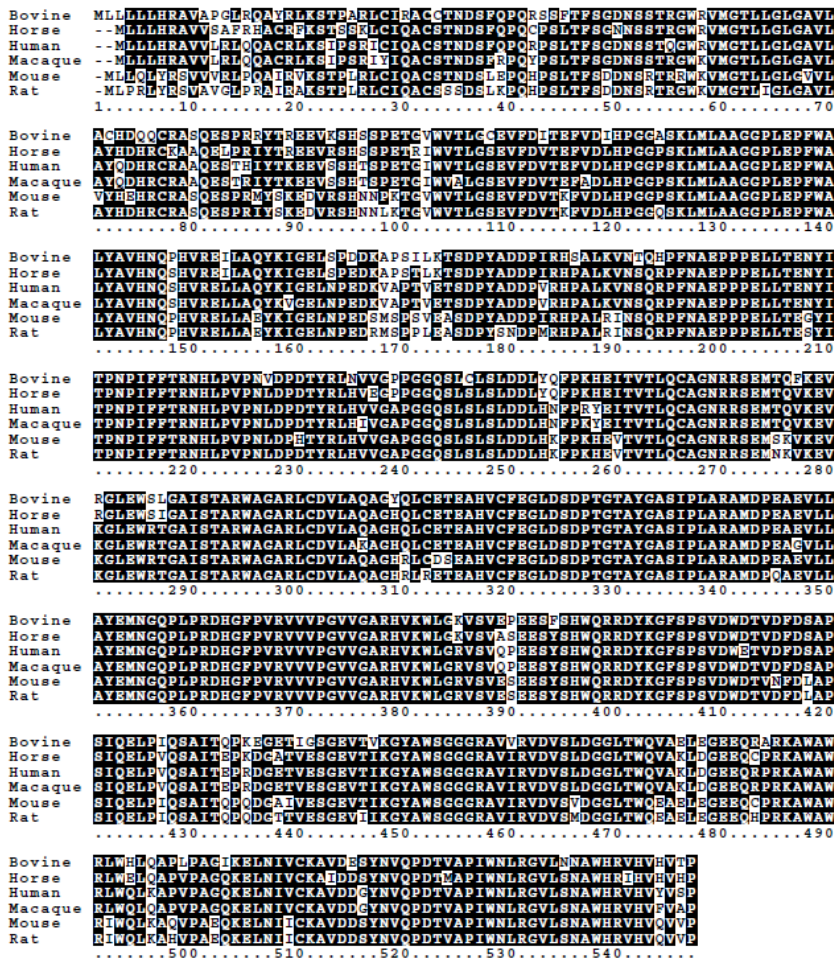


**Figure 2.1 Multiple sequence alignment of mammalian SO variants.** Alignment of mammalian SO sequences was conducted with CLUSTALW and images were generated with Boxshade. Residues are framed in black (high conservation), gray (moderate conservation) or white (no conservation). Protein accession numbers: NP\_001029538 (Bovine SO), XP\_001491902 (Horse SO), NP\_000447 (Human SO), BAD51985 (Macaque SO), NP\_776094 (Mouse SO), NP\_112389 (Rat SO).

Since mature mammalian SO lacks its first 80 residues including the hydrophobic stretch following mitochondrial processing (Kisker et al., 1997), a truncated variant of SO representing the mature protein was purified from *E. coli*. This protein variant was expressed at high yields and could be enriched to purity by means of sequential Ni-NTA affinity chromatography and anion-exchange chromatography (Figure 2.2 A). Expression was carried out in *E. coli* strain TP1000, which is able to synthesize the eukaryotic form of Moco (Palmer et al., 1996), while WT-*E. coli* mainly produces a nucleotide modified form of the cofactor. The enzymatic activity of SO requires efficient homodimerization, as monomeric mutant variants have been shown to be catalytically inactive (Wilson et al., 2006). The

oligomerization of purified SO was analyzed by means of HPLC based size exclusion chromatography, revealing the expected distribution of a major dimeric and a minor monomeric population of the protein (Figure 2.2 B, blue trace). Apart from the protein derived absorption at 280 nm, the heme cofactor mediated absorption at 413 nm was recorded during chromatography to assess the integration of the heme cofactor into SO. As the absorption of the protein at 413 nm closely followed its absorption at 280 nm, efficient heme cofactor integration into SO was observed (Figure 2.2 B, red trace). Next, the incorporation of Moco into purified SO was determined by HPLC-mediated detection of the Moco derivative FormA-dephospho. SO expressed from *E. coli* strain BL21, which does not accumulate the eukaryotic form of Moco, was supposed to deliver significantly less FormA-dephospho and was used as a negative control within the assay. The analysis revealed an approximately 40% Moco saturation of SO expressed from *E. coli* TP1000, while SO expressed from strain BL21 showed less than 10% Moco integration (Figure 2.2 C). These results are in line with values reported for other Moco proteins (Fischer et al., 2006b, Gruenewald et al., 2008).

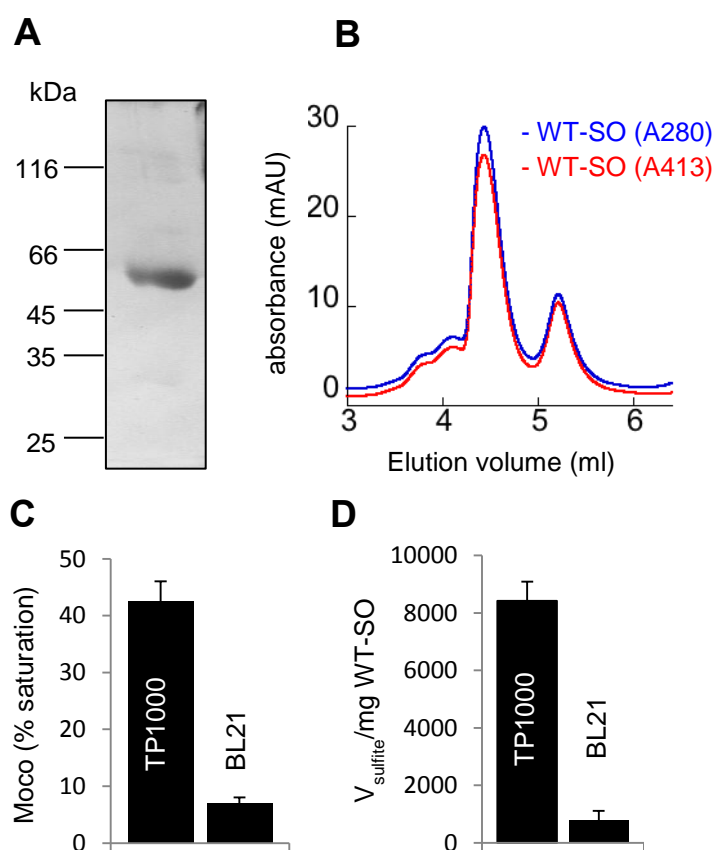


**Figure 2.2 Purification and characterization of MSO expressed in *E. coli*.** (A) SO was expressed in *E. coli* strain TP1000 for 48 h at room temperature and purified by sequential Ni-NTA and anion-exchange chromatography. Purity of SO preparation was assessed by 12% SDS-PAGE and subsequent coomassie blue staining. (B) Oligomerization of purified SO was determined by HPLC based size exclusion chromatography. Absorptions were measured at 280 nm (blue traces) and 413 nm (red traces). (C) Moco saturation of 100 pmol SO expressed from *E. coli* strains TP1000 and BL21, respectively, was determined by HPLC mediated detection of the fluorescent Moco derivative FormA. Error bars represent standard deviations (n=3). (D) Activities of purified SO variants from *E. coli* strains TP1000 and BL21 were determined by means of the sulfite:cytochrome *c* SO assay. Depicted are velocities of sulfite oxidation per mg SO within the reaction well. Error bars represent standard deviations (n=3).

The homodimerization as well as the integration of heme and Moco resulted in a catalytically active enzyme, which was finally determined by means of an *in vitro* SO activity-assay using cytochrome *c* as the final electron acceptor (Figure 2.2 D). The determined values of SO

activity are thereby consistent with SO activities described in the literature (Garrett et al., 1998)

### 2.1.2 Moco dependent mitochondrial localization of SO

The steps of SO maturation described in chapter 2.1.1 result in an active enzyme *in vitro*. The assembly however becomes more complex *in vivo*, where both SO and Moco additionally require a coordinated translocation to mitochondria after their cytosolic synthesis, a process which was not understood so far. Premature integration of Moco into SO within the cytosol and the concomitant folding would interfere with mitochondrial transport of the complex, as only unfolded proteins can enter mitochondria across the TOM and TIM complexes (Neupert and Herrmann, 2007). On the other hand, Moco has been shown to be a very unstable molecule if not associated to the protective environment of a protein, suggesting an immediate association of SO and Moco in the cytosol (Schwarz and Mendel, 2006).

To address this conflict and to identify possible mutual impacts of SO and Moco for their mitochondrial translocation, SO was transiently expressed in WT and Moco-deficient human fibroblasts. Immunostaining using an SO specific antibody (Figure 2.3 A) revealed the expected exclusive mitochondrial localization in WT fibroblasts, as demonstrated by the complete colocalization of SO and mitochondria stained with Mitotracker Red (Figure 2.3 B). To analyze the cellular distribution of SO in absence of Moco, SO was expressed in human fibroblasts with a mutation in the *MOCS1* gene. The *MOCS1* proteins catalyze the first step of the Moco synthesis pathway by converting GTP to cPMP in mammals (Hanzelmann et al., 2002), suggesting that *MOCS1*-deficient fibroblasts do not contain substantial amounts of Moco. While WT fibroblasts significantly reconstituted the Moco-deficient nitrate reductase in the *nit-1* assay, *MOCS1*-deficient fibroblasts did not deliver any considerable amounts of Moco (Figure 2.3 C). Surprisingly, expression of SO in the latter Moco-deficient fibroblasts revealed a diffuse distribution throughout the entire cell body with no clear mitochondrial localization left (Figure 2.3 D). No nuclear exclusion of the SO staining was observed, which would point to an apparent size of less than 60 kDa as seen for other proteins that are able to passively enter the nucleus (Nigg, 1997).

To confirm that Moco binding to SO is required for the mitochondrial targeting of the enzyme, a mutant variant of SO was designed, which should not be able to bind Moco. In a report listing several cases of isolated SO deficiency, two mutations in the Moco binding domain of human SO were described. (Johnson et al., 2002). The first mutation affected



Arg309, which is involved in the binding of Moco by forming salt bridges with the phosphate of the pterin (Kisker et al., 1997).

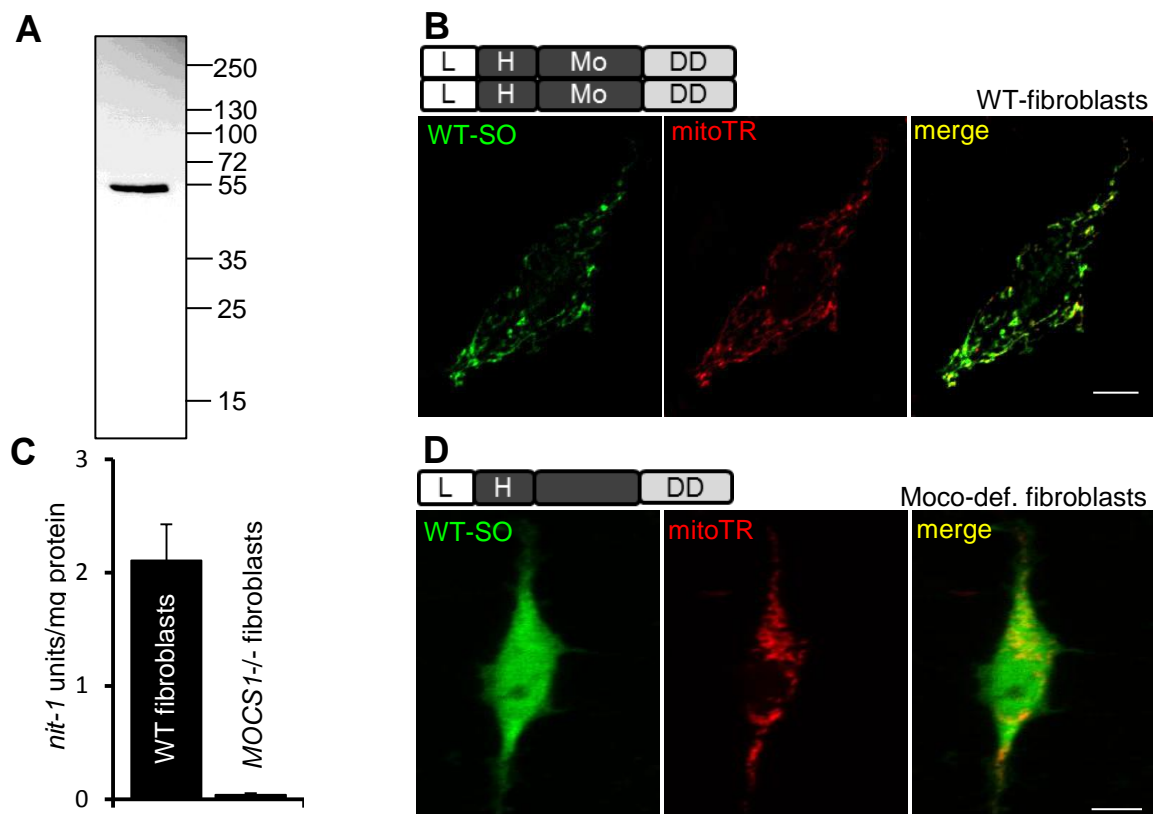


**Figure 2.3 Moco dependent localization of SO.** (A) SO was expressed in HEK-293 cells and total protein extract was loaded on a 12% SDS gel. Specificity of the SO-antibody was determined by Western blot. (B, D) SO was expressed for 48 h and detected by anti-SO immunostaining (green) using confocal laser scanning microscopy. Mitochondria were stained with Mitotracker Red CMXRos (mitoTR). Bar, 10 μm. Cartoons illustrate the status of cofactor insertion and oligomerization: L, leader sequence; H, heme; Mo, Moco; DD, dimerization domain. (C) Moco content of WT and MOCS1-deficient fibroblasts was determined by the *nit-1* assay. The depicted values represent an average of the *nit-1* activities expressed as units per mg total protein. Error bars represent standard deviations (n=3).

The described mutation to histidine at this position was proposed to prevent these hydrogen bond formations and to sterically interfere with surrounding residues. The second mutation involved Lys322, which binds the N1 as well as the 2-amino group of the pterin and also forms a salt bridge to the phosphate. A mutation to arginine was proposed to cause sterical problems in response to the larger side chain of arginine compared to lysine. Both mutations, R309H as well as K322R, resulted in a disease phenotype of the affected patients, suggesting that the activity of SO was disrupted and the integration of Moco might not have occurred in response to the structural problems outlined above (Johnson et al., 2002).

Given that the above mentioned mutant variants were not further characterized biochemically, the corresponding double mutation was introduced into mouse SO and the respective variant (SO-R367H-K380R) was characterized on cofactor integration and oligomerization in this study. SO-R367H-K380R was expressed in *E. coli* strain TP1000 from pQE80 and purified by sequential Ni-NTA and anion exchange chromatography (Figure 2.4 A). To determine the degree of Moco integration in the mutant variant, HPLC-based FormA analyses were conducted. While WT-SO was saturated with at least 40% cofactor, SO-R367H-K380R did not contain any significant amounts of Moco, demonstrating that mutations R367H and K380R as expected collectively interfere with efficient Moco integration into SO (Figure 2.4 B). Before analyzing the localization of the Moco-deficient SO variant, the status of oligomerization and heme cofactor integration was determined by size exclusion chromatography. While heme cofactor incorporation was unaffected as illustrated by the similar absorptions at 280 nm and 413 nm, the oligomerization behavior changed because SO-R367H-K380R mainly eluted as a monomer (Figure 2.4 C). These observations indicate that the integration of Moco into SO is a prerequisite for efficient homodimerization.

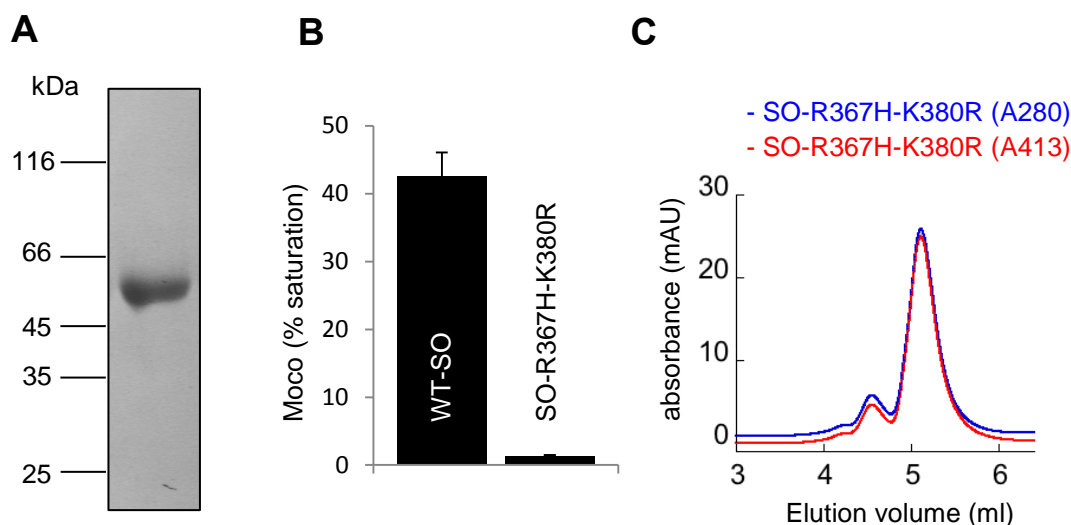


**Figure 2.4 Characterization of a Moco-deficient mutant variant of SO.** (A) SO-R367H-K380R was expressed in *E. coli* strain TP1000 for 48 h at room temperature. Purification occurred by sequential Ni-NTA and anion exchange chromatography. Purity was assessed by 12% SDS-PAGE and subsequent coomassie blue staining. (B) Moco content of 100 pmol WT-SO and SO-R367H-K380R was analyzed by HPLC mediated FormA analysis. Error bars represent standard deviations (n=3). (C) Oligomerization of purified SO-R367H-K380R was determined by HPLC based size exclusion chromatography. Absorptions were measured at 280 nm (blue traces) and 413 nm (red traces).

In order to confirm the importance of Moco for the sub-cellular localization of SO, the distribution of SO-R367H-K380R was analyzed in WT-HEK-293 cells by

immunocytochemistry. WT-SO exclusively localized to mitochondria (Figure 2.5 A), while SO-R367H-K380R was diffusely distributed within the cell (Figure 2.5 B), as previously seen for WT-SO in Moco-deficient cells. To quantitatively assess the degree of colocalization of SO and mitochondria and thus to figure out if a minor pool of SO may still be present in mitochondria in absence of Moco, the Pearson correlation coefficients (PCC) were determined. The PCC expresses full (100%) colocalization with a number of +1, while separate (excluding) localization is classified by -1. Consequently, zero represents a fully random, non-correlated distribution. (Manders et al., 1992).

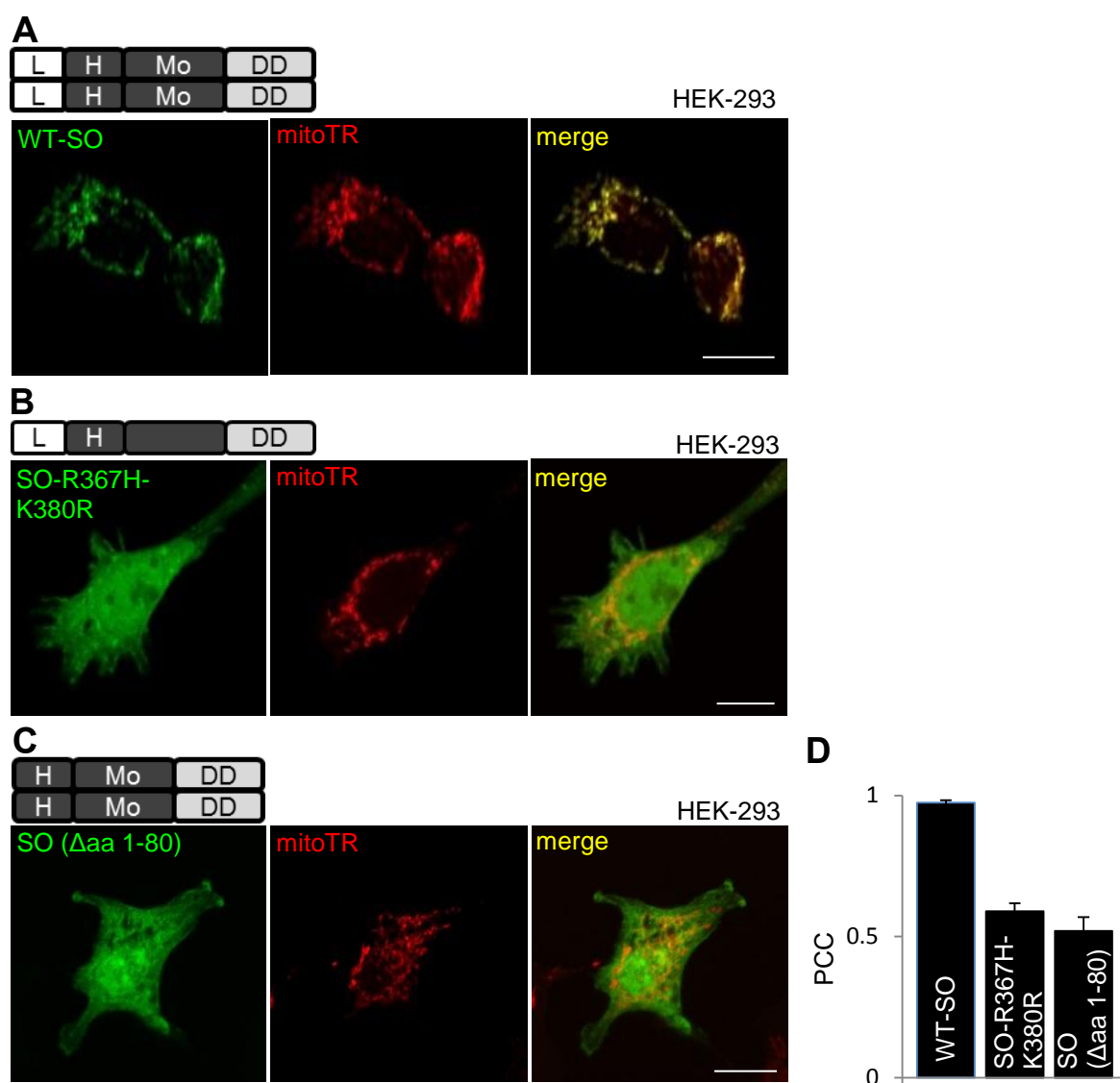


**Figure 2.5 Cellular distribution of Moco-deficient SO.** (A) WT-SO, (B) SO-R367H-K380R and (C) SO ( $\Delta$ aa 1-80) were expressed in HEK-293 cells for 48 h and detected by anti-SO immunostaining (green) using confocal laser scanning microscopy. Mitochondria were stained with Mitotracker Red CMXRos (mitoTR). Bar, 10  $\mu$ m. Cartoons illustrate the status of cofactor insertion and oligomerization: L, leader sequence; H, heme; Mo, Moco; DD, dimerization domain. (D) Pearson correlation coefficients were determined by means of the Perkin Elmers VOLOCITY software. Error bars represent standard deviations (n=5).

Under WT conditions, SO and mitochondria showed an expected average PCC of +0.97 (Figure 2.5 D, left panel). For SO-R367H-K380R, an average PCC value of +0.59 was determined (Figure 2.5 D, middle panel). As a negative control, a cytosolic variant of SO lacking residues 1-80 was used (Figure 2.5 C) and revealed an average PCC of +0.52 (Figure 2.5 D, right panel), indicating that the theoretically expected reading of “0” is not reached. Therefore, the recorded PCC values for Moco-deficient SO are in well agreement with the negative control.

The determination of the PCC values confirmed the obvious mislocalization of SO in absence of Moco, but could not quantitatively express if any pool of Moco-deficient SO is present in mitochondria. The negative control, SO lacking its N-terminal mitochondrial targeting sequence, was not present in mitochondria but still revealed a certain degree of colocalization with mitochondria, as mitochondrial areas were not clearly excluded from the antibody staining (Figure 2.5 C). Thus, a minor mitochondrial localization was difficult to be identified and to be distinguished from a non-mitochondrial distribution by immunocytochemistry.

To more precisely characterize the distribution of SO-R367H-K380R in the cell, the latter variant as well as WT-SO, each containing a C-terminal myc –tag, were expressed in HEK-293 cells for 48 h. Subsequently, mitochondrial and cytosolic fractions were separated by discontinuous density gradient centrifugation and SO variants were detected in both fractions by anti-myc Western blotting. Both fractions were efficiently separated, as demonstrated by the specific distribution of the marker proteins VDAC and gephyrin in mitochondrial and cytosolic fractions, respectively (Figure 2.6 A). Consistent with the localization data, WT-SO was exclusively detected in the mitochondrial fraction, while SO-R367H-K380R was mainly present in the cytosolic pool (Figure 2.6 A). The Moco-deficient variant of SO was however also detected in the mitochondrial fraction, finally demonstrating that the depletion of Moco did not completely prevent the mitochondrial targeting of SO, but that Moco is required for an efficient localization of SO to mitochondria. Quantification of band intensities revealed 100% localization of WT-SO in mitochondria (given that no signal was found in the cytosolic fraction), while only 30% of the Moco-deficient variant was found to be mitochondrial and 70% remained in the cytosol. This distribution was also confirmed by the application of Proteinase K (PK) to whole cell extracts after expression of WT and Moco-deficient SO variants, respectively. The sensitivity to PK was used as an alternative illustration of differential holo- and apo-SO distribution, since cytosolic proteins should be susceptible to proteolytic digestion, while mitochondrial proteins were expected to be protected from PK accessibility.

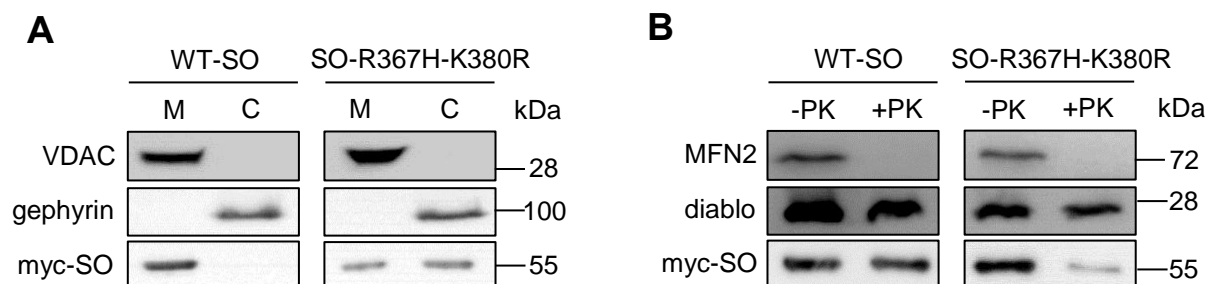


**Figure 2.6 Western blot analysis of Moco dependent distribution of SO.** (A) WT and SO-R367H-K380R were expressed in HEK-293 cells for 48 h. Cytosolic (lane C) and mitochondrial fractions (lane M) were separated from each other and total amounts of protein were determined in both fractions. Representative amounts of mitochondrial and cytosolic protein were loaded on a 12% SDS gel. VDAC and gephyrin were used as mitochondrial and cytosolic markers, respectively. Myc-tagged SO was stained using anti-myc antibodies. Similar results were obtained in three independent experiments. (B) WT-SO and SO-R367H-K380R were expressed in HEK-293 cells for 48 h. Whole cell extracts were treated with or without PK and loaded on a 12% SDS gel. MFN2 (mitochondrial outer membrane marker) and diablo (IMS marker) were detected as control proteins, SO variants were detected via their C-terminal myc-tags.

Indeed, the outer mitochondrial membrane protein MFN2 was susceptible to PK, as a large domain of the protein is exposed to the cytosol (Figure 2.6 B). In contrast, the IMS protein diablo was mainly protected from digestion. Consistent with the previous experiments outlined above, WT-SO was almost completely protected from PK, while SO-R367H-K380R was susceptible to PK-mediated hydrolysis and only a minor fraction was stabilized due to its mitochondrial localization (Figure 2.6 B).

Altogether, cellular and biochemical localization studies independently pointed out that SO requires the integration of Moco for an efficient mitochondrial localization, whereas the mechanism of Moco-dependent targeting of SO to mitochondria remained to be elucidated.

### 2.1.3 Mitochondrial import of SO

The cytosolic localization of SO in absence of Moco appeared to be unexpected, since SO contains a predicted mitochondrial targeting signal at its N-terminus (92.6% according to MitoProt II), which should be sufficient for the mitochondrial localization of a protein. To confirm that SO indeed contains an N-terminal mitochondrial targeting signal and to investigate if the impact of Moco for the localization of SO is related to this domain, the first 80 residues of SO were fused to GFP and expressed in WT and Moco-deficient fibroblasts. In both cases, GFP was efficiently targeted to mitochondria, confirming that SO in fact

contains an intrinsic and functional mitochondrial targeting signal, which functions independently of Moco (Figure 2.7 A, B).

Because the targeting signal of SO was able to localize GFP to mitochondria efficiently and independently from the presence or absence of Moco, the question arose of why SO and not GFP requires Moco for its mitochondrial localization. To unravel the underlying mechanisms of this coherency, the impact of Moco on the mitochondrial import of SO was first analyzed, as the diffuse distribution of SO in absence of Moco may result from an impaired import to mitochondria. The targeting signal of SO is not present in the mature protein (Kisker et al., 1997) and, as other known N-terminal mitochondrial targeting peptides, cleaved following mitochondrial import (Ono and Ito, 1984). This cleavage was expected to result in a shift of the electrophoretic mobility, serving as a marker for successful import of the protein to mitochondria.

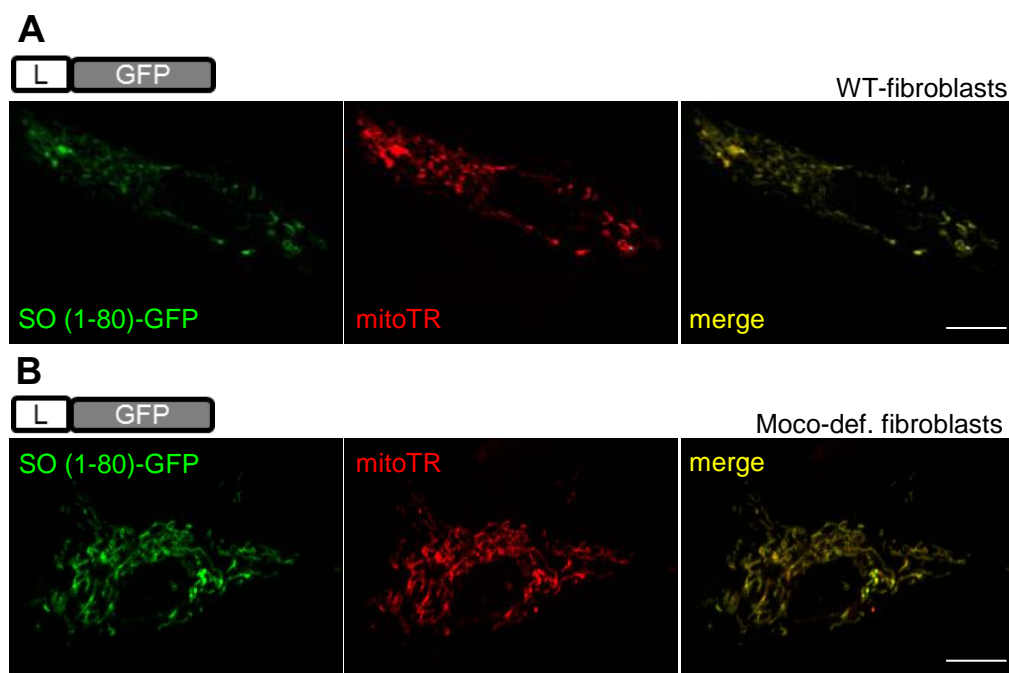


**Figure 2.7 SO contains an N-terminal mitochondrial targeting signal.** The SO leader sequence (L, residues 1-80) was fused to GFP and expressed in (A) WT or (B) MOCS1-deficient fibroblasts for 48 h. Mitochondria were stained with Mitotracker Red CMXRos (mitoTR). Bar, 10  $\mu$ m.

Therefore, WT-SO as well as the Moco-deficient SO-R367H-K380R variant was expressed in HEK-293 cells, while the unprocessed full-length variant was expressed in *E. coli* and subsequently purified. Western blotting against the C-terminal myc-tag revealed a similar molecular weight of both, the WT and the Moco-deficient variant of SO, each being detected at the same apparent size of approximately 53 kDa. This band size was clearly below the size of full-length, non-processed SO, suggesting that in HEK-293 cells, both

variants, WT-SO and SO-R367H-K380R, were processed in the same manner (Figure 2.8). Consequently, the primary mitochondrial import of SO and the subsequent cleavage of the mitochondrial targeting sequence are not dependent on the presence of Moco and occur efficiently in a Moco-deficient background.



**Figure 2.8 Moco independent mitochondrial processing of SO.** WT-SO and SO-R367H-K380R were expressed in HEK-293 cells for 48 h and cell extracts were loaded on an 8% SDS gel. As control, myc-tagged, full-length SO was expressed in *E. coli* strain TP1000. Proteins were detected by Western blot using anti-myc primary antibodies.

Ono and Ito (1984) reported an ATP- and membrane potential-dependent import of SO into mitochondria through the TOM and TIM machineries, while the involved peptidases and thus the import mechanism remained uncharacterized. Mature mouse SO lacks the first 80 residues and contains a predicted matrix processing peptidase (MPP) cleavage site at position 19 of the precursor form (Claros and Vincens, 1996). The remaining part of the leader sequence contains a predicted, hydrophobic transmembrane stretch at position 56-72 (Kyte and Doolittle, 1982). This signal sequence structurally resembles the mitochondrial targeting motifs of *S. cerevisiae* cytochrome  $b_2$  and the mammalian diablo protein (Figure 2.9 A). Both proteins have been shown to be imported based on bipartite mitochondrial targeting signals and processed by the inner membrane peptidase (IMP) complex (Glick et al., 1993, Burri et al., 2005), a hetero-oligomer composed of the two catalytic subunits IMP1 and IMP2 and a third non-catalytic subunit involved in substrate recognition. Deletion of any of the two catalytic subunits destabilizes and silences the complex activity (Nunnari et al., 1993, Gakh et al., 2002). In respect to the topological similarities of the N-terminal pre-sequences of SO compared to cytochrome  $b_2$  and diablo, the question arose if the IMP complex may also process SO.

Thus, the human IMP1 protein was knocked down by shRNA in HEK-293 cells. For this purpose, sense and antisense shRNA strands complementary to an appropriate region (according to predictions of the Invitrogen shRNA tool) of the human *IMP1* coding sequence were designed and each cloned into the pJET1.2 vector in fusion with the CMV promoter. Following transfection of sense and antisense shRNA-encoding plasmids into HEK-293 cells, the effects on processing of co-transfected, myc-tagged SO were examined. Significant knockdown of IMP1 was confirmed by Western blot, revealing only 20 % residual expression

after shRNA treatment (Figure 2.9 B). The decreased IMP levels resulted in the appearance of an additional band for endogenous diablo, representing the unprocessed precursor form in the positive control. SO of untreated cells appeared to be completely processed, while the shRNA-mediated IMP1 knockdown resulted in an additional accumulation of unprocessed SO (Figure 2.9 B). These data suggest that the IMP complex processes SO in the mitochondrial IMS to release it as a soluble protein.

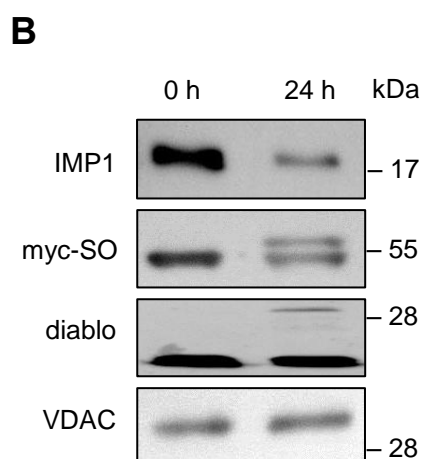
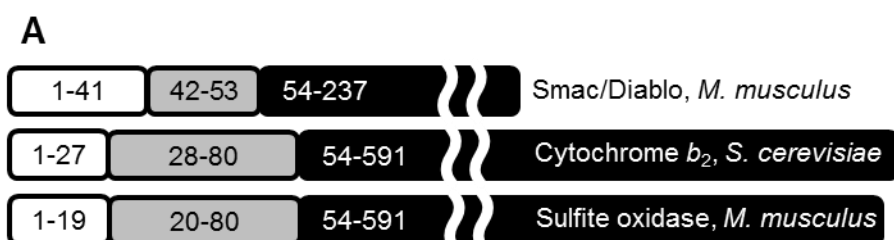


**Figure 2.9 Processing of SO by the IMP complex.**

(A) Structural comparison of Smac/Diablo (*M. musculus*), cytochrome  $b_2$  (*S. cerevisiae*) and SO (*M. musculus*). The first and last residues of matrix targeting peptide (white box), hydrophobic downstream region (light gray box) and mature protein (black box) are indicated. (B) Western blot analysis of SO (myc-SO), diablo, VDAC and IMP1 in response to IMP1 knockdown. Sense and antisense shRNA of *IMP1* as well as myc-tagged SO were co-expressed in HEK-293 cells for 0 and 24 h, respectively. Mitochondria were enriched by differential centrifugation and extracts were loaded on a 12% SDS gel.

#### 2.1.4 Retrograde translocation of SO to the cytosol in absence of Moco

Successful mitochondrial processing resulted in a truncated variant of WT- as well as of Moco-deficient SO-R367H-K380R. The primary mitochondrial import process of SO was thus not influenced by the presence or absence of Moco. However, a large SO proportion accumulated outside of mitochondria if Moco was not present. In respect to this conflict, the eventuality of a reverse translocation to the cytosol after mitochondrial import of Moco-deficient SO was investigated next. The TOM complex is known to allow bi-directional translocation of unfolded, small proteins (<20 kDa). For example, already imported Tim13 has been shown to re-enter the cytosol upon application of chelators that remove zinc ions required for its folding (Lutz et al., 2003). The import of other small proteins is converted into a vectorial process by the formation of internal disulfide bonds, thus being trapped by folding



within the IMS (Chacinska et al., 2004). Therefore, SO may require Moco in a similar manner to adopt its folding and to thereby prevent a backwards translocation to the cytosol.

To test a possible retrograde translocation of Moco-free SO, a mutant variant of SO was designed, which cannot be proteolytically processed by the IMP complex and should therefore remain anchored at the inner mitochondrial membrane, thus preventing a potential reverse translocation. Because the exact IMP cleavage site was not known and obvious consensus motifs for IMP mediated processing were not found, the SO peptide sequence containing the expected cleavage site (residues 66-86) was exchanged against the topologically similar part of the TIM50 protein (Figure 2.10 A). TIM50 is a protein of the inner mitochondrial membrane and is not processed by IMP, but apart from this follows an import pathway similar to that proposed for SO (Mokranjac et al., 2003). First, the SO-TIM50 chimera was expressed in HEK-293 cells to investigate its susceptibility to processing by the IMP complex. Western blotting against the C-terminal myc-tag revealed the accumulation of unprocessed SO-TIM50, running at the same size as the unprocessed precursor synthesized in *E. coli* (Figure 2.10 B). Therefore, the chimeric fusion prevented IMP-mediated processing of SO and its full release into the IMS, but caused a permanent association of SO with the inner mitochondrial membrane.

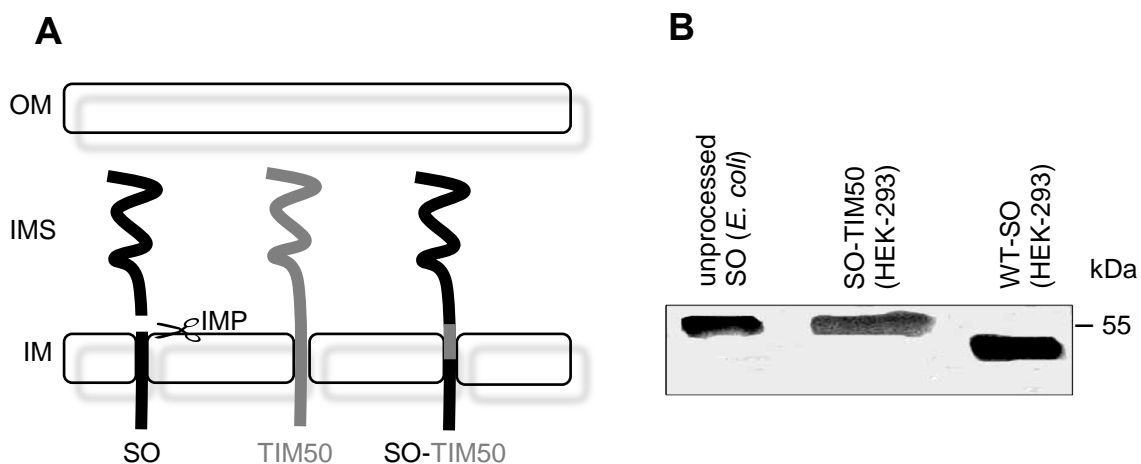


**Figure 2.10 Design of an unprocessed SO-TIM50 chimera.** (A) Scheme of the proposed import mechanism of SO and the known mechanism of TIM50 transport to mitochondria. To avoid cleavage and release of soluble SO in the IMS, the region containing the putative IMP cleavage site in SO (residues 64-84) was exchanged against the analogous part of TIM50 (residues 66-86), thus creating an SO-TIM50 chimera. (B) SO-TIM50 chimera and WT-SO were expressed in HEK-293 cells and enriched mitochondria were loaded on a 10% SDS gel to detect SO by anti-myc Western blot. The increased size of SO-TIM50 correlates well with the size of the unprocessed SO derived from *E. coli* TP1000.

Before analyzing the impact of Moco on the cellular distribution of this variant, its proper enzymatic activity had to be ensured to confirm the chimeric fusion did not interfere with the overall structure and folding of SO. For this purpose, WT-SO and SO-TIM50 were expressed in HEK-293 cells and SO enzymatic activities of whole cell extracts were determined in comparison to non-transfected cells. Both, WT and chimeric SO revealed a similar increase in SO activity compared to the control, demonstrating that the exchange of the respective region did not critically influence the overall structure of the protein (Figure 2.11).

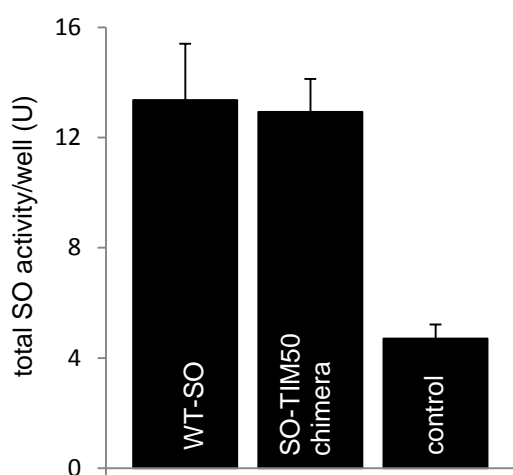


**Figure 2.11 Similar enzymatic activities of WT-SO and SO-TIM50.** WT-SO and SO-TIM50 chimera were expressed in HEK-293 cells and SO activities in crude proteins extracts were determined using the sulfite:cytochrome c SO assay. The depicted values correspond to the total activity of SO in the cuvette (10  $\mu$ g protein extract). As a control, non-transfected HEK-293 cell extracts were used representing the intrinsic activity of HEK293 cell SO. Error bars represent standard deviations (n=3).

Upon verifying membrane anchoring and full enzymatic activity of SO-TIM50, the impact of Moco on the cellular localization was determined next. The chimera was expressed in Moco-deficient fibroblasts, in which WT-SO showed a diffuse cellular distribution and no clear mitochondrial localization (compare Figure 2.3 D). In contrast, prevention of processing and thus anchoring of the protein at the inner mitochondrial membrane resulted in a complete mitochondrial localization even in absence of Moco (Figure 2.12).

In conclusion, the necessity of Moco for the mitochondrial localization of SO can be overcome by artificial attachment of the protein to the inner mitochondrial membrane. Both, membrane attachment and cofactor integration can hence keep SO within mitochondria. Further, these findings suggest that SO undergoes a reverse translocation in absence of Moco and that Moco integration into SO initiates folding and thereby trapping of SO within mitochondria.

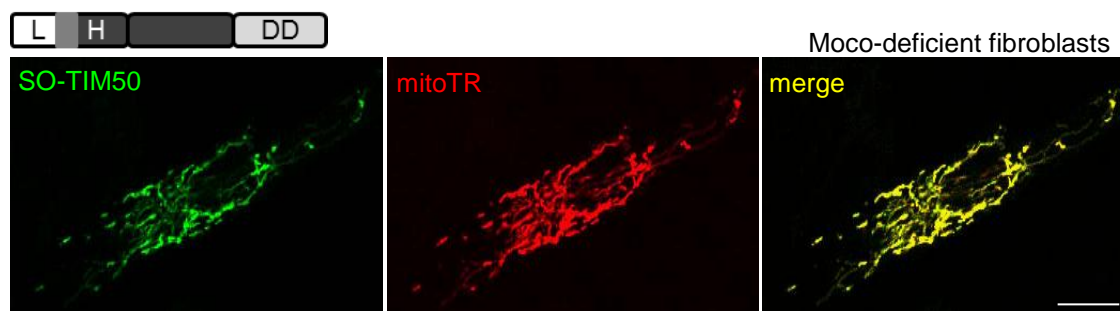


**Figure 2.12 Moco independent mitochondrial localization of SO-TIM50.** The SO-TIM50 chimera was expressed in Moco-deficient fibroblasts for 48 h and visualized by anti-SO immunostaining (green) using confocal laser scanning microscopy. Mitochondria were stained with Mitotracker Red CMXRos (mitoTR). Bar, 10  $\mu$ m. Cartoon illustrates the status of cofactor saturation and oligomerization: L, leader sequence; H, heme; DD, dimerization domain. The chimeric TIM50 sequence is illustrated in gray.

The data outlined above suggested a mechanism for the mitochondrial translocation of SO similar to Tim13 and other small proteins of the IMS. However, with a molecular weight of about 50 kDa as a monomer, SO appeared considerably larger than the small IMS proteins, which follow a folding-trap mechanism of maturation. Therefore, a retrograde movement of SO through the TOM complex after complete import seemed unlikely. Apart from small proteins of the IMS, a reverse translocation to the cytosol has been described for 55 kDa fumarase. This protein ensures its dual cytosolic and mitochondrial localization by reentering the cytosol after a partial translocation across the outer mitochondrial membrane (Knox et al., 1998, Sass et al., 2001). In contrast to small IMS proteins, fumarase does not completely cross the TOM complex before reverse translocation occurs, but keeps its C-terminus exposed to the cytosol, until folding of the latter domain triggers reverse translocation (Knox et al., 1998).

In this respect, the question arose if SO completes its translocation across the outer mitochondrial membrane via the TOM complex in absence of Moco or if Moco integration may be required as an additional driving force to “pull” the protein entirely into the mitochondrial IMS. To address this issue, SO-TIM50 as well as the Moco-deficient variant SO-TIM50-R367H-K380R, each labeled with a C-terminal myc-tag, were expressed in HEK-293 cells. Likewise WT-SO-TIM50 in Moco-deficient cells, the Moco-deficient chimera was efficiently targeted to mitochondria in WT cells (Figure 2.13 A). To assess if the C-terminal myc-tag of SO-TIM50-R367H-K380R remained exposed to the cytosol or if translocation was completed, mitochondria were enriched by differential centrifugation and exposed to PK treatment. All peptide sequences outside of mitochondria, including the C-terminal myc-tag, were thereby supposed to be hydrolyzed. While diablo (IMS control) levels remained

unaffected following PK application, the cytosolic protein gephyrin became entirely hydrolyzed (Figure 2.13 B).

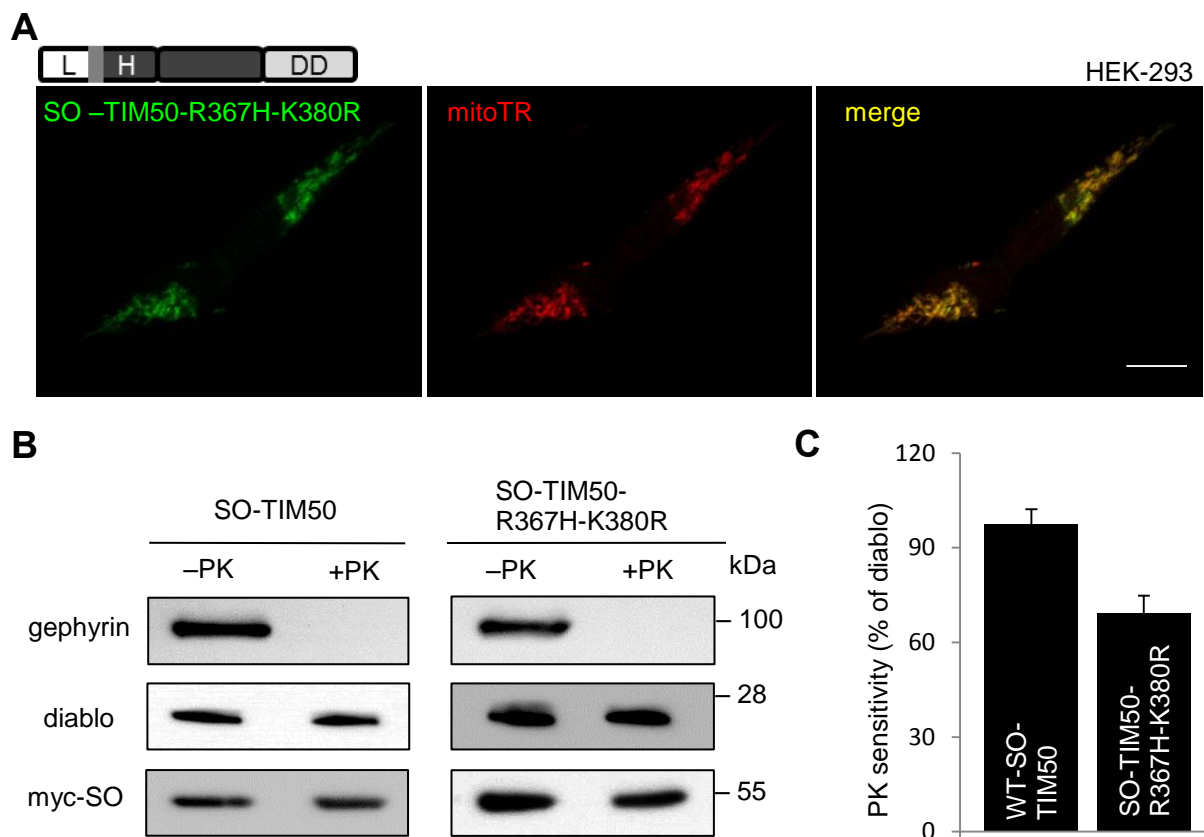


**Figure 2.13 Moco “pulls” SO across the outer mitochondrial membrane. (A)** SO-TIM50-R367H-K380R was expressed in HEK-293 cells for 48 h and visualized by anti-SO immunostaining (green) using confocal laser scanning microscopy. Mitochondria were stained with Mitotracker Red CMXRos (mitoTR). Bar, 10  $\mu$ m. Cartoon illustrates the status of cofactor saturation and oligomerization: L, leader sequence; H, heme; DD, dimerization domain. The chimeric TIM50 sequence is illustrated in gray. **(B)** SO-TIM50 and SO-TIM50-R367H-K380R, each containing a C-terminal myc-tag, were expressed in HEK-293 cells and mitochondria were subsequently enriched by differential centrifugation. After treatment with or without Proteinase K ( $\pm$ PK), extracts were loaded on a 10% SDS-gel and subsequently stained for diablo as a mitochondrial marker and for myc-SO, using Western blot with the respective antibodies. Efficient PK digestion was confirmed by anti-gephyrin Western blotting whole cell lysate. **(C)** Band intensities of SO-TIM50 and diablo upon PK treatment were each quantified relative to the respective untreated samples. The quotients of SO-TIM50 intensities were then determined in relation to those of diablo and depicted in the diagram. Error bars represent standard deviations (n=3).

WT-SO-TIM50 was protected from PK application, demonstrating an efficient translocation across the outer mitochondrial membrane. The depletion of Moco in contrast resulted in PK accessibility of about 30% of the myc-tagged C-termini (Figure 2.13 C). At first glance, this finding appeared divergent from figure 2.6 A, in which 70% of SO-R367H-K380R

were detected outside of mitochondria. However, anchoring of the SO-TIM50-R367H-K380R chimera at the inner mitochondrial membrane constituted an artificial driving force towards the IMS. Therefore, PK susceptibility of the Moco-deficient chimera was less strong as the cellular distribution of Moco-deficient SO would suggest.

In conclusion, the mitochondrial import of SO across the outer membrane is not efficiently completed in absence of Moco but arrested in the TOM complex, finally resulting in a reverse translocation of a major SO population to the cytosol.

### 2.1.5 The role of heme in the mitochondrial maturation of SO

Apart from Moco, mammalian SO requires a cytochrome  $b_5$  type heme as a second metal cofactor for its enzymatic activity (Kisker et al., 1997). The integration of heme cofactors results in folding of the respective domains and has also been shown to contribute to trapping of proteins in the IMS of mitochondria (Dumont et al., 1988, Esaki et al., 1999). Therefore, it was surprising that SO was not trapped in mitochondria when Moco was not present and that its localization was not rescued by heme integration (Figure 2.3 D, 2.5 B).

To analyze the role of heme for the mitochondrial localization of SO and to integrate this folding event into the overall maturation process, a heme-deficient mutant SO variant was designed next. In SO, the heme cofactor is not covalently attached, but is deeply buried in a hydrophobic cavity of the N-terminal domain and the iron is symmetrically coordinated by histidines 119 and 144 (Kisker et al., 1997). Since depletion of these histidines was expected to result in a loss of heme, both were exchanged against alanine using site-directed mutagenesis. The resulting SO-H119A-H144A variant was first expressed in *E. coli* strain TP1000 to analyze heme cofactor integration and the impact of the altered heme domain on Moco binding and SO oligomerization. Likewise WT- and Moco-deficient SO, SO-H119A-H144A was efficiently purified by Ni-NTA affinity- and anion exchange chromatography (Figure 2.14 A). Heme integration and oligomerization of the purified variant were determined by HPLC-based size exclusion chromatography. The marginal remaining heme specific absorption at 413 nm revealed that heme cofactor integration was indeed strongly reduced by the exchange of the coordinating histidines and demonstrated SO-H119A-H144A to be a heme-deficient variant of SO (Figure 2.14 B). In contrast to the primarily monomeric Moco-deficient SO variant, heme-deficient SO essentially eluted as a dimer, suggesting that heme integration is not a prerequisite for oligomerization of SO (Figure 2.14 B). As revealed by HPLC FormA analysis, Moco integration into SO-H119A-H144A occurred as efficient as into

WT-SO, confirming that binding of Moco to SO is not dependent on prior heme incorporation (Figure 2.14 C).

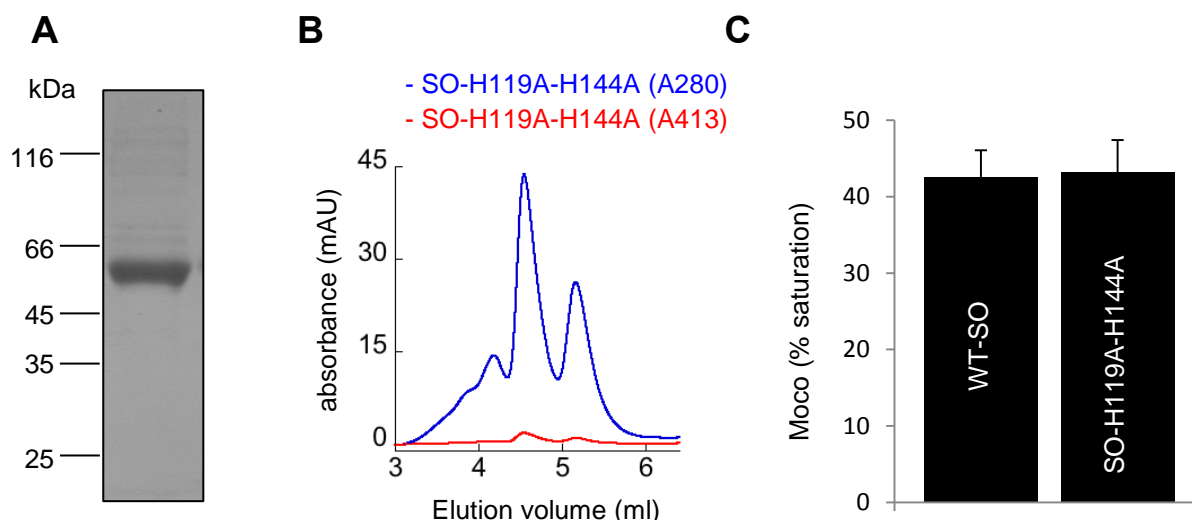


**Figure 2.14 Characterization of a heme deficient mutant variant of SO.** (A) SO-H119A-H144A was expressed in *E. coli* strain TP1000 for 48 h at room temperature. Purification occurred by sequential Ni-NTA and anion exchange chromatography. Purity was assessed by 12% SDS-PAGE and subsequent coomassie blue staining. (B) Oligomerization of purified SO-H119A-H144A was determined by HPLC based size exclusion chromatography. Absorptions were measured at 280 nm (blue traces) and 413 nm (red traces). (C) Moco content of 100 pmol WT-SO and SO-H119A-H144A was analyzed by HPLC FormA analysis. Error bars represent standard deviations (n=3).

To assess the significance of heme integration on mitochondrial localization of SO, the heme-deficient variant was expressed in HEK-293 cells. SO-H119A-H144A exclusively localized to mitochondria, suggesting that the heme cofactor is dispensable for mitochondrial trapping and that Moco, which was present in the latter variant, is not only essential but also sufficient for mitochondrial retention and localization of SO (Figure 2.15).

The mitochondrial localization of SO-H119A-H144A illustrated that heme incorporation and the accompanying folding of the respective domain is not essential for mitochondrial retention of SO, but that folding initiated by Moco integration was apparently sufficient. Still, the question remained why the presence of heme was not adequate to prevent the Moco-deficient SO variant from a reverse translocation to the cytosol. The integration of heme represents a folding event, which was shown to be involved in the transfer of cytochrome  $b_2$  across the outer mitochondrial membrane and its retention in the IMS (Esaki et al., 1999). Heterologous expression of SO-R367H-K380R in addition showed

that heme cofactor integration was not strictly dependent on Moco integration in *E. coli* (Figure 2.4 C).

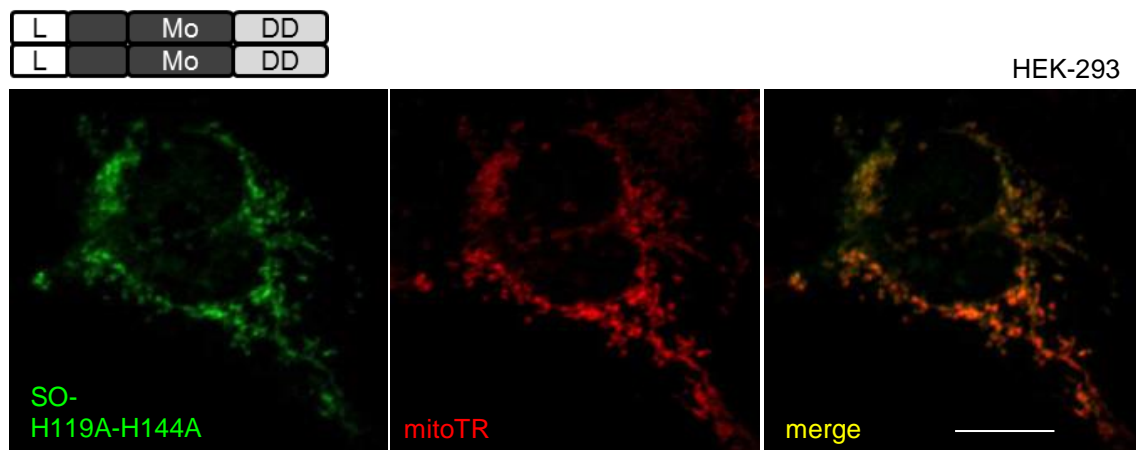


**Figure 2.15 Heme independent mitochondrial localization of SO.** SO-H119A-H144A was expressed in HEK-293 cells for 48 h and visualized by anti-SO immunostaining (green) using confocal laser scanning microscopy. Mitochondria were stained with Mitotracker Red CMXRos (mitoTR). Bar, 10  $\mu$ m. Cartoon illustrates the status of cofactor saturation and oligomerization: L, leader sequence; Mo, Moco; DD, dimerization domain.

The mitochondrial localization of SO-H119A-H144A illustrated that heme incorporation and the accompanying folding of the respective domain is not essential for mitochondrial retention of SO, but that folding initiated by Moco integration was apparently sufficient. Still, the question remained why the presence of heme was not adequate to prevent the Moco-deficient SO variant from a reverse translocation to the cytosol. The integration of heme represents a folding event, which was shown to be involved in the transfer of cytochrome  $b_2$  across the outer mitochondrial membrane and its retention in the IMS (Esaki et al., 1999). Heterologous expression of SO-R367H-K380R in addition showed that heme cofactor integration was not dependent on Moco integration in *E. coli* (Figure 2.4 C).

Therefore, the principle capability of the heme cofactor for trapping the SO-heme domain in the IMS was analyzed. To uncouple Moco insertion from heme integration, the isolated heme domains of WT- as well as of SO-H119A-H144A were expressed in HEK-293 cells. While the WT-heme domain localized to mitochondria (Figure 2.16 A), no clear mitochondrial localization, but rather a diffuse distribution within the entire cell body was observed for the heme-deficient heme domain (Figure 2.16 B). This finding suggests that in absence of heme, the heme domain is not folded and therefore it is able to move in a retrograde manner to the cytosol, as seen for full-length SO in absence of Moco.

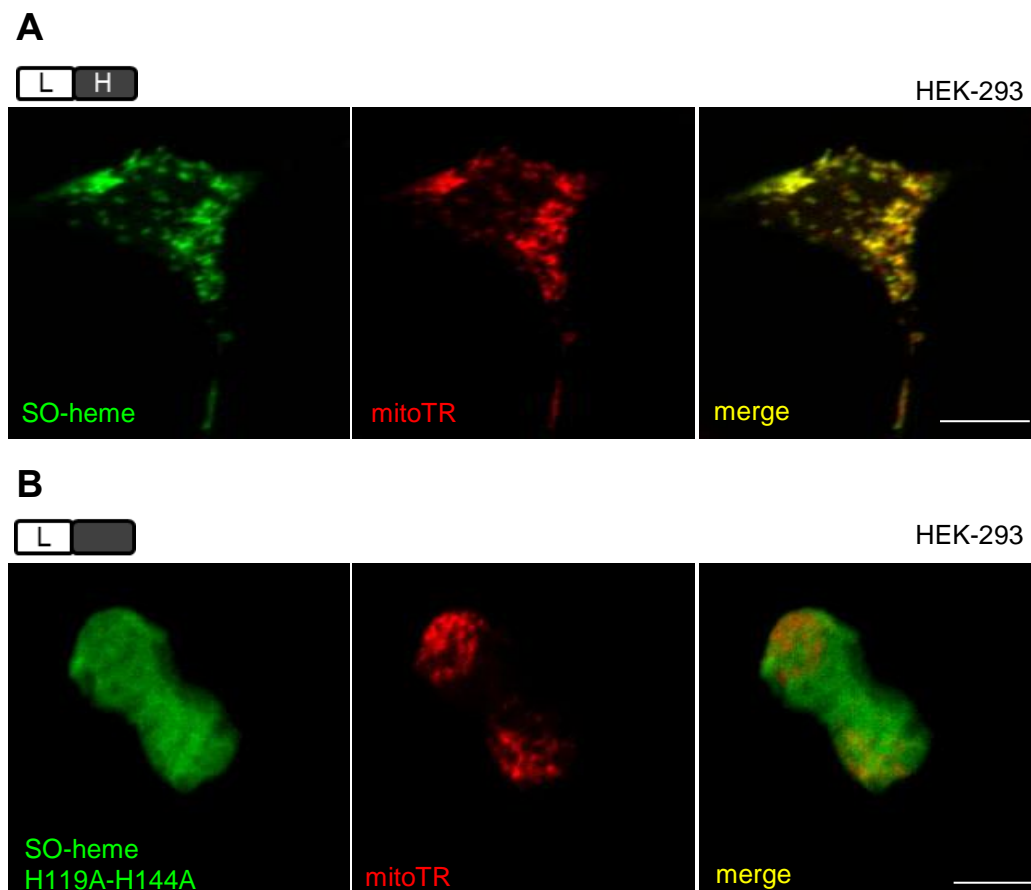


**Figure 2.16 Heme mediated trapping of the SO heme domain.** (A,B) WT-SO heme domain (A) and heme deficient SO-H119A-H144A heme domain (B) were expressed in HEK-293 cells for 48 h and visualized by anti-SO immunostaining (green) using confocal laser scanning microscopy. Mitochondria were stained with Mitotracker Red CMXRos (mitoTR). Bar, 10 μm. Cartoon illustrates the status of cofactor saturation and oligomerization: L, leader sequence; H, heme.

In conclusion, the heme cofactor is competent for trapping the SO heme domain in the IMS and following heme integration, reverse translocations from mitochondria to the cytosol can be prohibited. Because SO was not efficiently trapped in mitochondria in absence of Moco, the heme cofactor seems not to be integrated into SO sufficiently *in vivo*, pointing to a hierarchy of cofactor integration starting with Moco followed by heme insertion.

### 2.1.6 The impact of homodimerization on the mitochondrial maturation of SO

As a third event in the maturation of mammalian SO, homodimerization is required in addition to Moco and heme cofactor integration. Although not unequivocally shown in the literature so far, oligomerization events are conceivable to contribute to trapping mechanisms of mitochondrial IMS proteins. To position SO dimerization within the hierarchy of processes



that lead to SO maturation and to investigate the impact of dimerization on the mitochondrial localization of SO, a monomeric SO variant was created. This was of particular interest, given that Moco-deficient SO was shown to be monomeric too (Figure 2.4 C) and therefore the observed mislocalization of SO in absence of Moco could principally also reside from the monomeric nature of the resulting enzyme instead of the lack of Moco.

In mouse SO, glycine 531 is positioned in the dimerization interface of SO and a patient carrying a mutation leading to a replacement to aspartate at the respective site of the human enzyme suffered from isolated SO deficiency (Kisker et al., 1997). Consequently, this mutation was later confirmed to interfere with dimerization and to cause a predominately monomeric enzyme (Wilson et al., 2006). To examine the role of dimerization for the maturation of SO, glycine 531 was replaced by aspartate using site-directed mutagenesis and the respective SO variant was purified from *E. coli* by Ni-NTA affinity- and anion exchange chromatography (Figure 2.17 A). To verify the monomeric nature of the resulting SO-G531D variant and to investigate the status of heme integration, the purified protein was analyzed by HPLC-based size exclusion chromatography.

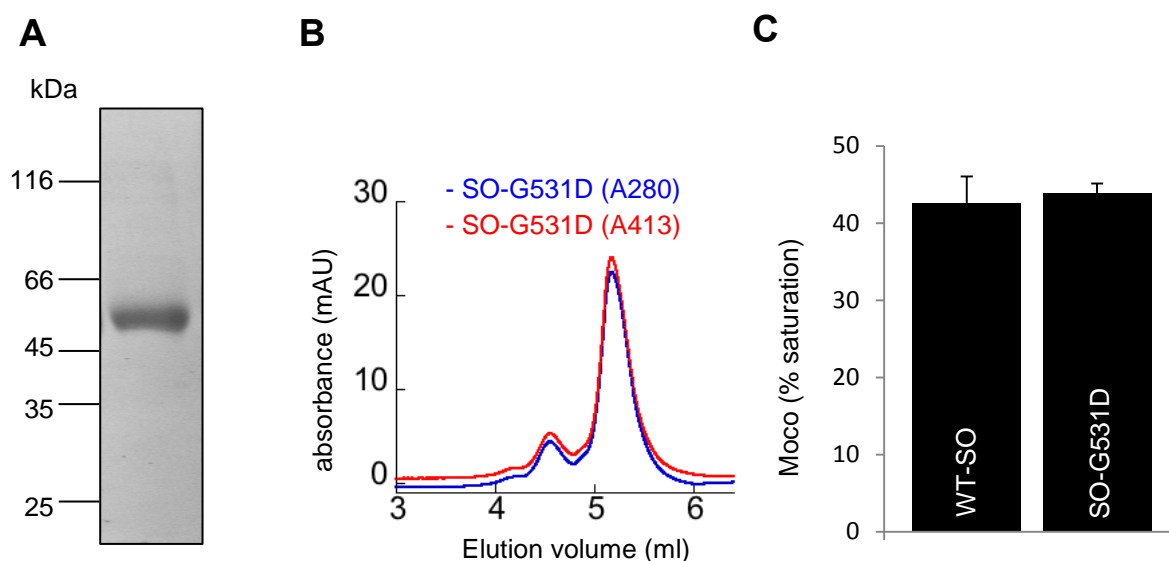


**Figure 2.17 Characterization of a monomeric mutant variant of SO.** (A) SO-G531D was expressed in *E. coli* strain TP1000 for 48 h at room temperature. Purification occurred by sequential Ni-NTA and anion exchange chromatography. Purity was assessed by 12% SDS-PAGE and subsequent coomassie blue staining. (B) Oligomerization of purified SO-G531D was determined by HPLC based size exclusion chromatography. Absorptions were measured at 280 nm (blue traces) and 413 nm (red traces). (C) Moco content of 100 pmol WT-SO and SO-G531D was analyzed by HPLC FormA analysis. Error bars represent standard deviations (n=3).

As expected, SO-G531D mainly eluted as a monomer, confirming that the introduced mutation indeed interfered with homodimerization. In addition, the strong heme-specific absorption at 413 nm revealed an efficient integration of the heme cofactor into SO and a mutual independence of heme integration and dimerization during the SO maturation process (Figure 2.17 B). The proper integration of Moco was confirmed by HPLC-based FormA determination, demonstrating that Moco integration occurs also independently on oligomerization of SO (Figure 2.17 C).

Next, the role of dimerization for the mitochondrial localization of SO was determined by expressing SO-G531D in HEK-293 cells. The monomeric variant of SO localized to mitochondria, demonstrating that dimerization is not required for mitochondrial retention of SO (Figure 2.18). This also confirms that the mislocalization of SO in absence of Moco is indeed due to the inaccessibility of Moco and not attributed to the secondary loss of homodimerization.

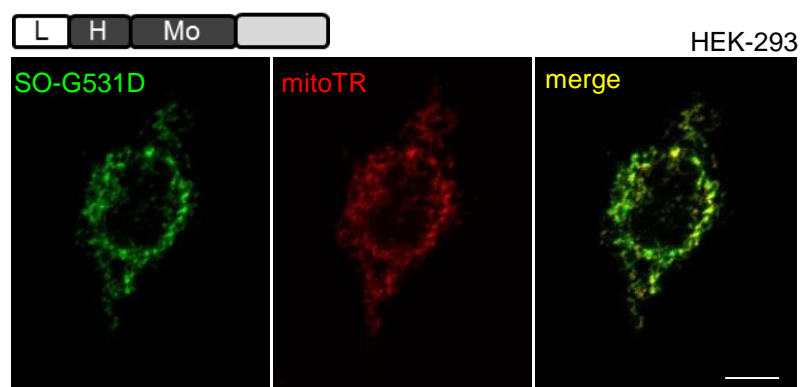


**Figure 2.18 Dimerization independent mitochondrial localization of SO.** SO-G531D was expressed in HEK-293 cells for 48 h and visualized by anti-SO immunostaining (green) using confocal laser scanning microscopy. Mitochondria were stained with Mitotracker Red CMXRos (mitoTR). Bar, 10  $\mu$ m. Cartoon illustrates the status of cofactor saturation and oligomerization: L, leader sequence; H, heme; Mo, Moco.

Summarizing the hierarchically organized cellular SO assembly, the integration of Moco constitutes a central component, which is not only a prerequisite for efficient mitochondrial targeting of SO, but which also triggers all further downstream maturation events. Following its translocation to mitochondria, SO becomes processed by the IMP complex and integrates Moco to complete the import across the outer membrane and to prevent a backwards translocation to the cytosol. The integration of Moco constitutes a pre-condition for dimerization and heme incorporation *in vivo*, both of which occur independent on each other and without any defined order.

### 2.1.7 SO-independent population of Moco in mitochondria

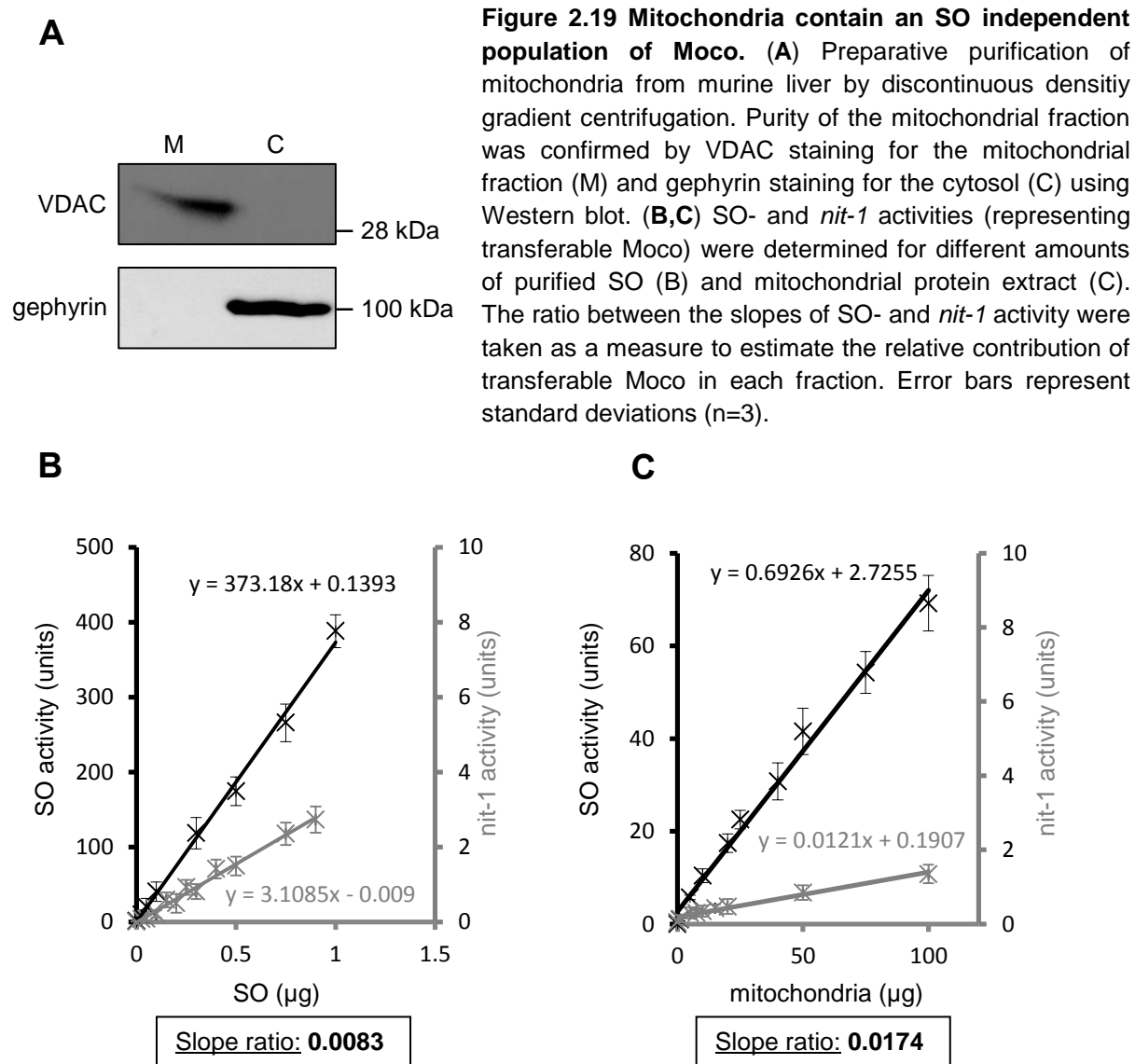
The dissection and characterization of the mitochondrial maturation of SO was initially triggered by the knowledge that Moco is very unstable and consequently, the question was asked how this instability may align with the mitochondrial maturation of SO. The findings of the current study contradict a combined mitochondrial transport of SO and Moco, as Moco was required for trapping SO in the IMS, suggesting that a SO-Moco complex cannot cross the TOM complex. This however opens the question of how Moco is stabilized from its cytosolic synthesis until its mitochondrial association with SO.

In autotrophic organisms, Moco storage proteins have been identified, which permit stabilization and cofactor insertion into the respective apo-enzymes (Fischer et al., 2006b, Kruse et al., 2010). In animals, similar Moco-binding chaperons have however not been identified so far. To address the problem of Moco stabilization and transport to mitochondria, the amount of Moco in mitochondria was quantified and placed in relation to the amount of SO activity. This was supposed to unravel if mitochondria contain an SO independent population of Moco that might be in transit to SO or bound by a yet not known Moco storing component. For this purpose, WT-SO was purified from *E. coli* strain TP1000 as illustrated in figure 2.2 A and mitochondria were purified from murine liver by discontinuous density gradient centrifugation (Figure 2.19 A). SO activities of purified SO and purified mitochondria were determined by means of the sulfite:cytochrome *c* SO assay *in vitro*. In parallel, the amounts of Moco were measured in both fractions based on the *nit-1* assay (Figure 2.19 B, C). For both, SO and mitochondria, dose dependent enzyme- and cofactor-activities were recorded with each of them showing a strong linear dependence. Finally, the fractional ratio between SO and cofactor activity was determined for the purified enzyme as well as the mitochondrial fraction.

In mitochondria, the amount of Moco referred to SO was twice as high as for isolated SO, suggesting a significant pool of Moco not to be attributed to SO. A part of this fraction might represent free Moco, which is in transit to SO, or it could be derived from a hitherto unknown mitochondrial Moco-binding protein. However, a second mitochondrial Moco-enzyme, the mitochondrial amidoxime-reducing component (mARC1 and mARC2), was recently discovered (Havemeyer et al., 2006) and most likely accounts for a major part of the SO-independent mitochondrial Moco activity.

When assuming an approximately similar contribution of both mARC proteins and SO to the *nit-1* based Moco activity, the mitochondrial Moco quantification does not promise the presence of major populations of free Moco in mitochondria or the presence of a Moco

storing component. Rather, these data suggest that SO and Moco immediately associate in mitochondria after their import to stabilize Moco and to prevent a reverse translocation of SO.



## 2.2 Mitochondrial maturation of mARC1

In chapter 2.1.7, a significant amount of SO independent Moco was discovered in mitochondria. A major proportion of this fraction is presumably attributed to the recently discovered mitochondrial Moco proteins mARC1 and mARC2 (Havemeyer et al., 2006, Gruenewald et al., 2008). In respect to the novel and unexpected mechanisms examined for SO and to achieve a comprehensive overview of the cell biology of mitochondrial molybdoenzymes, the mitochondrial maturation of mARC1 was analyzed in the second part of this study and compared to the findings on SO.

mARC1 was chosen as a representative for both mARC proteins, which closely resemble each other according to their primary structure (Figure 2.20) and secondary structure predictions (Mitoprot II, Phobius, (Kyte and Doolittle, 1982)).

```

marc1  MGAAGSSALARFVTLAQSRLPCWLGVAALGLTAVALGAVAWRRRAWPTRRRRLLQOVGTVAQ
marc2  MGAASSSALARLGLPARPWPRLWLVAAALGLAVALGTVAWRRRAWPTRRRRLLQOVGTVAK
1.....10.....20.....30.....40.....50.....60

marc1  LWIYPVKSCRGVPSVEAECTAMGLRSGNLRDRFWLVINQEGNMVVTARQEPRLVLISLTCD
marc2  LWIYPVKSCRGVPSVEAECTAMGLRSGNLRDRFWLVIKEDGHMVTARQEPRLVLISIIYE
.....70.....80.....90.....100.....110.....120

marc1  GDTITLSAAYTKDLELPIKTPETNAVHKCRVHGLSEIEGRDCGEATAOWITTSFLKSOPYRL
marc2  NNCLIFRAPDMDQVLEPSKQDSSNKLHNCRIFGLDIKGRDCGNEAAKWFNFKTEAYRL
.....130.....140.....150.....160.....170.....180

marc1  VHFEPHMRPARRPHQIADLFRPKDQIAYS DTSFLLILSEASLADLNSRIEKKVKRATNFRPN
marc2  VQFETNMKGRTRSRKLLPTLDQNFQVAYPDYCELLIMTDASLVDLNTRMKKKRMENFRPN
.....190.....200.....210.....220.....230.....240

marc1  IVISGCDVVAEDSWDELLIGDVELKRVMACSRCILTTVDPPDTGVMSRKEPLETLSYRQC
marc2  IVVTGCDAFBEDWDELLIGSVEVKVMACPRCILTVDPPDTGVDRKQPLDTLSYRQC
.....250.....260.....270.....280.....290.....300

marc1  DPSERKLYGKSPFLGQVYFVLENPGETIKVGDVYLLGQ
marc2  DPSERELYKLSPLFGIYYSVSKIGSLRVGDPVYRMV-
.....310.....320.....330.....

```

**Figure 2.20 Alignment of human mARC1 and mARC2.** Alignment of human mARC1 and mARC2 was conducted with CLUSTALW and Boxshade. Residues are framed in black (high conservation), gray (moderate conservation) or white (no conservation). Protein accession numbers: NP\_073583 (human mARC1), NP\_060368 (human mARC2).

The human *MOSC1* coding sequence (NP\_073583), encoding the mARC1 protein, was purchased from ImaGenes and amplified by PCR. Sequencing revealed two reproducible polymorphisms resulting in substitution of threonine 165 by alanine and methionine 187 by lysine. However, these polymorphisms also appear in the databases, e.g. as protein accessions NP073583, AAH10619 and EAW93921 and hence obviously represent naturally occurring polymorphisms.

### 2.2.1 Sub-cellular localization of mARC1

The mARC2 protein was identified and isolated from mitochondria by Havemeyer et al. (2006), suggesting a mitochondrial localization of mARC2. This was later confirmed by immunostaining in cell culture (Wahl et al., 2010) and identification of mARC2 in mitochondrial fractions purified from rat liver (Neve et al., 2012).

The sub-cellular localization of mARC1 was however not investigated so far, while the high degree of sequence similarity to mARC2 suggested a similar sub-cellular routing of both components. In addition, the exact localization to one of the four mitochondrial sub-compartments was neither unambiguously shown for mARC1 nor for mARC2 so far. First, the sub-cellular and sub-mitochondrial localization of mARC1 was analyzed *in silico* with the aim to identify potential mitochondrial targeting signals and/or transmembrane domains (Claros and Vincens, 1996, Kall et al., 2004) to obtain a first indication for its localization (Figure 2.21).

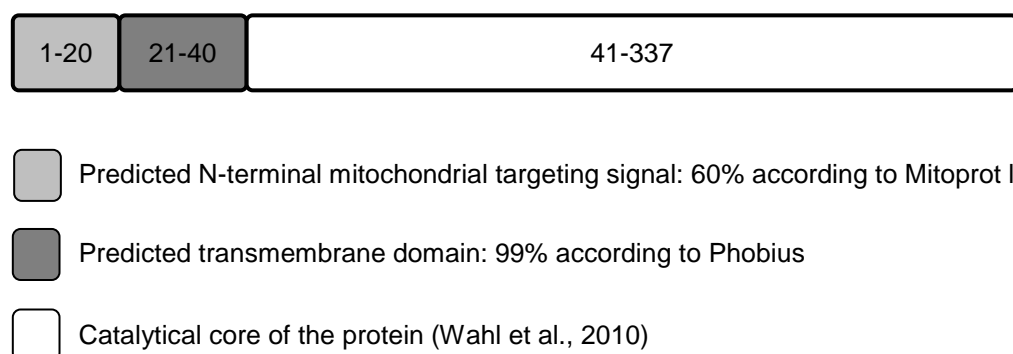


**Figure 2.21 Analysis and prediction of mARC1 sequence and structural motifs.** The peptide sequence of human mARC1 was analyzed by Mitoprot II (<http://ihg.gsf.de/ihg/mitoprot.html>) and Phobius (<http://phobius.sbc.su.se/>). Cartoon represents the predicted motifs with numbers illustrating the involved amino acids.

The analysis of the mARC1 peptide sequence revealed the presence of a potential N-terminal mitochondrial targeting signal and a downstream transmembrane domain with high probability scores. The remaining part of the protein was shown to be catalytically active *in vitro* in absence of residues 1-40 (Wahl et al., 2010), but was not predicted to contain any further mitochondrial targeting or transmembrane motifs and was hence termed as the catalytical core of the enzyme.

Considering the mitochondrial localization of mARC2 and the predictions above, mARC1 was expected to be directed to mitochondria too. In order to investigate its localization, mARC1 was fused to GFP via its C-terminus by expression of the *MOSC1* coding sequence in the pEGFP-N1 vector. Expression of mARC1-GFP in HEK-293 cells revealed the expected exclusive mitochondrial localization (Figure 2.22).

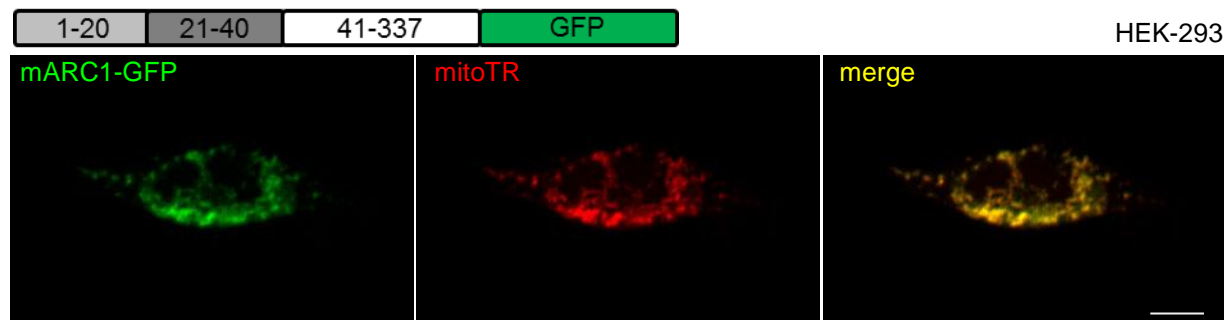


**Figure 2.22 Mitochondrial localization of mARC1-GFP.** mARC1-GFP (green) was expressed from pEGFP-N1 in HEK-2993 cells for 48 h and visualized by means of confocal laser scanning microscopy. Mitochondria were stained with Mitotracker Red CMXRos (mitoTR). Bar, 10  $\mu$ m. Cartoon illustrates the expression construct with the predicted mitochondrial targeting signal (light gray), the transmembrane domain (dark gray), the catalytical core (white) and GFP (green).

## 2.2.2 Localization of mARC1 within the mitochondrial compartments

Following the confirmation of its mitochondrial targeting, the localization of mARC1 was further investigated to finally assign it to one of the four mitochondrial subcompartments. Given the sequence analysis of mARC1 (Figure 2.21), a membrane association was predicted, which could either be the outer or inner mitochondrial membrane. However, as also shown for SO in the first part of this study, many mitochondrial proteins contain transmembrane domains in their precursor forms, which are lost during maturation in response to proteolytic processing, thus resulting in soluble mitochondrial proteins. The presence of a transmembrane domain in the precursor form does therefore not necessarily account for membrane spanning of the protein in its mature form.

To evaluate if mARC1 is either bound to a mitochondrial membrane or appears as a soluble protein, mitochondria were purified from HepG2 cells and mitochondrial membranes were separated from soluble fractions by alkaline treatment with 0.1 M  $\text{Na}_2\text{CO}_3$ . Thereby, closed vesicles or even whole organelles have been shown to be converted into open membrane sheets, accompanied by release of peripheral membrane- or soluble content proteins (Fujiki et al., 1982). Thus, upon incubation of mitochondria in  $\text{Na}_2\text{CO}_3$ , centrifugation resulted in an accumulation of mitochondrial membrane proteins in the pellet, while soluble proteins of the IMS or mitochondrial matrix were supposed to remain in the supernatant. This was confirmed by the exclusive detection of the respective marker proteins VDAC (outer membrane) and COX4 (inner membrane) in the pellet fraction and by the pure accumulation of the soluble proteins SMAC (IMS) and HSP60 (matrix) in the supernatant (Figure 2.23). Following this separation protocol, endogenous mARC1 protein was only detected in the

pellet fraction, demonstrating that mARC1 is membrane bound in its mature form and unlike SO, retaining its transmembrane domain during maturation (Figure 2.23).

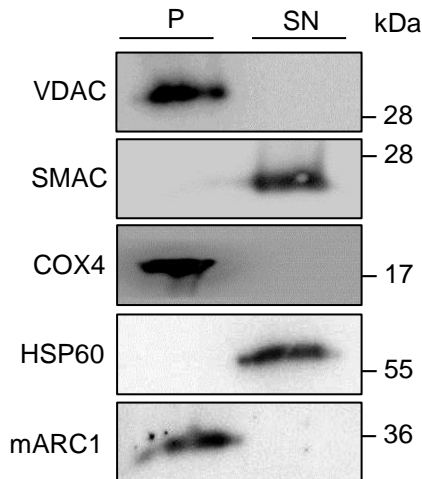


**Figure 2.23 Association of mARC1 with mitochondrial membranes.** Mitochondria were enriched from HEP-G2 cells by differential centrifugation and resuspended in 0.1 M  $\text{Na}_2\text{CO}_3$ , pH 11.5. After 30 min incubation on ice, mitochondrial fractions were separated by centrifugation at 100.000 x g for 60 min. Pellet (P) was directly resuspended in SDS loading buffer while proteins of the supernatant (SN) were first precipitated by TCA. Distribution of marker proteins and mARC1 was analyzed by 12% SDS PAGE and subsequent Western blot.

Given that inner and outer membranes were not separated during  $\text{Na}_2\text{CO}_3$  extraction, the localization of mARC1 was not finally assigned to a single mitochondrial sub-compartment. In addition, the spatial orientation of mARC1 within the respective membrane was not clarified.

To finally resolve the exact localization and membrane topology of mARC1, external proteases were applied to purified mitochondria in order to interpret protein stability against degradation in light of protein localization. Thereby, proteins of the outer membrane containing a soluble cytosolic domain were supposed to be degraded, while those residing in the inner mitochondrial compartments were expected to be protected from protease accessibility. Proteins of the inner membrane exposing a soluble domain to the IMS or completely soluble IMS proteins should be degraded only upon specific swelling of the outer membrane following the application of a hypotonic solution. The inner mitochondrial membrane, constituting a ~2.5-fold larger surface area compared to the outer membrane in HeLa cells (John et al., 2005), was expected to tolerate a mild hypotonic treatment, suggesting that proteins of the matrix were protected from digestion even after swelling.

Mitochondria were purified from HeLa cells to determine the sensitivity of endogenous mARC1 against PK. Upon exposure of PK to intact mitochondria, the outer membrane protein MFN2 was degraded, while the IMS and matrix control proteins remained unaffected (Figure 2.24 A). Swelling of the outer membrane resulted in the additional and complete degradation of SMAC upon PK exposure but an ongoing stabilization of matrix-residing



HSP60 was seen, demonstrating a specific swelling of the outer membrane and an intact inner membrane (Figure 2.24 A). Endogenous mARC1 was degraded following PK treatment of intact mitochondria, demonstrating its integration into the outer mitochondrial membrane (Figure 2.24 A).

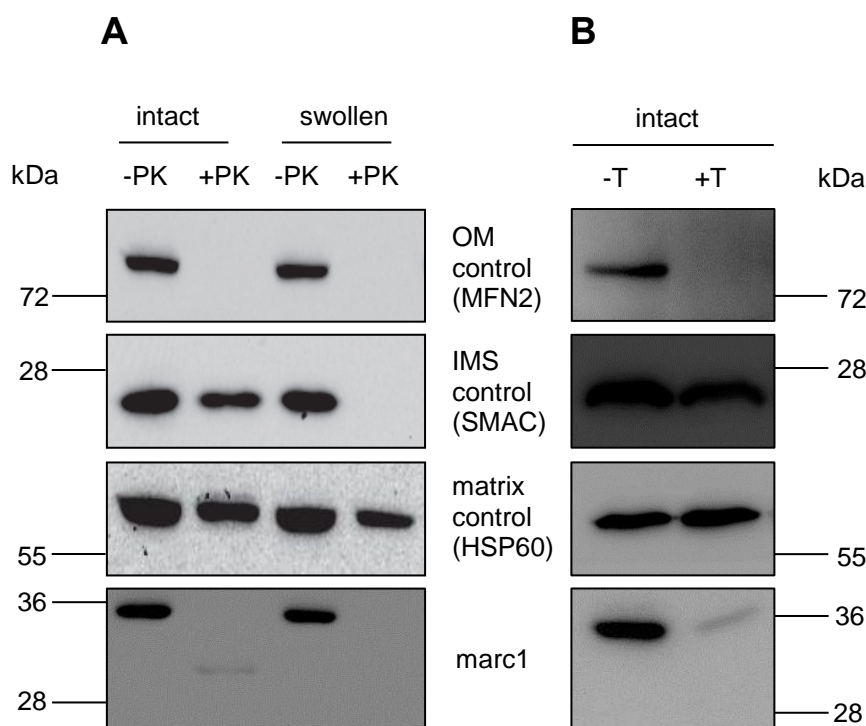


**Figure 2.24 mARC1 localizes to the outer mitochondrial membrane.** Mitochondria were enriched from HeLA cells and treated with 100  $\mu$ g/ml **(A)** PK or **(B)** trypsin for 10 min at 4°C. Swelling occurred by incubating mitochondria in 10 mM HEPES, pH 7.4 for 10 min prior to protease application. After protease inactivation and TCA precipitation, mitochondrial proteins were loaded on a Tris/Tricine gradient SDS-PAGE (8-17.5%) with subsequent Western blotting.

Notably, a proteolytic fragment of ~30 kDa of mARC1 was formed upon PK treatment of intact mitochondria (Figure 2.24 A), which allowed to examine the topology of mARC1 in the outer membrane. The truncated version may either constitute a protease protected fragment being exposed to the mitochondrial IMS or be exposed to the cytosol but being partially stable to PK application. Considering the predictions in figure 2.21 and the presence of the antibody epitope within residues 182-212, two orientations of mARC1 in the outer membrane were possible: Either, the C-terminus may be exposed to the IMS and the 20 residues upstream of the transmembrane domain are facing the cytosol ( $N_{(out)}-C_{(in)}$  orientation), or the N-terminus may point towards the IMS while the core of the protein remains cytosolic ( $N_{(in)}-C_{(out)}$  orientation). Compared to the intensity of full-length mARC1 in absence of PK, the truncated fragment following PK treatment was hardly detectable. This

finding together with the size of the sequence preceding the transmembrane domain (2 kDa), which would be degraded in the event of an outside orientation, suggests that the weak signal at 30 kDa is derived from an incomplete degradation of the large C-terminal catalytic core facing the cytosol.

To confirm the proposed  $N_{(in)}-C_{(out)}$  orientation of mARC1, trypsin was chosen as a second protease. Assuming the C-terminal core of mARC1 to be directed towards the IMS, a similar protease protected fragment as seen upon PK application should appear following trypsin treatment. Since no smaller fragment was detected after trypsin exposure (Figure 2.24 B), the truncated fragment seen in figure 2.24 A was confirmed to form due to incomplete degradation by PK and demonstrated the exposure of the C-terminal core domain of mARC1 to the cytosol. Following trypsin application, no truncated fragments of mARC1 were detected, although the full-length protein did not completely disappear. However, in analogy to the signal intensity differences between full-length and truncated mARC1 upon PK application, the full-length fragment appeared considerably weaker upon trypsin exposure, while the IMS control remained unaffected (Figure 2.24 B). This finding in aggregate suggests the C-terminal core of mARC1 to be tightly folded and thus to be partially stable to PK and trypsin mediated degradation. Taken together, both protease treatments of mitochondria revealed the localization of mARC1 in the outer mitochondrial membrane with an  $N_{(in)}-C_{(out)}$  orientation.

### 2.2.3 Mitochondrial targeting of mARC1

Upon determination of its localization and membrane orientation, the question arose of how mARC1 is directed to the outer mitochondrial membrane. The predictions of figure 2.21 suggested the presence of a weak N-terminal mitochondrial targeting signal and a downstream transmembrane domain. To determine the functions of both motifs in mitochondrial translocation of mARC1, both sequence motifs were fused to GFP and localized in HEK-293 cells.

First, the putative N-terminal mitochondrial targeting signal (MTS) consisting of residues 1-20 were fused to GFP. Expression in HEK-293 cells revealed a heterogeneous sub-cellular distribution of the fusion with some cells revealing a complete mitochondrial localization and others showing a weaker mitochondrial targeting, accompanied by a diffuse distribution throughout the cell (Figure 2.25 A). Statistical analyses revealed about 50% of the cells to display a complete and efficient mitochondrial targeting, while full-length mARC1-GFP was exclusively targeted to mitochondria in nearly all cells (Figure 2.25 B). These

distributions suggested residues 1-20 to constitute a weak mitochondrial targeting signal and are thus in line with the predictions of MITOPROT II and the low amphipathic character with only two basic residues within this region.

Given that classical MTS are usually not present in outer mitochondrial membrane proteins (Walther and Rapaport, 2009), the matrix-targeting ability of the N-terminal 20 residues of mARC1 was investigated in the next step. mARC1 ( $\Delta$ 21-337)-GFP expressed in HEK-293-cells accumulated in purified mitochondria and was protected against externally added protease, while PK treatment after solubilization of mitochondrial membranes using 1% Triton resulted in efficient degradation (Figure 2.25 C). Thus, residues 1-20 of mARC1 were confirmed to constitute a classical but weak MTS, which is able to drive an attached marker protein to the mitochondrial matrix.

However, mARC1 was shown not to be targeted to the mitochondrial matrix and the transport efficiency of the full-length protein was demonstrated to exceed the targeting capability of the isolated N-terminus. This suggested the presence of an additional targeting motif within the mARC1 protein, which would on the one hand ensure a complete mitochondrial localization and on the other hand induce sorting of mARC1 to the outer mitochondrial membrane.

In order to analyze the combined impact of N-terminal targeting signal and the downstream transmembrane domain for mitochondrial targeting, residues 1-40 of mARC1 were fused to GFP and expressed in HEK-293 cells. In contrast to the isolated N-terminal targeting signal, co-expression with the transmembrane domain triggered GFP translocation to mitochondria as efficiently as it was seen with the full-length mARC1 protein (Figure 2.25 D). The reconstitution of the entire mitochondrial translocation upon fusion of the transmembrane domain thus indicated a function of the latter in mitochondrial transport of mARC1.

Consistently, it could be confirmed that residues 21-40, when fused to GFP, were sufficient to mediate a complete mitochondrial localization, demonstrating the transmembrane domain to constitute a mitochondrial targeting signal on its own (Figure 2.25 E). Thus, the mARC1 N-terminal domain contains two autonomous motifs triggering mitochondrial sorting of mARC1.

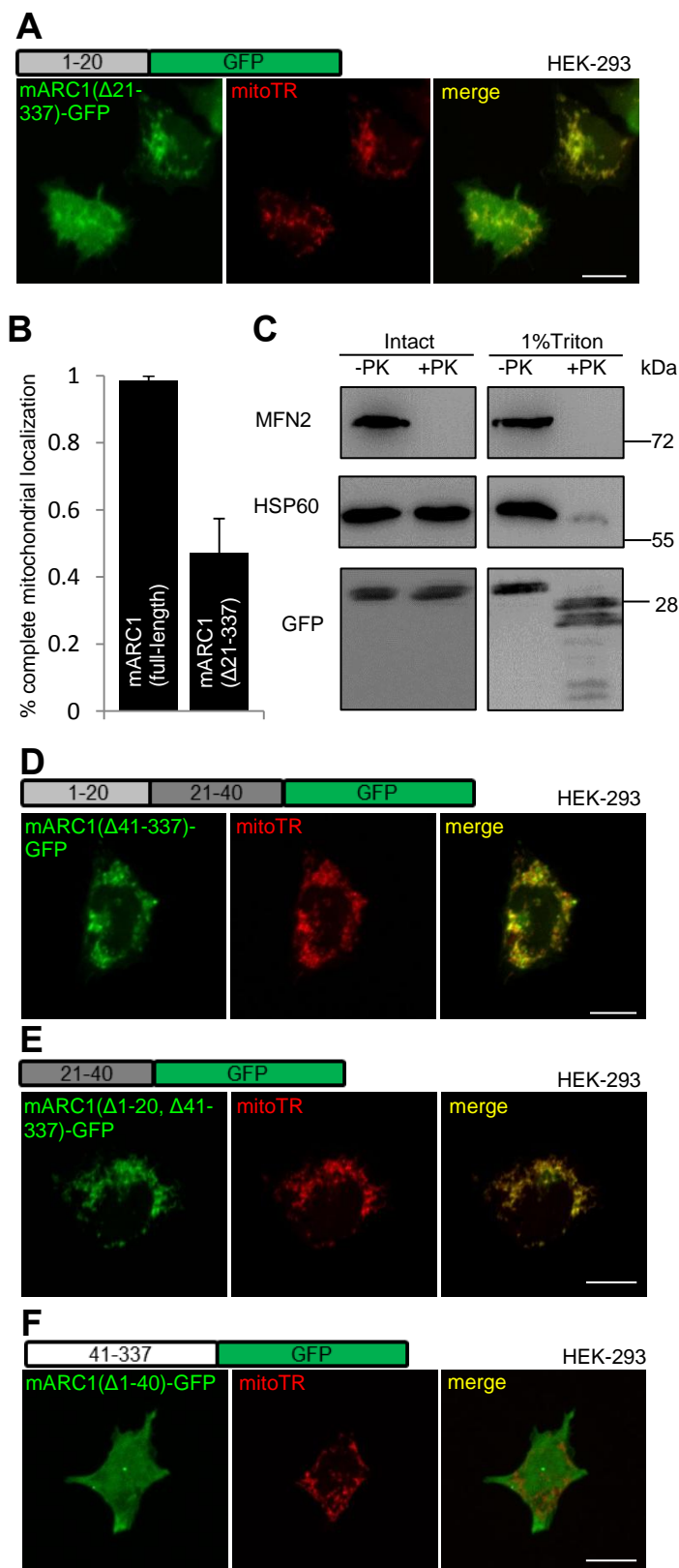


**Figure 2.25 Mitochondrial targeting motifs of mARC1.**

(A) Sub-cellular localization of mARC1( $\Delta$ 21-337)-GFP. (B) Statistical quantification of mitochondrial localization of mARC1( $\Delta$ 21-337)-GFP compared to mARC1-GFP.

Cells revealing a complete mitochondrial localization of the respective construct were counted and depicted as percent. Each 50 cells were analyzed, error bars represent standard deviations ( $n=3$ ). (C) mARC1( $\Delta$ 21-337)-GFP was expressed in HEK-293 cells for 48 h. Mitochondria were enriched and treated  $\pm$  1% Triton for 10 min prior to the addition of 100  $\mu$ g/ml PK for 10 min at 4°C. After protease inactivation and TCA precipitation, mitochondrial proteins were loaded on a 12% SDS-PAGE with subsequent Western blotting. (D) Sub-cellular localization of mARC1( $\Delta$ 41-337)-GFP. (E) Sub-cellular localization of mARC1( $\Delta$ 1-20, $\Delta$ 41-337)-GFP. (F) Sub-cellular localization of mARC1( $\Delta$ 1-40)-GFP.

Constructs of (A), (D), (E) and (F) were expressed in HEK-293 cells for 48 h and pictures were obtained by means of confocal laser scanning microscopy. Mitochondria were stained with Mitotracker Red CMXRos (mitoTR). Bar, 10  $\mu$ m.

Finally, the catalytic core of mARC1 was fused to GFP and expressed in HEK-293 cells. No mitochondrial localization was observed and instead, the construct was diffusely

distributed within the entire cell (Figure 2.26 F). In conclusion, residues 41-337 of mARC1 do not contain any further mitochondrial targeting signals, suggesting that the mitochondrial localization of mARC1 is solely mediated by its N-terminal domain.

Thereby, mARC1 is classified as a novel signal-anchored protein of the outer mitochondrial membrane, which share N-terminal transmembrane domains simultaneously constituting membrane anchor and targeting signal (Shore et al., 1995).

In analogy to mARC1, SO likewise contains an N-terminal mitochondrial targeting motif. As illustrated in the first part of this study, the SO targeting signal itself was however not sufficient for mitochondrial localization, but Moco was in addition required for mitochondrial trapping of SO. To determine the role of Moco for the mitochondrial targeting of mARC1, the latter was expressed in MOCS1-deficient fibroblasts, in which SO showed a diffuse distribution within the cell (Figure 2.3 D). To allow immunodetection in cultured cells, mARC1 was expressed with a C-terminal myc-tag. In contrast to SO, mARC1 did not require Moco for its mitochondrial localization, but was efficiently targeted even in absence of its cofactor (Figure 2.26).

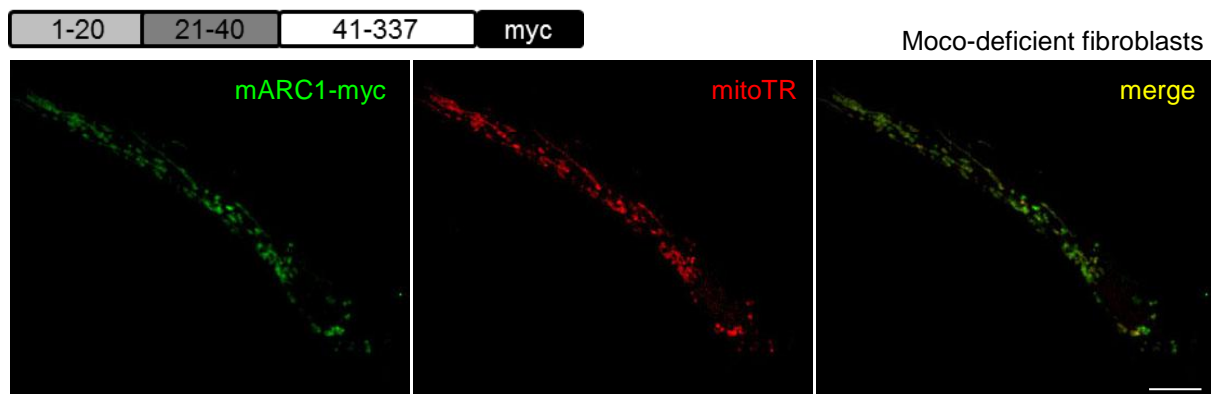


**Figure 2.26 Moco independent mitochondrial targeting of mARC1.** mARC1-myc was expressed in MOCS1-deficient fibroblasts for 48 h and visualized by anti-myc immunostaining (green) using confocal laser scanning microscopy. Mitochondria were stained with Mitotracker Red CMXRos. Bar, 10  $\mu$ m. Cartoon illustrates the expression construct with the predicted mitochondrial targeting signal (light gray), the transmembrane domain (dark gray), the catalytical core (white) and the C-terminal myc-tag (black).

The Moco independent mitochondrial localization of mARC1 was expected in respect to its association with a mitochondrial membrane. The non-mitochondrial distribution of Moco-deficient SO was based on its solubility and could be rescued by artificial attachment of the protein to the inner mitochondrial membrane. Therefore, a similar demand on Moco for

mitochondrial retention of mARC1 is not required and its N-terminal targeting motifs are sufficient for accurate mitochondrial localization.

## 2.2.4 Mechanims of mitochondrial mARC1 import

After identification and dissection of the internal motifs responsible for mitochondrial localization of mARC1, the overall import mechanism was finally characterized *in vitro* to achieve a comprehensive understanding of the mitochondrial maturation of mARC1. The amino terminal 20 residues of mARC1 constitute a classical but weak N-terminal MTS. These motifs are usually cleaved after import by mitochondrial peptidases, resulting in N-terminal truncation of the respective mature proteins. In addition, predictions by MITOPROT II (Claros and Vincens, 1996) suggested the presence of a potential peptidase cleavage site at position 44. In order to probe a potential mitochondrial processing of mARC1, the apparent molecular weight of *in vitro* translated mARC1 was compared to that of mARC1 synthesized in cells using SDS-PAGE and Western blot analysis, assuming that processing will result in a reduced size as compared to the *in vitro* synthesized precursor protein. For this purpose, mARC1 was translated in a cell free reticulocyte lysate system and labeled by  $^{35}\text{S}$ -methionine incorporation. Thereby, untagged mARC1, containing five methionine residues, and myc-tagged mARC1, containing two additional methionines within the tag, were synthesized to compare their radioactive signal intensities (Figure 2.27).

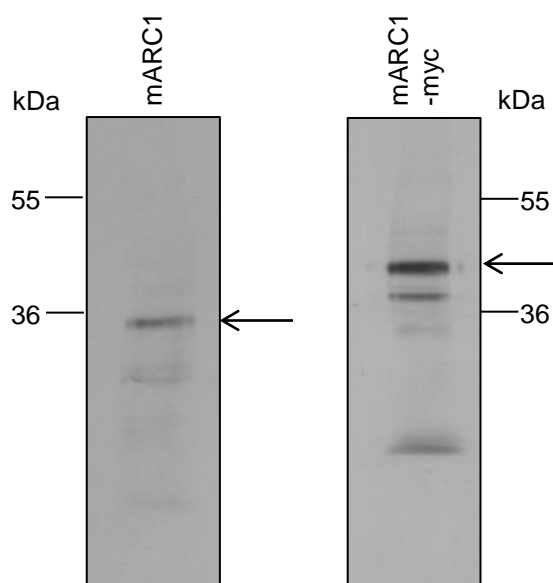


**Figure 2.27** *In vitro* translation of mARC1. mARC1 (A) and mARC1-myc (B) were translated in a cell free reticulocyte lysate system. Radioactive labeling occurred by integration of  $^{35}\text{S}$ -methionine during translation. In each lane, 2  $\mu\text{l}$  of lysate were loaded on a 12% SDS gel and detected by subsequent Western blot analysis. The membrane was exposed to an X-ray film overnight before development of signals. Arrows point to the respective mARC1 variants at the expected sizes.

The analysis of the *in vitro* translation revealed a considerably stronger intensity of myc-tagged mARC1 compared to the untagged variant, but also depicted more impurities, presumably representing premature translation termination or alternative sites of translation initiation. However, in both cases mARC1 was predominantly synthesized as the expected full-length precursor. The significantly bigger size of the myc-tagged precursor is attributed to a long C-terminal extension of this variant, which harbors a linker region and the myc-tag.

To investigate a possible mitochondrial processing of mARC1, untagged and myc-tagged mARC1 were comparatively expressed in HEK-293 cells. The molecular weights of both variants were each compared to the respective *in vitro* translated precursors by Western blotting and revealed similar sizes of *in vitro* and *in vivo* expressed mARC1 (Figure 2.28). Thus, mARC1 is not processed in mitochondria and retains both identified targeting motifs during maturation.

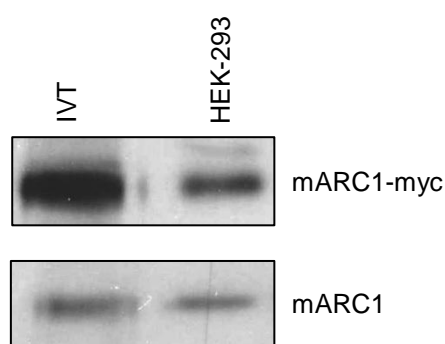


**Figure 2.28 mARC1 is not processed.** mARC1 and mARC1-myc were translated *in vitro* as described in figure 2.27 and in parallel expressed in HEK-293 cells for 48 h. Each 4  $\mu$ l lysate and 30  $\mu$ g cell extract, respectively, were loaded on a 12% SDS gel with subsequent Western blotting. *In vitro* translated (IVT) mARC1 was detected by overnight exposure to an X-ray film, while mARC1 expressed *in vivo* was subsequently detected by anti-mARC1 antibody staining. Images of both detections were merged for final size comparisons.

Detection of successful *in vitro* import into mitochondria is usually performed based on protection to external protease application or based on processing and truncation of the imported precursor. However, as mARC1 is exposed to the cytosol and not processed following successful import, mitochondrial translocation was monitored based on the proposed ability of mARC1 to form a complex with its electron donors cytochrome  $b_5$  reductase and cytochrome  $b_5$  in the outer mitochondrial membrane.

First, mARC1 complex formation was determined by expression of the protein in HEK-293 cells. Mitochondria were purified and extracts were loaded on Blue Native-PAGE (BN-PAGE) to characterize mARC1 oligomerization in the outer membrane and to thus define the native mARC1 protein pattern to be expected upon successful *in vitro* import. Western blot detection of the C-terminal myc-tag revealed mARC1 to reside in three high oligomeric protein complexes each of which of more than 350 kDa in size, while mitochondria

purified from untransfected cells did not show any of these signals, thus ensuring antibody specificity and successful transient expression of mARC1 (Figure 2.29 A).

Successful *in vitro* import of mARC1 was expected to reproduce the complexes seen after cellular expression of the protein in HEK-293 cells. The incubation of *in vitro* synthesized precursors with purified mitochondria indeed resulted in a time-dependent formation of similar high-oligomeric structures, suggesting successful import of mARC1 (Figure 2.29 B).

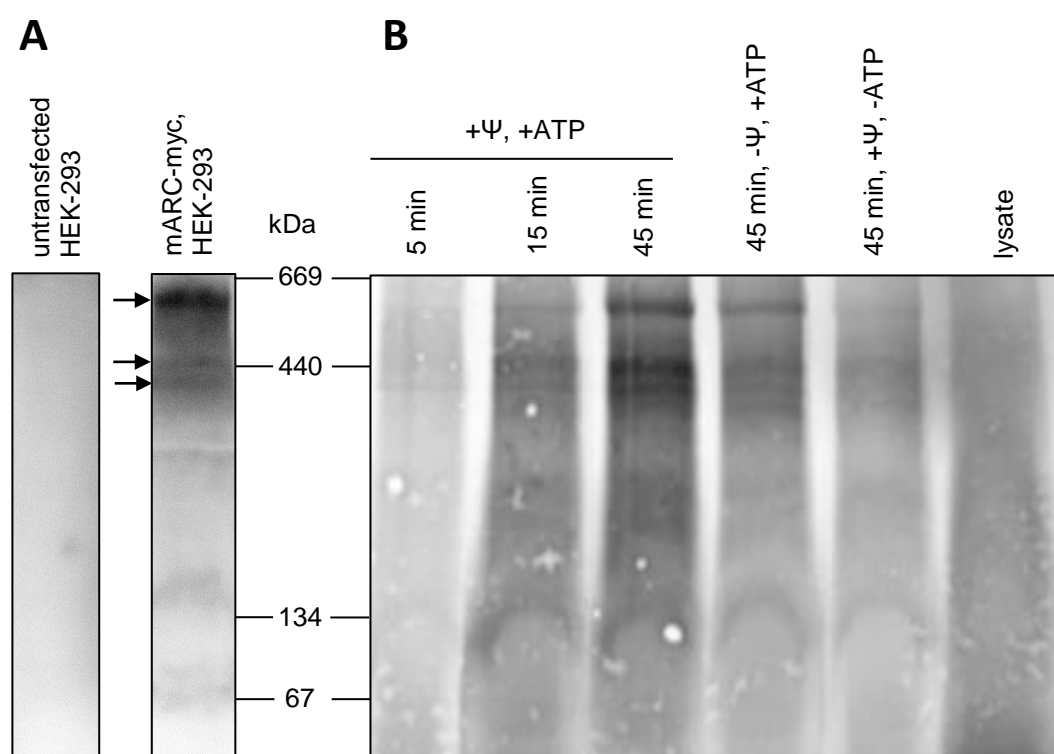


**Figure 2.29 Mitochondrial *in vitro* import of mARC1.** (A) Mitochondria were enriched from HEK-293 cells expressing mARC1-myc or from untransfected cells and mitochondrial proteins were extracted from enriched mitochondria by detergent application. Proteins were loaded on a 4-16% Bis-Tris acrylamide gradient BN-PAGE with subsequent western blotting. mARC1-myc containing complexes were detected by anti-myc antibody detection. Arrows point at high molecular weight bands that were also identified upon *in vitro* import of mARC1-myc in (B). (B) Import of *in vitro* translated mARC1-myc occurred into mitochondria purified from HEK-293 cells. Import reactions were performed at 37°C and stopped after 5, 15 or 45 min. Membrane potential deficient mitochondria (-Ψ) were obtained by the addition of 20 μg/ml valinomycin prior to the import reaction. After import, mitochondrial proteins were extracted by detergent application and subsequently loaded on a 4-16% Bis-Tris acrylamide gradient BN-PAGE, followed by western blotting. Radioactive signals were detected by 2 weeks exposure to an X-ray cassette.

These complexes were also detected upon depletion of the membrane potential by valinomycin, demonstrating, as usual for proteins residing in the outer mitochondrial



membrane (Walther and Rapaport, 2009), that an intact membrane potential is not required for mitochondrial transport of mARC1. Since the general function of N-terminal MTS is based on an intact membrane potential, the membrane potential independent integration of mARC1 into the outer mitochondrial membrane indicated that the MTS does not contribute to mARC1 targeting in a conventional manner. Depletion of external ATP significantly decreased the efficiency of complex formation, illustrating that extramitochondrial ATP is required for mARC1 assembly into high oligomeric structures. The specificity of complex formations was ensured by application of mARC1-precursors in absence of mitochondria, which did not result in any detectable mARC1-specific oligomers (Figure 2.29 B).

In summary, mARC1 is directed to the outer mitochondrial membrane based on its bipartite N-terminal targeting motif. With the transmembrane domain constituting the critical signal for correct sorting, mARC1 is a novel member of the small family of signal-anchored outer mitochondrial membrane proteins. The membrane potential independent but ATP requiring mechanism of membrane insertion results in an  $N_{(in)}-C_{(out)}$  orientation of mARC1 and its final integration into high-oligomeric protein complexes

## **3 Discussion**

### **3.1 Maturation of mammalian SO**

#### **3.1.1 Moco-dependent mitochondrial localization of SO**

The formation of functional SO implies a complex and highly organized multi-step maturation procedure. The transport of SO and Moco to mitochondria, the mitochondrial processing of SO, the integration of Moco and heme as well as homodimerization need to occur in a defined order to ensure efficient SO maturation.

In the current study, Moco was identified as a key component of SO assembly, which does not only ensure mitochondrial localization, but also heme integration and dimerization. In absence of Moco, about 70% of SO was not found in mitochondria but instead mislocalized to the cytosol, although processing of the N-terminal targeting peptide revealed that the protein was initially imported into mitochondria. Since anchoring of SO in the inner mitochondrial membrane resulted in mitochondrial localization in absence of Moco, unfolded and Moco-free SO was proposed to undergo a passive backshift to the cytosol.

Cofactor-dependent mitochondrial localization has been described earlier for cytochrome *c*, which requires the heme cofactor as well as the heme integrating cytochrome *c* heme lyase to ensure efficient localization in the mitochondrial IMS (Dumont et al., 1988, Nargang et al., 1988). Similarly, IMS proteins of the Mia40-dependent import pathway have been found outside of mitochondria in absence of Mia40 (Chacinska et al., 2004). Such a folding-mediated trapping of small IMS proteins has also been described for Tim13, which contains four conserved cysteine residues binding a zinc ion as a cofactor. Application of external chelators after *in vitro* import of Tim13 to mitochondria resulted in re-appearance of Tim13 outside of mitochondria and thus in reverse translocation after zinc loss and unfolding of the protein (Lutz et al., 2003). These retrograde movements across the TOM complex are possible in respect to the small size of the respective proteins on the one hand and considering that folding depicts the only vectorial driving force towards the IMS on the other hand. The TOM complex is known to be a passive translocation channel undergoing only weak interactions with the passing proteins (Ungermann et al., 1994). Unfolded small proteins therefore tend to bi-directionally diffuse through the TOM complex and thus do not achieve efficient mitochondrial targeting. However, all of the described proteins lack N-terminal pre-sequences, become imported independently of the membrane potential and therefore belong to IMS proteins that require so-called folding-trap mechanisms for mitochondrial import (Neupert and Herrmann, 2007).

SO was in contrast shown to contain a bipartite N-terminal targeting signal and its molecular weight of more than 50 kDa as a monomer considerably exceeds those of the small IMS proteins. Furthermore, its import was shown in a previous study to be based on the classical pre-sequence pathway, which requires ATP and an intact membrane potential across the inner mitochondrial membrane (Ono and Ito, 1984). Unlike small IMS proteins, SO therefore receives an additional driving force for mitochondrial sorting based on its N-terminal targeting signal. Thus, SO combines the N-terminal bipartite targeting peptide with the ATP- and membrane potential-dependent translocation across the inner mitochondrial membrane of the members of the pre-sequence pathway with a cofactor-dependent trapping mechanism known for members of the folding-trap/Mia40 import pathway.

N-terminal targeting signals are essential elements triggering mitochondrial transport and depletion of the latter from the respective proteins usually prevents mitochondrial localization. In most cases, these motifs are not only essential, but also sufficient for targeting (Baker et al., 2007). The N-terminal domain of SO is also required for mitochondrial routing and its depletion results in cytosolic accumulation of the precursor. However, the N-terminal sorting signal of SO was not sufficient for mitochondrial localization, given that the integration of Moco was additionally required for mitochondrial retention. Absence of Moco finally resulted in a backwards translocation to the cytosol.

Other exceptions in which MTS are not entirely sufficient for mitochondrial sorting are highlighted by a number of proteins with dual subcellular localizations. A single translation product of the mitochondrial cysteine desulfurase Nfs1 was shown to localize to mitochondria and the nucleus (Naamati et al., 2009). The Nfs1 distribution mechanism was determined to require at least partial mitochondrial entry of all precursors. The authors proposed minor nuclear import, which was suggested to occur after reverse translocations of Nfs1 subpopulations to the cytosol. Similarly, eclipsed amounts of mitochondrial aconitase were identified in the cytosol and were suggested to appear upon reverse translocation from mitochondria (Regev-Rudzki et al., 2005). In addition, a small fraction of the cytosolic signaling protein Ecsit was found in mitochondria, while the mechanism of its dual distribution remained uncharacterized (Vogel et al., 2007). The probably best understood mechanism of reverse translocation-mediated dual localization of a protein is displayed by fumarase. Fumarase is a mitochondrial matrix protein becoming imported based on a conservative N-terminal targeting motif. A fraction of fumarase was shown to move in a retrograde fashion to the cytosol following its mitochondrial processing, thus resulting in a dual localization of the protein (Knox et al., 1998). This particular proportion, destined as the cytosolic pool, therefore does not completely cross the TOM complex while being in transit to the mitochondria, because a C-terminal folding event outside of mitochondria constitutes a

reverse driving force towards the cytosol (Sass et al., 2001). These described examples resemble SO in a way, that all proteins contain N-terminal MTS, which not in all cases result in mitochondrial localization but permit reverse translocations to the cytosol. In contrast to SO, these retrograde movements however depict a cellular instrument to achieve dual subcellular localization of a single translation product. Further, folding mediated by Moco integration essentially contributes to mitochondrial import of SO, while C-terminal folding of fumarase constitutes an active driving force for backwards translocation to the cytosol.

The reverse translocation in absence of Moco indicated an active function of Moco for the mitochondrial import of SO. Consistently, a chimeric SO-TIM50 variant anchored in the inner mitochondrial membrane was not completely translocated across the TOM complex, but the C-terminal domain partially remained exposed to the cytosol if Moco was not present. The incorporation of Moco in contrast resulted in folding of the protein and a completion of the transport across the TOM complex. Therefore, two distinct mechanisms appear to drive SO translocation across the outer mitochondrial membrane: The N-terminal targeting signal directs the SO N-terminus across the outer and inner mitochondrial membrane, while the C-terminus is not imported and remains exposed to the cytosol. The integration of Moco is required as a second translocation mechanism to pull the entire protein across the outer mitochondrial membrane. In absence of Moco, SO apparently undergoes bidirectional Brownian thermal motion upon cleavage by the IMP the complex, resulting in reverse translocation of a major population of SO. Integration of Moco seems to ratchet the Brownian motion and to drive translocation of the C-terminal domain across the outer membrane. Still, in absence of Moco, 30% of SO remained mitochondrial and was not re-exported to the cytosol. While the N-terminal part of SO is actively targeted towards the mitochondrial matrix, the remaining part of the protein requires Moco integration to shift the equilibrium of passive diffusion towards the IMS to complete translocation. In absence of Moco and after cleavage by the IMP complex, no direction is favored and SO may move towards both the cytosol and IMS. The mitochondrial fraction of Moco-deficient SO may therefore arise from SO arrested in the TOM complex and another subpopulation which randomly enters the IMS. The majority of SO however undergoes a complete reverse translocation to the cytosol, although not triggered by an apparent driving force as described for fumarase (Sass et al., 2001). The cytosolic accumulation of SO may occur since its N-terminal targeting signal is processed in mitochondria and once SO has left the TOM complex in the reverse direction, the signal for re-entering mitochondria is lost. Furthermore, diffusion towards the cytosol may be favored in respect to the narrow space between outer and inner boundary membrane, which might interfere with passive protein entry, as also observed for small IMS proteins mainly accumulating outside of mitochondria if not folded (Lutz et al., 2003, Chacinska et al., 2004).

The bipartite mechanism of mitochondrial import of SO resembles the translocation of yeast cytochrome  $b_2$  (Glick et al., 1993). In analogy to SO, cytochrome  $b_2$  contains a bipartite N-terminal targeting signal and is cleaved by IMP1 to generate a soluble IMS protein (Nunnari et al., 1993). Cytochrome  $b_2$  contains a non-covalently bound heme as a single cofactor, which is required during import to pull the C-terminal domain of the protein across the outer mitochondrial membrane. Prevention of heme integration and thus of folding of the heme domain resulted in an arrest of translocation within the TOM complex, while the incorporation of heme was required to shift the Brownian thermal motion of the C-terminal domain towards the IMS (Esaki et al., 1999). The mitochondrial maturation of SO and cytochrome  $b_2$  therefore reveal striking mechanistic parallels, with each depending on two distinct events, both being essential for the efficient completion of protein translocation towards the IMS.

### 3.1.2 The SO import vs. other proteins with bipartite targeting signals

The Moco-dependent mitochondrial maturation of SO depicts a novel connection between the classical pre-sequence pathway and folding-trap mechanisms of small IMS proteins. Both, N-terminal pre-sequence and cofactor-mediated trapping are required to ensure comprehensive mitochondrial localization of SO. As described above, a related mechanism was also found for yeast cytochrome  $b_2$ , which resembles SO in respect to its analogous bipartite N-terminal targeting signal. However, such a demand on these two distinct mechanisms triggering a complete translocation towards the mitochondrial IMS is not common to all proteins containing bipartite N-terminal targeting signals, but rather unique to SO and cytochrome  $b_2$  as known so far.

Therefore, the question arises of why these two proteins require two distinct mechanisms for targeting, while other proteins containing bipartite targeting signals are efficiently targeted to mitochondria solely based on their N-terminal targeting signals.

Most IMS proteins are small and are targeted according to the folding trap pathway, while the sub-group of soluble proteins with bipartite targeting signals is rather small. Apart from SO and cytochrome  $b_2$  (Cytb2), the pro-apoptotic protein SMAC/DIABLO (Burri et al., 2005), the soluble fraction of the dual localized yeast Mcr1 (Haucke et al., 1997), the apoptotic DNase endonuclease G (EndoG) (Ohsato et al., 2002, Neupert and Herrmann, 2007) as well as the heme-synthesizing coproporphyrinogen oxidase (CPO) (Grandchamp et al., 1978, Neupert and Herrmann, 2007) are known IMS proteins with bipartite N-terminal targeting signals.

To address why cytochrome  $b_2$  and SO may need additional cofactor integration for mitochondrial transport, both proteins were compared to the pool of other proteins containing bipartite targeting signals. The demand on cofactor integration may be based on two conceivable reasons: First, the MTS of SO and cytochrome  $b_2$  may be considerably weaker than those of the other proteins, suggesting that the driving force exerted by the MTS might not be strong enough to complete translocation of the whole protein across the outer membrane. Second, the size of SO and cytochrome  $b_2$  might be larger, resulting in an incomplete translocation in spite of a functional mitochondrial targeting signal. Therefore, both parameters were compared among all mentioned proteins with bipartite targeting signals (Table 3.1). The matrix targeting capability of the proteins were thereby analyzed by MITOPROT II and the obtained percentages expressing the probability of matrix targeting were taken as an indicator for the strength of the N-terminal targeting signal (Dinur-Mills et al., 2008). While SO was predicted to contain a MTS with more than 90% probability, the MTS of cytochrome  $b_2$  revealed 83% prediction. SO and cytochrome  $b_2$  thereby achieve higher matrix localization scores than EndoG, Mcr1 and CPO. Since the MTS of all the compared proteins are sufficient for mitochondrial targeting as known so far, the scores obtained for SO and cytochrome  $b_2$  suggest that their MTS are likewise strong enough to permit complete mitochondrial import.

**Tab. 3.1 Comparison of IMS proteins with bipartite N-terminal targeting signals**

Protein	MTS prediction (%) <sup>1</sup>	Mature protein size (kDa)	species
SO	92.6	53	mouse
Cytb2	82.6	57	yeast
SMAC	98.7	24	mouse
EndoG	76.3	27	human
Mcr1	75	27	yeast
CPO	60	34	human

<sup>1</sup>Predictions according to Mitoprot II (Claros and Vincens, 1996)

Notably, SO and cytochrome  $b_2$  reveal a considerably larger size in their mature form compared to other proteins containing bipartite N-terminal targeting signals. These differences of more than 20 kDa could explain, why SO and cytochrome  $b_2$  may need cofactor integration as an additional driving force for translocation across the TOM complex. Since a hydrophobic stop-transfer signal arrests MTS-mediated translocation across the TIM complex, a long C-terminal end of the protein may not completely enter the IMS but remain exposed to the cytosol. Shorter C-termini may in contrast be completely imported into the IMS before translocation becomes arrested. The import of SO and cytochrome  $b_2$  may therefore represent a mechanism two ensure translocation of bigger soluble proteins into the

narrow IMS. As the comparisons of table 3.1 and the resulting hypothesis are based on only few known examples of proteins with bipartite targeting signals, an experimental verification would be essential and could be achieved by artificially elongating the C-terminus of SMAC/DIABLO, for instance. According to the outlined theory, increasing the size of the mature protein to more than 50 kDa should interfere with complete translocation across the TOM complex and result in partial C-terminal exposure to the cytosol.

The principle stated above does however not apply to proteins with bipartite targeting signals, which do not become cleaved but remain anchored in the inner mitochondrial membrane. Yeast Yme2 contains an N-terminal targeting signal followed by a single transmembrane domain and is therefore expected to be imported by a similar stop transfer mechanism (Neupert and Herrmann, 2007). The IMS domain of the protein thereby reveals a molecular weight of ~60 kDa. However, Yme2 is not soluble and anchoring in the inner membrane accompanied by lateral diffusion of the transmembrane domain may constitute a driving force towards the IMS, which may be analogous to cofactor mediated trapping of large soluble IMS proteins. Thus, also larger inner membrane proteins may well be imported based on this anchor-diffusion model (Glick et al., 1991). Similarly, the anchored SO-TIM50 chimera revealed only minor C-terminal exposure to the cytosol in absence of Moco. Anchoring seems in this case to replace cofactor triggered translocation across the outer membrane.

Taken together, mitochondrial proteins exposing large IMS domains and containing bipartite N-terminal targeting signals appear to require two distinct mechanisms for efficient mitochondrial import. The N-termini of these proteins are translocated based on N-terminal targeting signals, while the C-terminal domains seem to require additional driving forces for transfer across the TOM complex. The C-termini of integral inner membrane proteins may be imported based on the anchor-diffusion model, as already proposed by Glick et al. (1991), while large soluble IMS proteins seem to require cofactor-mediated folding for a vectorial transfer of the C-terminus across the outer membrane.

### **3.1.3 The role of heme and dimerization in the mitochondrial maturation of SO**

In spite of several striking similarities between the assembly mechanisms of SO and cytochrome  $b_2$ , the maturation of SO is more complex, which additionally requires integration of a second cytochrome  $b_5$  type heme cofactor. Therefore, and considering the related function of heme in the maturation of cytochrome  $b_2$ , the question arose of why only Moco but not heme can mediate the second part of SO import by trapping the protein in the IMS.

Integration of heme cofactors result in folding of the respective domains and have been shown to contribute to trapping of cytochrome *c* (Dumont et al., 1988) and cytochrome *b<sub>5</sub>* (Esaki et al., 1999) in the mitochondrial IMS. These data suggest that following heme incorporation into proteins, reverse translocations to the cytosol are prohibited.

Nevertheless, SO was not trapped in mitochondria when Moco was not present, allowing the conclusion that heme integration could not rescue SO localization or that heme integration was prohibited. Considering the observations of Esaki et al. (1999), the principle capability of the SO heme cofactor to mediate trapping was analyzed. The isolated heme domain was only efficiently targeted to mitochondria upon heme integration, while heme depletion resulted in a diffuse cellular distribution of the construct. The mechanisms triggering the non-mitochondrial localization of the heme domain in absence of its cofactor may follow the cofactor-dependent mitochondrial trapping of the small IMS proteins. After processing, the isolated heme domain accounts for a molecular weight of ~10 kDa and seems, in analogy to the small IMS proteins, to bi-directionally diffuse through the TOM complex if not folded. These observations confirmed that following heme-mediated folding of the SO heme domain, a reverse translocation to the cytosol is prevented. Thus, upon hypothetical integration of heme into the N-terminal heme domain in absence of Moco, at least the heme domain of full-length SO should remain mitochondrial. The diffuse cellular distribution of SO in absence of Moco in contrast suggests that SO entirely leaves mitochondria if Moco is not present.

In conclusion, the heme cofactor seems not to be efficiently incorporated into SO *in vivo* if Moco is not present and therefore does not rescue the mitochondrial localization of SO. In contrast to the *in vivo* situation in HEK cells, overexpression of Moco-deficient SO in *E. coli* revealed the incorporation of heme, demonstrating that heme integration is not strictly dependent on prior Moco incorporation. However, recombinantly expressed SO is accumulating in *E. coli* and therefore constantly exposed to heme integration. In contrast, when expressed in mammalian cells, the reverse translocation from mitochondria in absence of Moco kinetically competes with heme integration. Assuming that heme integration is a kinetically less favored event in absence of Moco, SO would integrate heme in *E. coli* due to high expression and accumulation, but would not incorporate heme *in vivo* where the reverse translocation occurs presumably faster than heme integration. Given the fact that 30% of the Moco-deficient SO was located to mitochondria, heme integration might have occurred in those cases preventing the retrograde backshift of a fraction of SO in absence of Moco. Therefore, the presence of the apo-SO Moco binding domain appears to slow down heme integration significantly and ultimately Moco insertion becomes the rate limiting step in the overall SO maturation process.



Apart from prosthetic groups, oligomerization events are also conceivable to contribute to trapping mechanisms of proteins in the IMS. Given the fact that a monomeric variant of SO localized to mitochondria, oligomerization does not seem to be required for mitochondrial retention of SO. Since Moco-deficient SO mainly forms monomers, Moco integration apparently presents a prerequisite for dimerization, thus inducing structural rearrangements of the dimerization domain allowing oligomerization. In contrast to heme integration, which can occur upon overexpression in *E. coli* in absence of Moco, efficient dimerization appears to be strictly dependent on prior Moco integration.

The overall *in vivo* maturation of SO therefore is subject to a molecular hierarchy. The integration of Moco thereby occurs first, which is in line with the crystal structure of holo SO, demonstrating that Moco is deeply buried within the protein (Kisker et al., 1997). In this respect, Moco was previously proposed to be either incorporated prior to or during completion of SO folding and dimerization (Mendel, 2007). Upon Moco binding, integration of heme and dimerization can occur efficiently, while both events do not seem to depend on each other, since heme deficient SO revealed adequate dimerization and monomeric SO displayed regular heme integration.

### 3.1.4 Processing of SO in the IMS

Following N-terminal translocation across the inner membrane, SO was shown in this study to be processed by the IMP complex in order to become released as a soluble protein. This was determined by shRNA mediated knockdown of the *IMMP1* gene product and co-expression of SO in HEK-293 cells. Considering the half-life of endogenous SO being approximately four days (Ono and Ito, 1982a), the effect of 24 h IMP1 downregulation were only apparent upon the transient expression of SO following transfection.

SO far, not many other mitochondrial proteins are known to be processed by this protease and all hitherto characterized substrates were identified in *S. cerevisiae*. The only identified yeast substrates are the mitochondria encoded Cox2, which is co-translationally inserted into the inner membrane by Oxa1 prior to Imp-mediated processing (Ott and Herrmann, 2010), nuclear encoded Mcr1 (Hahne et al., 1994), Gut2 (Esser et al., 2004), cytochrome *c*<sub>1</sub> and cytochrome *b*<sub>2</sub> (Nunnari et al., 1993). In addition, the murine variant of SMAC/DIABLO was shown to be processed by the IMP complex in *S. cerevisiae* (Burri et al., 2005).

In the current study, the identification of SO as a novel substrate of the IMP complex occurred in a mammalian system and therefore represents the first experimental confirmation

of a functional IMP complex in mammals. IMP1, which was shown by downregulation of its mRNA to mediate processing of SO, does not follow obvious consensus motifs for cleavage (Chen et al., 1999). The precise IMP cleavage site within the SO protein is unclear, while the unprocessed SO-TIM50 chimera suggested processing to occur between residues 66-86. Further, the crystallization of mature chicken SO purified from liver tissue revealed residues 1-80 not to be present in the mature protein, suggesting IMP cleavage to take place adjacent to residues 80 of chicken SO (Kisker et al., 1997).

Cytochrome  $b_2$  was shown to be processed in two steps, with MPP mediated cleavage of the matrix exposed N-terminus preceding IMP cleavage in the IMS (Gasser et al., 1982). Such a double cleavage was suggested to occur for all proteins with bipartite targeting signals (Schmidt et al., 2010) and may also apply for SO maturation. This could be further investigated by purification of MPP and incubation with SO precursors *in vitro* or by shRNA-mediated downregulation of MPP in cell culture in order to monitor potential changes of the SO processing pattern.

Efficient IMP cleavage of cytochrome  $b_2$  is dependent on a correctly folded heme domain that is stabilized by the bound cofactor (Glick et al., 1993). IMP-mediated processing of SO in contrast does not seem to require cofactor-mediated folding but can occur before Moco integration into SO, since SO was released as a soluble protein from mitochondria in absence of Moco. Thus, integrating IMP cleavage into the hierarchy of SO assembly, Moco integration and processing seem to occur independent on each other.

### 3.1.5 Moco stabilization

As isolated Moco has been shown to be intrinsically instable (Deistung and Bray, 1989), its cellular transport and stabilization following its cytosolic synthesis has been subject to intensive debates in the past (Hille, 2002, Schwarz and Mendel, 2006, Mendel, 2007). Fast association of Moco with either its apo-proteins or stabilizing Moco binding proteins has been proposed and could occur co-translationally in the cytosol (Schwarz et al., 2009). Co-translational integration into the family of mitochondrial Moco-enzymes would however interfere with mitochondrial transport and consistently, the findings of the current study support a selective association of SO and Moco in the mitochondrial IMS. The functional trapping of SO demonstrates that Moco associated with SO does not cross the TOM channel and remains inside mitochondria. In addition, the folded monomeric Moco-containing domain of SO comprises a diameter of approximately 4 nm (Kisker et al., 1997), while the diameter of the open pore of the TOM complex accounts for a maximum of only 2 nm (Ahting et al., 1999). A combined import of any Moco-SO complex across the TOM pore therefore appears

to be very unlikely, but SO and Moco rather seem to enter mitochondria independently. In the cytosol, Moco association with SO presumably is prohibited by association of chaperones to SO, which keep the latter in an import competent state. This further raises the question of how Moco is stabilized during its transport to mitochondria. In the green algae *Chlamydomonas reinhardtii*, a Moco carrier protein was identified (Fischer et al., 2006a) and a novel class of Moco-binding proteins was recently reported for *Arabidopsis thaliana* (Kruse et al., 2010). Similar Moco-binding chaperons, which stabilize Moco and promote Moco insertion into apo-proteins, were however not found in animals so far. Alternatively, Moco may be stabilized in the reducing environment of the animal cell for some time and thereby passively diffuse into the mitochondrial IMS.

The quantitative analysis of the mitochondrial Moco population revealed an uncharacterized pool of SO-independent Moco, which approximately corresponded to the same amount of Moco as bound by SO. Both mARC proteins are expected to contribute significantly to this population of Moco, thus potentially indicating mitochondria to lack further abundant Moco proteins or significant populations of free Moco. This in turn suggests a rapid association of Moco with its mitochondrial apo-enzymes and is in line with the proposed immediate association of SO and Moco to ensure trapping in the IMS.

### 3.1.6 Assembly and maturation of SO

The findings of the first part of this study in aggregate allowed to build a model summarizing the complex mitochondrial maturation of SO (Figure 3.1). SO and Moco are synthesized in the cytosol and become transferred to mitochondria separately.

While Moco may enter the IMS by passive diffusion through porins of the outer mitochondrial membrane, SO is actively imported to mitochondria based on its bipartite N-terminal targeting signal. The ATP- and membrane-potential dependent translocation across the inner mitochondrial membrane is arrested by a hydrophobic stop-transfer motif downstream of the N-terminal matrix signal (Ono and Ito, 1982b).

SO is subsequently released from the inner membrane by IMP mediated cleavage to generate a soluble protein. In absence of Moco, this results in reverse translocation of SO to the cytosol, as SO translocation across the outer membrane is not completed if Moco is not present. Alternatively, binding of Moco initiates SO folding and constitutes an additional driving force for a vectorial translocation of the SO C-terminal domain across the TOM complex. Following Moco insertion into SO and completion of import, heme integration and homodimerization occur independent on each other to accomplish the hierarchical assembly of SO.

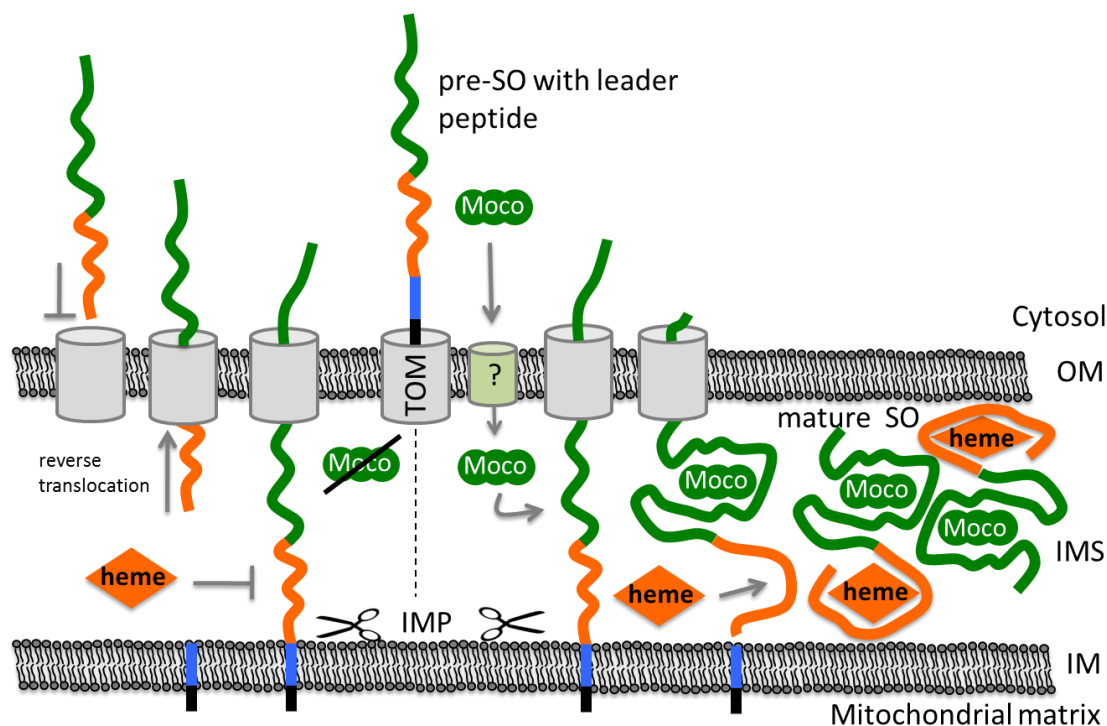


**Figure 3.1 Assembly and maturation of mammalian SO.** SO is depicted with its N-terminal targeting signal (black), its hydrophobic stop-transfer signal (blue), its heme domain (orange) and the Moco- and dimerization domain (green). See text for details. IM, inner membrane; IMP, inner membrane peptidase; IMS, IMS; OM, outer membrane; TOM, translocase of the outer membrane.

## 3.2 Sub-cellular localization and sorting of human mARC1

### 3.2.1 Localization of mARC1 to the outer mitochondrial membrane

In a screen for the missing third component of the pro-drug activating N-reductive system, mARC2 was identified as the fifth eukaryotic Moco-containing enzyme (Havemeyer et al., 2006). It was isolated from enriched outer mitochondrial membrane fractions and consistently, mARC2 was recently detected in purified rat liver outer mitochondrial membranes (Neve et al., 2012). Contradictingly, mARC2 was also identified during a large scale proteomic characterization of mouse liver inner mitochondrial membranes (Da Cruz et al., 2003). Furthermore, the subcellular localization of a close homologue, mARC1, has not been studied so far. However, the high degree of similarities to mARC2 in respect to sequence and function strongly suggests a similar subcellular distribution of both enzymes.

In the second part of this work, the sub-cellular localization of mARC1 was determined and revealed its integration into the outer mitochondrial membrane. This was shown by PK and trypsin treatments of purified mitochondria, which resulted in degradation

of mARC1 from intact mitochondria. The depletion of full-length mARC1 following PK exposure was accompanied by the simultaneous appearance of a truncated fragment of about 30 kDa. The very weak intensity of the corresponding protein band after PK treatment suggested, that this fragment has derived from incomplete degradation of the cytosolic C-terminal core of mARC1, which presumably reflects the tight folding of this domain. However, swelling of the outer mitochondrial membrane resulted in complete degradation of mARC1 and also prevented formation of the truncated fragment seen upon PK treatment of intact mitochondria. The more efficient degradation of mARC1 following outer membrane disruption may be attributed to the increased PK accessibility of the protein, which would be reflected by the concomitant degradation of the protein from both terminal ends.

Furthermore, the size of the truncated fragment following PK treatment appears about 5 kDa smaller than the full-length protein, while a protease protected fragment seen upon a hypothetical inverse  $N_{(out)}-C_{(in)}$  membrane orientation of mARC1 is expected to be 2 kDa smaller than the full-length fragment. The difference of 5 kDa may well be attributed to the size of the N-terminal targeting signal and the transmembrane domain, suggesting PK to cleave efficiently between transmembrane domain and the folded cytosolic core of the catalytic mARC1 domain.

In conclusion, mARC1 was defined to expose its C-terminal core domain to the cytosol, while the soluble N-terminus is facing the mitochondrial IMS.

Assuming a similar localization of mARC1 and mARC2, these results are in line with the previous studies detecting mARC2 in purified outer membrane fractions (Havemeyer et al., 2006, Neve et al., 2012). The mitochondrial protease treatment approach conducted in this study in addition addressed and clarified the membrane orientation of mARC 1 and thus for the first time affords a comprehensive view of mARC protein localization. The enzymatic activity of mARC requires its integration into a three-component enzyme system, in which electrons are transferred from NADH cytochrome  $b_5$  reductase via cytochrome  $b_5$  to mARC (Wahl et al., 2010). Both, NADH cytochrome  $b_5$  reductase (Borgese and Pietrini, 1986, Borgese et al., 1996) as well as cytochrome  $b_5$  (Fukushima et al., 1972, Ito, 1980) are well-known components of the outer mitochondrial membrane exposing their catalytic domains to the cytosol. The current findings of an  $N_{(in)}-C_{(out)}$  orientation of mARC1 in the outer mitochondrial membrane are thus in well agreement with the catalytic interplay of the three components, which all expose their functional domains to the cytosol to build an efficient inter-molecular electron transport chain.

### 3.2.2 Targeting of mARC1 to the outer mitochondrial membrane

The localization of mARC1 to the outer mitochondrial membrane is defined by its N-terminal region, which is composed of a weak MTS and a downstream transmembrane domain. Fusion of the transmembrane domain with GFP revealed the latter to be sufficient for mitochondrial sorting of mARC1. Considering its N-terminal transmembrane segment, which is required for targeting and membrane anchoring, mARC1 is classified as a novel and only the fifth known signal-anchored protein. All members of this small group of proteins share anchoring to the outer mitochondrial membrane based on their N-terminal transmembrane domains (Shore et al., 1995). In analogy to mARC1, the transmembrane segment of signal-anchored proteins is in most cases sufficient for mitochondrial targeting, which was also found for TOM20 (Kanaji et al., 2000) and TOM70 (Suzuki et al., 2002) as two prominent representatives of this protein family.

Although the transmembrane domain is adequate for correct sorting when fused to GFP and recombinantly expressed in HEK-293 cells, the N-terminus of mARC1 contains an additional MTS. This motif is comparatively weak, as illustrated by the inefficient mitochondrial sorting of a fusion of residues 1-20 to GFP and the presence of only two basic residues with a much less amphipathic character compared to other classical N-terminal MTS (Table 3.2) (Neupert and Herrmann, 2007). In previous studies, the soluble N-terminal domain upstream of the transmembrane segment of signal-anchored proteins was shown to have supportive functions by increasing the efficiency of targeting, which is primarily mediated by the transmembrane domain. Investigations of a fusion of dihydrofolate reductase with the N-terminal bitopic domain of yeast Tom70 revealed the three basic residues upstream of the transmembrane segment to enhance the rate of outer membrane insertion (McBride et al., 1992). In spite of similarities to the N-terminus of mARC1, the N-termini of other signal-anchored proteins could however not be shown to be autonomous MTS. This is also illustrated by the parameters depicted in table 3.2, in which the soluble N-termini of all currently known signal-anchored proteins are compared. The parameters of the MTS of SO, TIM50, SMAC and cytochrome  $b_2$  (Cytb2) are also shown in the table for better comparability (shaded blue).

Predictions conducted by MITOPROT II revealed the mARC1 N-terminus to constitute a MTS with 65% probability. This was clearly below the values calculated for SO, TIM50, SMAC as well as Cytb2 and is thus in line with the less number of basic residues and the weak mitochondrial targeting efficiency of residues 1-20 of mARC1 when fused to GFP. The MTS predictions of mARC1 in contrast exceed the scores obtained for the N-termini of

Tom70, TOM20 and OM45. Since the number of basic residues is quite similar among mARC1 and the latter three components and all proteins exhibit the same subcellular localization, the weak N-terminal MTS of mARC1 may have similar supportive functions during mitochondrial targeting.

**Tab. 3.2 Analysis of matrix-targeting capability of different protein N-termini**

Protein	compartment	size (residues) <sup>1</sup>	MTS prediction (%) <sup>2</sup>	basic residues	species
mARC1	OM	20	65	2	human
Tom70	OM	10	35	3	yeast
TOM20	OM	5	20	1	human
OM45	OM	5	40	1	yeast
Mcr1	OM/IMS	11	75	4	yeast
SO	IMS	20	92.6	4	mouse
TIM50	IM	27	99.3	5	human
SMAC	IMS	20	97.9	4	human
Cytb2	IMS	27	82.6	7	yeast

<sup>1</sup>Soluble domains N-terminal of transmembrane segments

<sup>2</sup>Predictions according to Mitoprot II (Claros and Vincens, 1996)

Consequently, the mARC1 N-terminus may thus function as a primary receptor for the outer mitochondrial membrane, as described for the analogous segments of other signal-anchored proteins such as TOM70 and TOM20 (McBride et al., 1992, Kanaji et al., 2000, Suzuki et al., 2002). The similarities between the soluble N-termini of mARC1 and other signal-anchored proteins suggest a smooth transition between outer membrane receptor and weak MTS of signal-anchored proteins. In any case, the downstream transmembrane domain seems to ensure correct localization and to suppress potential weak matrix signals within the upstream segment, which do thus not affect import in a conventional manner and ultimately not drive the protein to the mitochondrial matrix. Yeast Mcr1 is another signal-anchored protein with higher MTS scores than mARC1 which will be discussed later.

The mechanisms by which signal-anchored proteins enter the outer mitochondrial membrane are not completely understood. The import of TOM20 and TOM70 was however shown not to essentially require pre-existing primary TOM20 and TOM70 receptors (Ahting et al., 2005) and OM45 was recently shown to adopt a helical transmembrane conformation in artificial bilayers (Merklinger et al., 2012). Since signal-anchor domains of the known signal-anchored proteins are functionally interchangeable (Ahting et al., 2005), Dukanovic and Rapaport (2011) proposed a common initial membrane insertion step of all signal anchored proteins.

While TOM20 and TOM70 are thought to require a pre-existing TOM complex for correct assembly after their initial membrane insertion, the TOM complex was proposed to be dispensable for the assembly of the other signal-anchored proteins (Dukanovic and Rapaport, 2011). Accordingly, mARC1 may also insert into an artificial bilayer in absence of the TOM complex, while its N-terminal targeting signal suggests an interaction to the primary import receptors TOM20 and TOM22. Potential interactions of mARC1 to the primary TOM import receptors could be probed *in vitro* following heterologous expression and purification of TOM20/22 fragments and mARC1, respectively. Binding could be analyzed by pull-down and immunoprecipitation experiments or biochemically characterized by isothermal titration calorimetry and surface plasmon resonance spectroscopy. Alternatively, cross-linking during *in vitro* import of mARC1 with subsequent co-immunoprecipitations could be used to identify interactions to any TOM components.

These putative interactions to the primary TOM receptors seem not to be strictly essential, as the mARC1 transmembrane domain was shown to be an autonomous targeting signal, but they may increase the efficiency of targeting. Still, a fusion of the mARC1-transmembrane domain with GFP revealed a complete mitochondrial localization in cell culture, indicating an efficient mitochondrial targeting even in absence of the N-terminal MTS. However, considering the extended two-days expression of the construct in cell culture, the long cellular accumulation of the construct may finally result in a comprehensive mitochondrial localization. This system may therefore not be sensitive enough to detect potential decreased mitochondrial targeting efficiencies due to the lack of a functional IMS. The cooperating effect of the mARC1-MTS could rather be experimentally tested by repeating the *in vitro* import experiments with a truncated mARC1 variant lacking residues 1-20 or with a variant in which both positively charged residues of the MTS are exchanged by a neutral residue. The time dependent formation of the high-oligomeric complexes seen upon *in vitro* mitochondrial import could then be taken as a measure for the efficiency of complex formations in WT and truncated mARC1 variants.

It is currently unknown, if signal anchored proteins become membrane inserted co- or post-translationally, but the N-terminal MTS of mARC1 may facilitate immediate transfer of the translating ribosome to mitochondria and an efficient and rapid insertion into the outer mitochondrial membrane.



### 3.2.3 Outer membrane targeting of mARC1 vs inner membrane sorting of SO

A comparison of the primary structures of mARC1 and SO reveals surprising similarities, as both mitochondrial Moco enzymes share an N-terminal MTS followed by a hydrophobic transmembrane domain. Interestingly, these related N-terminal motifs confer different sub-mitochondrial localizations of both proteins, with the transmembrane domain of SO traversing the inner mitochondrial membrane and mARC1 being anchored in the outer membrane.

What are the mechanistic frameworks determining inner or outer mitochondrial membrane localization of SO and mARC1, respectively? And what are the parameters defining inner or outer membrane insertion of signal-anchored proteins and proteins with bipartite targeting signals in general?

SO and mARC1 are directed to their destined membrane solely based on their N-terminal regions, which thus also define association to the inner or outer membrane. The MTS were already compared in table 3.2, now the transmembrane segments of both proteins as well as of other signal-anchored proteins or inner membrane/IMS proteins with a bipartite targeting signal are compared in table 3.3. Depicted hydrophobicity scores were calculated with the program HydroMCalc (Tossi et al., 2002).

**Tab. 3.3 TM domain comparison between signal-anchored proteins and inner membrane/IMS proteins with bipartite targeting signals**

Protein	Compartment	Hydrophobicity <sup>1</sup>	size (residues)	species
mARC1	OM	2.4	20	human
Tom70	OM	1.02	18	yeast
TOM20	OM	1.71	18	human
OM45	OM	1.43	17	yeast
Mcr1	OM/IMS	2.01	20	yeast
SO	IMS	2.78	17	mouse
TIM50	IM	2.77	20	human
SMAC	IMS	1.22	19	human
Cytb2	IMS	1.38	17	yeast
Cue1	ER	4.58	19	yeast

<sup>1</sup>Predictions according to (Tossi et al., 2002)

The calculations of table 3.3 reveal the signal-anchored proteins TOM20, Tom70 and OM45 to contain a transmembrane segment of moderate hydrophobicity. Considering the lack of a functional MTS, these proteins do not receive a driving force towards the inner mitochondrial membrane but insert into the outer membrane. The mARC1 protein displays a stronger MTS prediction than other signal-anchored proteins, which appears to be balanced

by a more hydrophobic transmembrane domain, ultimately resulting in the same submitochondrial localization. SO and other proteins with bipartite targeting signals residing in the inner membrane or the IMS are characterized by even stronger N-terminal MTS. The hydrophobicity scores of the transmembrane domains appear divergent, with SO revealing a comparably strong value, while the transmembrane segments of SMAC or cytochrome *b*<sub>2</sub> depict only moderate degrees of hydrophobicity.

Comparing mARC1 with SO or the other proteins containing bipartite targeting motifs, mARC1 contains a weaker MTS, which is apparently not sufficient to drive the downstream transmembrane motif across the outer mitochondrial membrane. A weak MTS as seen for mARC1 seems to result in transmembrane domain mediated insertion into the outer mitochondrial membrane, while, as illustrated by SO, a stronger MTS may even translocate a more hydrophobic transmembrane segment across the outer membrane. Targeting to the inner or outer mitochondrial membrane may thus be regulated by the opposing forces of MTS and transmembrane domain.

In this context, yeast Mcr1 is a very interesting intermediate protein. Similar to SO and mARC1, Mcr1 contains an N-terminal MTS and a downstream transmembrane domain, which were shown to mediate dual localization of the protein to the outer membrane and to the IMS (Hahne et al., 1994). This is achieved by two distinct import mechanisms, with the intermembrane space form of Mcr1 entering the Tom40 import channel and being transported to the Tim23 complex, while the outer mitochondrial membrane isoform is inserted independent on Tom40 or the primary Tom import receptors (Meineke et al., 2008). These two independent mechanisms suggest that sorting of both isoforms diverge early, already before entering the TOM complex.

Notably, this dual distribution is also reflected in the parameters of tables 3.2 and 3.3. The MTS of Mcr1 appears to be stronger than the MTS of all other signal-anchored proteins including mARC1, but weaker than the motifs of the proteins with classical bipartite targeting signals. The hydrophobicity scores of the Mcr1 transmembrane domain likewise reveal intermediate values, which seem to be low enough to allow passage of a proportion of the proteins across the outer membrane, but also strong enough to permit retention of a sub-population of the proteins in the outer mitochondrial membrane. Consistent with this hypothesis, weakening the hydrophobicity of the Mcr1 transmembrane domain by mutating two alanines in the middle of the hydrophobic motif against glutamine prevented outer membrane arrest and caused a complete IMS localization of the protein (Haucke et al., 1997).

These mechanistic insights into Mcr1 trafficking further support the concept of the outer membrane localization of mARC1 compared to the inner membrane/IMS localization of SO to be controlled by the strength of the MTS and the degree of hydrophobicity within the downstream transmembrane domain. However, the import pathways of both Mcr1 isoforms are subject to two distinct mechanisms and membrane insertions of signal-anchored proteins are independent of the TOM complex. Further, a lateral opening of TOM40 was not observed so far and is under debate due to thermodynamic considerations (Rapaport, 2005). In aggregate, sorting of signal-anchored proteins and proteins with bipartite targeting-signals might be based on the strengths of the parameters shown in tables 3.2 and 3.3, while sensing these signals and sorting decisions must occur before translocation or membrane insertion, respectively, initiates.

As only five signal-anchored proteins and a limited number of proteins with bipartite targeting signals are known, the quantitative significances of the analyses shown in tables 3.2 and 3.3 are rather low. The outlined coherencies could therefore be experimentally tested by introducing additional basic residues into the mARC1-MTS or by exchanging the mARC1-MTS against the stronger MTS of SO. According to the hypothesis stated above, increasing the strength of the mARC1-MTS would cause inner membrane targeting of the modified protein. Alternatively, weakening of the SO-MTS might result in a premature arrest of SO-translocation in the outer mitochondrial membrane.

The sorting of mARC1 and other signal-anchored proteins to the outer mitochondrial membrane does not only have to be differentiated from inner membrane targeting, but also from mislocalization to the ER. Targeting to the ER is based on strongly hydrophobic motifs (Hegde and Keenan, 2011). Cue1 was chosen as a representative for a signal-anchored protein of the ER membrane (Biederer et al., 1997) and the hydrophobicity scores depicted in table 3.3 reveal a significantly higher hydrophobicity of Cue1 compared to all mitochondrial membrane proteins. Consistent with these differences, increasing the hydrophobicity of transmembrane segments of signal-anchored proteins has been shown to cause mislocalization to the ER (Waizenegger et al., 2003). Furthermore, Merklinger et al. (2012) observed that insertion of OM45 into artificial lipid bilayers is significantly increased when exposing the protein to an outer membrane-like lipid composition compared to a bilayer with ER-like lipid composition. This suggests that apart from the degree of hydrophobicity, target-membrane compositions may also constitute cellular sorting-signals for signal-anchored proteins.

The cellular trafficking of mARC1 and other signal-anchored proteins thus appears to be subject to a fine-tuned mechanism, with minor modifications in the N-terminal domain or the target membrane potentially causing protein mislocalizations.

### 3.2.4 *In vitro* import of mARC1

The *in vitro* characterization of the mitochondrial import of mARC1 revealed characteristics typical for proteins residing in the outer mitochondrial membrane (Dukanovic and Rapaport, 2011). Therefore, mARC1 was not processed during import and did not require a membrane potential across the inner mitochondrial membrane. This is consistent with a supportive function of the mARC1-MTS in mediating efficient outer membrane targeting of the protein, rather than a conventional and membrane potential-dependent role of the MTS in mitochondrial import of mARC1. The depletion of external ATP from the import buffer however significantly interfered with successful targeting of mARC1. ATP might be required for the release of mARC1 from cytosolic chaperons and thereby being essential for an efficient integration into the outer membrane. A similar role of external ATP during mitochondrial import has been described earlier for other membrane-anchored proteins (Wachter et al., 1994).

Interestingly, membrane integration of mARC1 resulted in the formation of high-oligomeric complexes as depicted by BN-PAGE following *in vitro* import or 48 h expression of mARC1 in cell culture, suggesting that mARC1 is part of these complexes in its final and active form. Given the molecular weight of mARC1, cytochrome *b*<sub>5</sub> reductase and cytochrome *b*<sub>5</sub> (total ~90 kDa), one can speculate that these three proteins might form a large multimeric complex with several copies per subunit. However, mARC1 and cytochrome *b*<sub>5</sub> reductase have been shown to be monomeric following expression in *E. coli*, while cytochrome *b*<sub>5</sub> revealed the formation of homo-dimeric complexes (Wahl et al., 2010). Alternatively, mARC1 may be part of a so far unknown membrane-bound multienzyme complex hosting other yet to be identified proteins. Isolation and characterization of these complexes could occur by co-immunoprecipitation of mARC1 with subsequent mass-spectrometric identifications of the co-precipitated components. The identified candidates could in the next steps be confirmed by appropriate and specific antibodies, which would be added to the mitochondrial *in vitro* import reactions of mARC1 prior to BN-PAGE analyses. Assuming a co-association of mARC1 and the respective candidate protein in the same complexes, addition of the antibodies should result in a shift of the complex seen on BN-PAGE. Another strategy to confirm potential components of the high-oligomeric structures could involve cross-linking of the complexes with subsequent identification of the proteins by western blotting using specific antibodies.

### 3.2.5 Assembly and maturation of mARC1

In summary, the findings of the second party of this study, the mitochondrial maturation of mARC1, can be illustrated in a model (Figure 3.2).

Following its cytosolic translation, mARC1 may be bound by chaperones guiding the protein to the outer mitochondrial membrane and preventing the transmembrane domain from being exposed to the cytosol. Release from chaperones might thus represent the ATP-dependent step of the mitochondrial import of mARC1. Insertion into the outer mitochondrial membrane is triggered by the N-terminal region of mARC1, which is composed of a weak MTS and a downstream transmembrane domain.

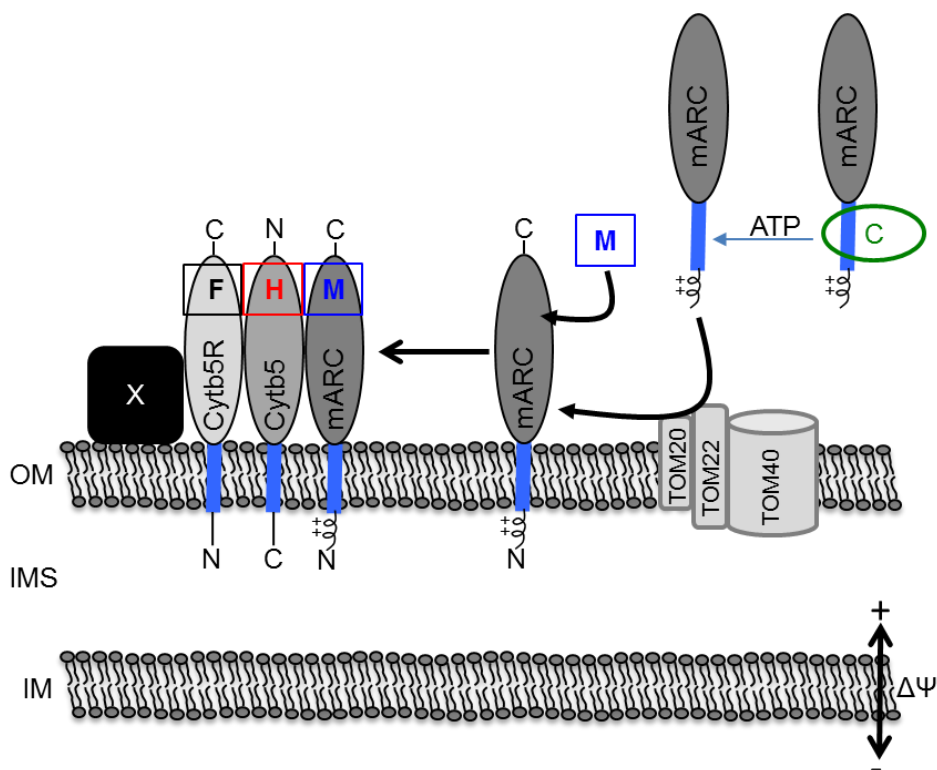


**Figure 3.2 Assembly and maturation of human mARC1.** mARC1 is depicted with its N-terminal targeting signal (black), its transmembrane domain (blue) and its catalytic core (dark gray). mARC1 is part of unknown multiprotein complexes (X) in the outer mitochondrial membrane. Cytochrome  $b_5$  reductase (Cytb5R) and cytochrome  $b_5$  (Cytb5) are shown with their transmembrane domains (blue). See text for details. C, chaperone (green circle); F, flavin adenine dinucleotide; H, heme; IM, inner membrane; IMS, IMS; M, Moco; OM, outer membrane; TOM, translocase of the outer membrane.

The MTS is supposed to function as a supportive receptor for the outer mitochondrial membrane and considering the known interactions of these motifs with the primary TOM receptors, the mARC1-MTS might initially interact with TOM20 and TOM22 to afford first contacts between the protein and its target membrane. The membrane insertion of mARC1

occurs membrane potential independently and is mediated by the transmembrane domain, which constitutes the targeting signal and membrane anchor, thus defining mARC1 as a novel signal-anchored protein of the outer mitochondrial membrane.

Thereby, mARC1 exposes its catalytic core domain to the cytosol and presumably integrates Moco after insertion into the outer membrane in analogy to the unfolded translocation of all mitochondrial proteins. Following membrane insertion and Moco integration, mARC1 builds an intermolecular electron-transport chain with cytochrome  $b_5$  reductase and cytochrome  $b_5$  but also forms high-oligomeric structures of currently unknown identity.

## **4 Material and methods**

### **4.1 Material**

#### **4.1.1 Organisms**

Different prokaryotic and eukaryotic organisms were used during the current study. *E. coli* cells were used for plasmid amplification and protein expression and are listed in table 4.1. Mammalian cells were used for localization studies and protein expression and are listed in table 4.2., while *N. crassa* cells (table 4.3) were used for *nit-1* reconstitution assays.

**Tab. 4.1 *E. coli* cells used in this study**

Strain	Reference	Genotype	Purpose
DH5 $\alpha$	(Hanahan, 1983)	<i>F</i> -, <i>supE44</i> , $\Delta$ <i>lacU169</i> , ( $\phi$ 80 <i>lacZ</i> $\Delta$ <i>M15</i> ), <i>hsdR17</i> , <i>endA1</i> , <i>gyrA96</i> , <i>thi-1</i> , <i>relA1</i> , <i>recA56</i>	Plasmid amplification
TP1000	(Palmer et al., 1996)	<i>F</i> -, $\Delta$ <i>lacU169</i> , <i>araD139</i> , <i>rpsL150</i> , <i>relA1</i> , <i>ptsF</i> , <i>rbsR</i> , <i>flbB</i> , ( $\Delta$ <i>mobAB</i> )	Protein expression in <i>E. coli</i>
BL21	(Weiner et al., 1994)	<i>F</i> -, <i>ompT</i> , <i>hsdS</i> ( <i>rB-mB</i> -), <i>dcm</i> +, <i>Tetr</i> , <i>gal</i> $\lambda$ ( <i>DE3</i> ), <i>endA</i> , <i>The</i> [ <i>argU</i> , <i>proL</i> , <i>camr</i> ]	Protein expression in <i>E. coli</i>

**Tab. 4.2 Mammalian cells used in this study**

Strain	Reference	Description	Purpose
HEK-293	(Graham et al., 1977)	Human embryonic kidney cells	Protein localization, mitochondrial purification, general protein expression
<i>MOCS1</i> -/- fibroblasts	Jochen Reiss, University of Göttingen	Human fibroblasts, $\Delta$ <i>MOCS1</i>	Protein localization
WT fibroblasts	Jochen Reiss, University of Göttingen	Human fibroblasts, WT	Protein localization
HEP-G2	(Knowles et al., 1980)	Human liver carcinoma cells	Protein localization
HeLA cells	(Scherer et al., 1953)	Human cervical carcinoma cells	Protein localization

**Tab. 4.3 *N. crassa* cells used in this study**

Strain	Reference	Genotype/description	Purpose
<i>nit-1</i>	(Nason et al., 1971)	FGSC : 34, allele : 34547, mating type : a/A linkage group: IR, genetic background : M, mutagen : UV	<i>nit-1</i> reconstitution assay

#### 4.1.2 Plasmids

Empty plasmids (table 4.4) from different companies were used for cloning and subsequent expression of proteins.

**Tab. 4.4 Plasmids used in this study**

Plasmid	Resistance	Source	Purpose
pQE80	Ampicillin	Qiagen	Protein expression in <i>E. coli</i>
pcDNA3.1 myc/HisA	Ampicillin	Invitrogen	General protein expression in mammalian cells, protein localization studies
pEGFP-N1	Kanamycin	Clontech	Protein localization
pJET1.2	Ampicillin	Fermentas	Expression of IMMP1I shRNA

#### 4.1.3 Enzymes and chemicals

Enzymes for cloning and DNA modifications were purchased from Fermentas, New England Biolabs, Roche and Stratagene. Cell culture media and buffers were purchased from PAA laboratories. Chemicals and solutions were obtained from Applichem, Biomol, Fluka, Merck, MP Biomedicals, Promega, Riedel deHaen, Roche, Roth, Serva, Sigma-Aldrich and VWR-Prolabo.



#### 4.1.4 Antibodies

Different primary (table 4.5) and secondary (table 4.6) antibodies from different companies were used for western blot detection or immunocytochemistry.

**Tab. 4.5 Primary antibodies used in this study**

Antibody	Dilution	Source	Application
Mouse monoclonal to SO	1:1000	Abcam	Western blot, immunocytochemistry
Mouse monoclonal to actin	1:400	Santa Cruz	Western blot
Rabbit polyclonal to IMMP1L	1:500	Abgent	Western blot
Rabbit polyclonal to MOSC1	1:1000	Abcam	Western blot
Rabbit polyclonal to smac/diablo	1:1000	Abcam	Western blot
Mouse monoclonal to VDAC	1:1000	Abcam	Western blot
Mouse monoclonal to gephyrin (3B11)	1:20	(Smolinsky et al., 2008)	Western blot
Mouse monoclonal to myc-tag (9E10)	1:5	Cell supernatant	Western blot, immunocytochemistry
Rabbit polyclonal to GFP	1:1000	Abcam	Western blot
Mouse monoclonal to HSP60	1:2000	Biomol	Western blot
Rabbit polyclonal to MFN2	1:1000	Sigma	Western blot
Mouse monoclonal to COX4	1:500	Santa Cruz	Western blot

**Tab. 4.6 Secondary antibodies used in this study**

Antibody	Dilution	Source	Purpose
Goat anti-mouse HRP coupled	1:10000	Santa Cruz	Western blot
Donkey anti-rabbit HRP coupled	1:10000	Pierce	Western blot
Alexa Fluor 488 anti-mouse	1:200	Invitrogen	Immunocytochemistry

## 4.2 Methods

### 4.2.1 Biochemical methods

#### 4.2.1.1 Expression of recombinant SO variants in *E. coli*

Different variants of mouse SO were expressed in *E. coli* strain TP1000 in this study. Therefore, the respective plasmids were transformed into the *E. coli* cells, which were then plated on agar medium. Single colonies were selected and grown over night at 37°C in LB medium (10 g/l tryptone, 10 g/l NaCl, 5 g yeast extract/l) containing the respective antibiotics (100 µg/ml ampicillin, 25 µg/ml kanamycin). 50 ml of precultures were each added to 3l of main cultures, which were grown for 3 h at 25°C and 90 rpm shaking. Expressions of SO variants were induced by the addition of 0.1 mM IPTG and 150 µM Na-molybdate and cells were harvested after further 48 h incubation at 25°C and 90 rpm shaking.

#### 4.2.1.2 *E. coli* cell disruption

*E. coli* cells were disrupted after expression of recombinant proteins according to the following protocol:

- 1) Cell pellets were thawed on ice and subsequently resuspended in ~20 ml lysis buffer (100 mM Tris pH 7.5, 300 mM NaCl, 15 mM imidazole).
- 2) Cells were opened by means of the cell disruptor (Constant systems) at 2.5 kbar.
- 3) The sample was sonicated on ice for 2 min to shear genomic DNA (50% interval).
- 4) Finally, a 40 min centrifugation (20.000 x g) was applied to get rid of cell particles. The obtained crude extract (supernatant) was used for further purification steps

#### 4.2.1.3 Purification of recombinantly expressed SO variants

All SO variants were expressed from pQE80 in fusion with an N-terminal His-tag. The binding of Nickel to histidines facilitated affinity purification of the variants by means of a Ni-NTA matrix. For this purpose, Ni-NTA matrix (Qiagen) was filled into a column and protein crude extract was loaded onto the matrix. After one step of washing with lysis buffer, the proteins were eluted from the matrix by the addition of an elution buffer (100 mM Tris pH 7.5, 300 mM NaCl, 400 mM imidazole). Imidazole strongly binds Nickel and removes the protein from the matrix. Since the eluted proteins were only enriched but not purified, an additional anion exchange chromatography was performed, which was used in combination with a Aekta FPLC system. Therefore, the Ni-NTA eluted protein was diluted 1:5 in 50 mM Tris/acetate pH 8.0 and applied on a SourceQ 30ml matrix (15 µm particles, Dr. Maisch).

All bound proteins were stepwise eluted from the matrix by application of a salt gradient (0-1 M NaCl) and according to their affinity to the matrix based on their negative charges.

#### 4.2.1.4 Concentration of purified proteins

Purified proteins were concentrated by means of Amicon Ultra Centrifugal Filters (Millipore). Depending on the molecular weight of the proteins, size exclusions of 3-100 kDa were chosen. The centrifugations occurred at 4°C and according to the instructions of the manufacturer.

#### 4.2.1.5 Analytical size exclusion chromatography

Size exclusion chromatography separates proteins according to their size. This can either be used for purification purposes or to determine the oligomerization status of a given protein. In the current study, size exclusion chromatography (column: ACQUITY BEH200; 1.7 µm particles; Waters) was used with an HPLC system (Agilent) to characterize the oligomerization of different SO variants. The analysis was performed as described by the supplier.

#### 4.2.1.6 Buffer exchange

Buffer exchange was performed with PD10 columns (GE Healthcare). Therefore, the columns were equilibrated with the target buffer, followed by application of 2.5 ml of protein. Proteins were finally eluted by the addition of 3.5 ml of target buffer.

#### 4.2.1.7 Determination of protein concentration

The concentration of purified proteins was determined by means of a Nanodrop Spectrophotometer (Thermo Scientific) based on the Lambert-Beer Law. Concentrations of protein crude extracts or mitochondria were determined by means of the Bradford solution, which is based on the binding of Coomassie Brilliant Blue G-250 (Rotiquant) to aromatic and basic residues of the protein. The accompanying change in absorption maxima (465 nm to 595 nm) was determined by means of a photometer (Thermo Electron Corporation) and taken as a measure for the amount of protein relative to a standard protein curve.

#### 4.2.1.8 SDS-PAGE

Sodium-dodecyl sulfate polyacrylamide gel electrophoresis (SDS-PAGE) is performed to separate denatured proteins according to their electrophoretic mobility. SDS is an anionic detergent which denatures and negatively charges proteins. Depending on the size of the proteins, different amounts of SDS will bind and provide a negative charge which correlates to the size of the protein. Thereby, proteins will be separated in the gel according to their size. The gel consists of an upper stacking gel and a lower resolving gel with varying percentages of acrylamide (depending on the molecular weight of the proteins of interest). Before loading the samples on the stacking gel, they were denatured by the addition of 5x SDS-loading dye (50% glycerol, 3.5% SDS, 15%  $\beta$ -mercaptoethanol, 0.02% bromophenol blue) and 5 min heating at 95°C. Afterwards, the gel was stained with Coomassie Blue solution (40% methanol, 10% acetic acid, 0.2% Coomassie Brilliant Blue G 250) and destained with destaining solution (40% methanol, 10% acetic acid) or further analyzed by Western blot.

#### 4.2.1.9 Western blot

After SDS PAGE, Western blot was used to specifically detect proteins of interest by immunostaining. In the current study, the proteins of the SDS gel were transferred to a polyvinylidene difluoride (PVDF) membrane by means of a semi-dry blotting system (C.B.S. Scientific). The transfer was conducted with transfer buffer (25 mM Tris, 192 mM glycine, 10% methanol) and three sheets of whatman paper on each side of the gel and membrane. After transfer, the membrane was blocked 1 hour with 5% milk in TBST buffer. The incubation with the primary and secondary antibodies occurred as recommended by the manufacturers. After both antibody incubations, the membrane was washed 4 times for 5 min with TBST. The secondary antibodies used in this study were coupled to horseradish peroxidase and finally visualized by SuperSignal West Pico/Femto Chemiluminescent substrate (Thermo Scientific). The signals were detected by means of an Enhanced Chemiluminescence Camera System (Decon).

#### 4.2.1.10 Blue Native-PAGE

Blue Native-PAGE (BN-PAGE) was applied to separate native protein complexes according to their sizes. In the current study 4%-16% acrylamide gradient gels were applied. Therefore, 4.5 ml of a 4% and 16% acrylamide solution, respectively, were each mixed with 20  $\mu$ l 20% APS and 3  $\mu$ l TEMED in a gradient gel mixer to cast the BN-gel. The stacking gel was

composed of 7 ml 4% acrylamide solution, 30  $\mu$ l 20% APS and 10  $\mu$ l TEMED. Before loading, the samples were supplied with 10x BN-loading dye (5% Coomassie blue G, 500 mM  $\epsilon$ -amino n-caproic acid, 100 mM Bis-Tris pH 7.0). All empty wells were filled with empty well buffer (20 mM Bis-Tris pH 7.4, 50 mM NaCl, 10% glycerol) and as a molecular weight marker a mix of 10 mg/ml thyroglobulin, 10 mg/ml ferritin, 10 mg/ml BSA and empty well buffer was used. 50 mM Bis-Tris pH 7.0 was used as the anode buffer during the run, while the cathode buffer was composed of 50 mM tricine, 15 mM Bis-Tris (unbuffered) and 0.02% Coomassie blue G. After the entry of the samples into the resolving gel, the cathode buffer was exchanged against a coomassie free equivalent. The gel was run at 10 mAmp and 600 volts at 4°C.

#### 4.2.1.11 Sulfite:Cytochrome c assay

SO activity was photometrically determined based on the increased absorption of reduced cytochrome c compared to the oxidized form at 550 nm. The measurements occurred at room temperature by means of an ELISA reader in a 96-well plate. Following components were mixed in the wells:

8  $\mu$ l 1 M Tris/Acetate pH 8.0

10  $\mu$ l 5 mM deoxycholic acid

35  $\mu$ l 0.5 mM KCN

108  $\mu$ l SuOx buffer (0.1 M Tris/acetate pH 8.0 + 0.1 mM EDTA)

12  $\mu$ l cytochrome c (10 mg/ml)

Afterwards, 0-15  $\mu$ l SO was added. In case less than 15  $\mu$ l were added, SuOx buffer was used to fill the protein solution to 15  $\mu$ l.

The reaction was started by the addition of 12  $\mu$ l Na-sulfite (5 mM), followed by a direct starting of OD measurement in the ELISA reader. 30 measurements at 550 nm in time intervals of 4 sec were conducted to determine the catalytic activity of SO.

#### 4.2.1.12 HPLC Form A analysis

Moco and can be detected and quantified by means of its fluorescing oxidation product Form A via HPLC. Moco gets oxidized to Form A in an acidic reaction with  $I_2/KI/HCl$  solution. The fluorescence spectra of Form A (excitation 370 nm, emission 450 nm) allow the detection of the component after elution from the HPLC column.

Moco oxidation to Form A occurred as follows:

- 1) 140  $\mu$ l of the sample were supplied with 17.5  $\mu$ l acidic oxidation mix (1.5/2% I<sub>2</sub>/KI solution in 1M HCl) and incubated at room temperature in the dark overnight.
- 2) The sample was centrifuged for 5 min at 15000 rpm, the yellowish supernatant was taken.
- 3) 20  $\mu$ l of freshly prepared 1% ascorbic acid solution was added to the supernatant to reduce the residual I<sub>2</sub>.
- 4) 70  $\mu$ l 1M Tris (unbuffered) and 5  $\mu$ l 1 M MgCl<sub>2</sub> were added.
- 5) 5  $\mu$ l alkaline phosphatase (1:10 diluted in 20 mM Tris pH 8.3) was added; the reaction was conducted for 30 min at room temperature in the dark.
- 6) Samples were centrifuged for 5 min at 21.000 x g, the supernatant was put into a new tube.
- 7) After another 1:10 dilution, the samples were transferred into HPLC tubes to start the analysis.

HPLC analysis was performed on a reverse phase column (250 x 4.6 mm 5  $\mu$ m C18, Dr. Maisch GmbH). Elution of FormA occurred by application of a methanol gradient.

#### 4.2.1.13 Nit-1 assay

The nit-1 assay was used to detect free Moco in mitochondrial extracts and protein solutions. The assay was conducted as follows:

- 1) 1-20  $\mu$ l protein (~2.5-50  $\mu$ g) was pipetted to 19.5  $\mu$ l nit-1 extract (containing 2 mM GSH) on ice. As a reference, one sample was not incubated with cell extracts but otherwise treated as all other samples.
- 2) Samples were degased in a desiccator and incubated over night at 4°C in the dark.
- 3) Samples were taken out of the desiccator and 1/10 volume of 1% NADPH was added, followed by an incubation time of 10 min at room temperature.
- 4) 1.5 volumes of degased 0.1 mM FAD/0.1 mM KNO<sub>3</sub> (1:2) was added. Samples were incubated for 20 min at room temperature in the dark.
- 5) Samples were heated at 95°C for 5 min and subsequently cooled on ice for a few min.
- 6) Finally, 2.5 volumes of SA/NED (1:1) solution were added. After 30 min of incubation at room temperature, samples were centrifuged and analysed in the ELISA reader at 540 nm on a multi-well plate.

#### 4.2.1.14 TCA precipitation

TCA precipitation was conducted to precipitate proteins in solution in this study. Therefore, 20 µl of a 72% TCA solution were each added to 100 µl protein solution. After 30 min incubation on ice, samples were centrifuged at maximum speed for another 30 min at 4°C. The precipitated protein pellets were rinsed with ice cold acetone two times and each centrifuged for 10 min at 4°C. Finally, the pellets were dried for 20 min in the fume hood and resolved in 30 µl SDS loading dye by shaking at 1.600 x rpm at 50°C.

### **4.2.2 Molecular biological methods**

#### 4.2.2.1 Cloning

For cloning, DNA fragments were first amplified by PCR from cDNA libraries or plasmid templates. After purification, PCR products and target vectors were digested by the respective restriction enzymes and ligated by means of a T4 DNA ligase. To ensure efficient ligation, a four to one insert:vector ratio was applied during the ligation process. The ligated plasmids were finally transformed into *E. coli* strain DH5α. Single colonies were analysed by colony PCR and DNA plasmids were tested on the correct sequence by restriction digest and sequencing (GATC Biotech AG).

#### 4.2.2.2 Plasmid amplification and purification

For plasmid amplification, single colonies of *E. coli* strain DH5α containing the plasmid were grown over night in LB medium containing the appropriate antibiotics. Plasmid extraction and purification occurred by means of the NucleoSpin Plasmid (Macherey-Nagel) according to the instructions of the manufacturer.

#### 4.2.2.3 Site directed mutagenesis

For the introduction of defined mutations into plasmid DNA, sense and antisense primers of the desired region containing the mutation were designed. The mutations were introduced by means of the QuikChange Lightning Site Directed Mutagenesis Kit (Stratagene) and according to the protocol supplied by the manufacturer.

#### 4.2.2.4 Fusion PCR

Fusion of two DNA fragments occurred by fusion PCR. Therefore, both DNA fragments were first amplified by PCR. The forward primer for the amplification of the second fragment

contained 10 nucleotides at the 5' end complementary to the 3' end of the first fragment. Both PCR products were fused by seven PCR cycles with an annealing temperature corresponding to the overlapping part of the two fragments. Finally, the product was amplified by 30 cycles after the addition of the respective forward and reverse primers.

### **4.2.3 Cell biological methods**

#### 4.2.3.1 Cultivation of mammalian cells

All mammalian cell types were cultivated in Dulbecco's modified eagle medium (D-MEM) supplied with 10% fetal calf serum (FCS) and 2mM L-glutamate at 37°C and 10% CO<sub>2</sub>. The cells were adherently grown on 10 cm dishes and detached by trypsin/EDTA application 2-3 times a week to dilute cells 1:4 or 1:8.

#### 4.2.3.2 Transfection of mammalian cells

The transfection of plasmid DNA into mammalian cells occurred to transiently induce the expression of genes from pcDNA3.1, pEGFP-N1 or the pJET1.2 vector. HEK-293 cells as well as human fibroblasts were transfected with PEI (polyethylenimine, 1mg/ml, pH 7.4). For the transfection of a 10 cm plate, 51.2 µl PEI were added to 1ml of D-MEM medium without FCS and glutamate. Transfections of smaller plates were adjusted accordingly. After incubation for 5 min at room temperature, 12.8 µg DNA was added and incubation was continued for another 20 min. Finally, the mixture was added to the cells. For co-transfections of two plasmids on a 10 cm plate, 70 µl PEI were added to 1ml of D-MEM medium without additives. Each 12.8 µg DNA were added and incubated as described above.

#### 4.2.3.3 shRNA mediated knockdown of gene products

In the current study, the human *IMP1* mRNA was downregulated by shRNA. Therefore, an appropriate RNA region was first predicted by an online shRNA design tool (Invitrogen). The region containing the highest probability of efficient gene product knockdown was chosen and sense and antisense primers representing the desired region were synthesized. In parallel, the CMV promoter was amplified by PCR and each fused to the sense and antisense fragments by fusion PCR. Finally, both constructs were separately ligated into the pJET1.2 vector and subsequently co-transfected into HEK-293 cells. The efficiency of knockdown was determined 24 h after transfection by anti-IMP1 Western blotting of the cell lysate.



#### 4.2.3.4 Harvesting and disruption of mammalian cultured cells

Cultured cells were detached by trypsin/EDTA application and pelleted for 5 min at 800 x g. After rinsing cells once with PBS, they were resuspended in the buffer of choice and sonicated two times for 20 sec. Finally, disrupted cells were centrifuged at 21.000 x g at 4°C for 10 min and the protein content of the supernatant was determined by means of the Bradford reagent.

#### 4.2.3.5 Microscopic preparations

Proteins and cell organelles were visualized by confocal laser microscopy and fluorescence microscopy in the current study. Proteins were either visualized by posttranslational fusion to GFP or by immunocytochemistry. In any case, HEK-293 cells or human fibroblasts were grown and transfected in 12-well plates on collagenized cover slips. After 48 h of protein expression, cells were washed three times with PBS and fixed by 20 min incubation in 4% paraformaldehyde. After additional three washing steps, cells expressing GFP tagged proteins were directly mounted on microscope slides containing a drop of Mowiol solution (20 g Mowiol in 80 ml PBS and 40 ml glycerol containing ¼ volume bleaching protection: 2.5 g n-propylgallat in 50 ml PBS and 50 ml glycerol). Preparations were dried over night at 37°C and subsequently analyzed by microscopy. Cells destined for immunocytochemistry were not immediately mounted after fixation but first incubated in 0.2% Tween-20 in PBS for 20 min to permeabilize the cells. After three steps of washing with PBS, cells were briefly incubated with 1% BSA and afterwards covered with the primary antibody (in PBS, concentrations according to the manufacturer) for one hour at 37°C. Cells were washed three times with PBS and incubated with the secondary antibody (1:200 dilution in PBS) for another hour at 37°C. After three washing steps with PBS, cells were finally mounted on microscope slides as described above.

#### 4.2.3.6 Staining of mitochondria

Mitochondria were visualized in the current study by means of Mitotracker Red CMXRos (Invitrogen). A 1mM stock solution in anhydrous DMSO was diluted 1:20000 in D-MEM medium and incubated for 2 h with the cells at 37°C prior to fixation. The dye was visualized by fluorescence microscopy or confocal laser microscopy by excitation at 543 nm.

#### 4.2.3.7 Confocal laser microscopy

Microscopic preparations were analyzed by a Nikon Eclipse Ti confocal microscope. Green fluorescent dyes were excited at 488 nm, red fluorescent dyes were excited at 543 nm.

#### 4.2.3.8 Determination of the Pearson Correlation Coefficient

The Pearson Correlation Coefficient (PCC) was determined to quantify the degree of colocalization of two dyes in a microscopic preparation. The PCC values were determined by means of the Volocity software (Perkin Elmer).

### **4.2.4 Methods to study mitochondrial localization and import of proteins**

#### 4.2.4.1 Enrichment of mitochondria

Mitochondria were enriched from cultured cells according to the following protocol:

- 1) Cultured cells were scraped from 10 cm plates in 5 ml PBS and pelleted at 800 x g.
- 2) Cells were resuspended in 3 ml solution A (20 mM Hepes pH 7.6, 220 mM mannitol, 70 mM sucrose, 1 mM EDTA, 0.5 mM PMSF, 2 mg/ml fatty acid free BSA).
- 3) The suspension was transferred to a teflon homogenizer (Sartorius) and homogenized with 20 strokes at 1000 rpm.
- 4) The homogenate was centrifuged at 800 x g, 4°C for 5 min and the supernatant containing mitochondria was collected.
- 5) The pellet was resuspended in 3 ml solution A and steps 3-4 were repeated 1-2 times.
- 6) The supernatants were combined and centrifuged at 12.000 x g, 4°C for 5 min.
- 7) The supernatant was removed and the pellets were resuspended in 1 ml of solution B (solution A lacking PMSF and BSA) and centrifuged at 12.000 x g, 4°C for 5 min.
- 8) Mitochondrial pellets were carefully resuspended in an appropriate volume of solution B and concentrations were determined by means of the Bradford reagent.

The enrichment of mitochondria from murine liver occurred as described above. The liver was cut into small pieces before pottering.

#### 4.2.4.2 Purification of mitochondria

To obtain mitochondria of high purity, mitochondria were first enriched as described above. 200-500 µl crude mitochondria were subsequently loaded on a discontinuous density gradient of 0.5 ml 80% (v/v) on the bottom, 2 ml 52% (v/v) in between and 2 ml 26% (v/v) percoll on the top in a 13 x 51 mm centrifuge tube. The 80% percoll solution was prepared by

mixing 4 parts 100% percoll with 1 part of 5x solution B to maintain isotonic conditions during the centrifugation procedure. The 52% and 26% percoll solutions were diluted from the 80% percoll solution with 1x solution B. The gradient was centrifuged at 23000rpm for 45 min at 4°C in a Beckman MLS-50 rotor. The fraction containing the purified mitochondria was carefully aspirated from the 26%-52% interface, diluted to a final volume of 1.5 ml with solution B and centrifuged at 16.000 x g, 4°C for 10 min to remove residual percoll. This washing step was repeated once or twice. The final pellet of purified mitochondria was resuspended in solution B.

#### 4.2.4.3 Na<sub>2</sub>CO<sub>3</sub> extraction of mitochondrial proteins

For the separation of soluble and membrane bound mitochondrial proteins, enriched mitochondria were resuspended in 0.1M Na<sub>2</sub>CO<sub>3</sub>, pH 11.5 to a concentration of 0.3 mg/ml. Mitochondria were incubated 30 min on ice and centrifuged at 100000g for one hour at 4°C. The pellet was washed with H<sub>2</sub>O and resuspended in SDS loading buffer. The supernatant was precipitated with TCA as described above.

#### 4.2.4.4 Protease treatment of mitochondria

The submitochondrial localization of proteins was determined by means of external PK and trypsin addition in this study. Either, the localization of endogenous proteins were determined, or proteins were first transiently expressed in cell culture from a plasmid. Mitochondria were enriched as described above and concentrated to 1 mg/ml. PK and trypsin were freshly prepared and dissolved in 10 mM HEPES pH 7.6 to a concentration of 5 mg/ml. 2 µl of protease were added to 100 µl of mitochondria to obtain a final concentration of 100 µg/ml. The samples were incubated at 10 min on ice and inhibition of PK occurred by PMSF with a final concentration of 1 mM for further 10 min on ice. Trypsin was inhibited by means of a specific trypsin inhibitor using 30x excess of inhibitor compared to trypsin. Finally, mitochondrial proteins were precipitated by TCA as described above and digestions were analyzed by Western blot.

#### 4.2.4.5 Hypotonic swelling of mitochondria

The outer mitochondrial membrane was selectively disrupted by hypotonic swelling of mitochondria in 10 mM HEPES pH 7.6 for 15 min at 4°C. Efficiency and selectivity of outer membrane disruption was examined by PK treatment and subsequent Western blotting with antibodies detecting marker proteins of the respective mitochondrial subcompartments.

#### 4.2.4.6 *In vitro* translation

Proteins were synthesized in a cell free reticulocyte lysate system as radioactive precursors for mitochondrial *in vitro* import studies. Transcription and translation occurred by means of the TnT Coupled Reticulocyte Lysate Systems (Promega). As a DNA template, 1 µg pcDNA 3.1 containing the respective coding sequence was applied. In respect to the T7 promoter of the plasmid, transcription was conducted by a T7 RNA polymerase in the assay. The proteins were radioactively labeled during translation by the addition of <sup>35</sup>S methionine (Hartmann Analytic). The translation occurred according to the protocol of the manufacturer and translation was stopped by the addition of 5x stop translation buffer (to 1x; 1.25 M sucrose, 10 mM methionine). The efficiency of translation was determined by SDS-PAGE and Western blot. The Western blot membrane was exposed to a Fuji medical X-ray film for 12 h and the film was developed in a CURIX 80 system (AGFA).

#### 4.2.4.7 Mitochondrial *in vitro* import studies

To study the import of a protein into mitochondria *in vitro*, mitochondria were first enriched from HEK-293 cells and the precursor protein was synthesized *in vitro*. Mitochondria were pelleted and gently resuspended in import buffer (250 mM sucrose, 5 mM magnesium acetate, 80 mM potassium acetate, 10 mM sodium succinate, 1 mM DTT freshly from stock, 0.1 mM ATP pH 7.4 freshly from stock, 20 mM Hepes-KOH pH 7.6) to a final concentration of 1 mg/ml. Import reactions were each carried out with 100 µl mitochondria and 5 µl radioactive precursor in 1.5 ml Eppendorf tubes at 37°C and 400 rpm shaking under eight conditions:

A1) 5 min import reaction, + $\Delta\Psi$

A2) 15 min import reaction, + $\Delta\Psi$

A3) 45 min import reaction, + $\Delta\Psi$

A4) 45 min import reaction, - $\Delta\Psi$  (addition of 2 µl 1 mg/ml valinomycin prior to the import reaction)

A5) 45 min import reaction, + $\Delta\Psi$ , -ATP (preparation of import buffer without ATP)

After the import reaction, samples A1-A5 were centrifuged at 12.000 x g for 5 min and rinsed with 150 µl import buffer lacking ATP and DTT. Pellets were resuspended in 100 µl detergent buffer (1% digitonin, 20mM Bis-Tris, 50mM NaCl, 10% glycerol) and incubated 30 min on ice. Samples were centrifuged at maximum speed and supernatants were loaded on BN-PAGE with subsequent Western blotting. The Western blot membrane was exposed to an X-ray

cassette (Fuji) for at least one week and signals were detected by a Typhoon Trio Variable Mode Imager (Amersham Biosciences).

## 5 Appendix

### 5.1 Primers

Tab. 5.1 Primers used in this study

Name	Sequence ( <b>RESTRICTION SITE</b> ), 5'→3'	Purpose
5'FW FLMSO-GFP	ccc <b>AAGCTT</b> atgctgctgcagctatacag	Cloning, SO
3'REV MSO ohne stop1	ccg <b>GAATTC</b> tgggaccacctgaacatggac	Cloning, SO
5'FW ohneleaderMSO-GFP	ccc <b>AAGCTT</b> atggagtcaccacggatgtactc	Cloning, SO
153-for	cagc <b>GAGCTC</b> atggagtcaccacggatg	Cloning, SO
154-rev	ctgcag <b>GTCGAC</b> tatgggaccacctgaac	Cloning, SO
His119Ala sense	cacaaaatttggacctggctccaggaggaccatcaaa	Mutagenesis, SO
His119Ala antisense	ttttgatggctcctctggagccagggtccacaaattttgtg	Mutagenesis, SO
His144Ala sense	gccctctatgctgtggccaaccagcccatgt	Mutagenesis, SO
His144Ala antisense	acatggggctggttggccacagcatagagggc	Mutagenesis, SO
Arg367His sense	catggctccctgtacacgtgggtggttctctggtg	Mutagenesis, SO
Arg367His antisense	caccaggaaccaccacgtgtacaggaagccatg	Mutagenesis, SO
Lys380Arg sense	tgcccgatgctcagatggctcggcagag	Mutagenesis, SO
Lys380Arg antisense	ctctgccgagccatctgacatgacgggca	Mutagenesis, SO
Gly531Asp sense	tctggaacctcgggacgtactcagcaatgc	Mutagenesis, SO
Gly531Asp antisense	gcattgctgagtacgtcccgaaggttccaga	Mutagenesis, SO
5'FW TIM50	atggcggcctcggcggctctgtt	Cloning, SO-TIM50
3'REV TIM50	tcagggctgcttgagcgaggcc	Cloning, SO-TIM50
5'FW TIMmembraneÜberhang	gataactcaaggactattgcgctctggatcgccggttgctc gga	Cloning, SO-TIM50
3'REV TIMmembrane	aaaaatatagacgatgct	Cloning, SO-TIM50
5'FW MSOTIMÜberhang	agcatcgtctatattttcacaacaaccctaaaactggagtc tgggta	Cloning, SO-TIM50
3'REV MSOTIM	agtccttgagttatcatca	Cloning, SO-TIM50
5'FWmARC1-GFP	ccc <b>AAGCTT</b> atgggcgccgcccggctcctc	Cloning, mARC1
3'REVmARC1-GFP	cgg <b>GGTACC</b> aactggcccagcaggtacacag	Cloning, mARC1
3'RevmARC1pcDNA	ccg <b>GAATTC</b> ctggcccagcaggtacacag	Cloning, mARC1
3'RevmARC1pcdnastop	ccg <b>GAATTC</b> tactggcccagca	Cloning, mARC1
3'RevmARC1erste20	cgg <b>GGTACC</b> aagggccgggattgcgagga	Cloning, mARC1
3'RevmARC1erste44	cgg <b>GGTACC</b> aatgcgcccagcagcgacag	Cloning, mARC1
5'FWmARC1hydrophob	ccc <b>AAGCTT</b> atggggtggctcggggttgcc	Cloning, mARC1
5'FWmARC1ohneleader	ccc <b>AAGCTT</b> atgtggcccacgcccggcg	Cloning, mARC1

## 5.2 Constructs

**Tab. 5.2 Constructs used in this study**

CDS	Construct	Restriction sites	Source
MSO	pcDNA3.1:WT-MSO	HindIII+EcoRI	this study
MSO	pcDNA3.1: WT-MSO, stop codon	HindIII+EcoRI	this study
MSO	pcDNA3.1: WT-MSO, $\Delta$ aa1-80	HindIII+EcoRI	this study
MSO	pcDNA3.1: WT-MSO, $\Delta$ aa166-546	HindIII+EcoRI	this study
MSO	pcDNA3.1: MSO-R367H-K380R, stop codon	HindIII+EcoRI	this study
MSO	pcDNA3.1: MSO-R367H-H380R	HindIII+EcoRI	this study
MSO	pcDNA3.1: MSO-H119A-H144A, stop codon	HindIII+EcoRI	this study
MSO	pcDNA3.1: MSO-H119-H144A, $\Delta$ aa166-546	HindIII+EcoRI	this study
MSO	pcDNA3.1: MSO-G531D, stop codon	HindIII+EcoRI	this study
MSO	pcDNA3.1: WT-MSO, $\Delta$ aa64-84, Insert: aa66-86 of mouse TIM50	HindIII+EcoRI	this study
MSO	pcDNA3.1: MSO-R367H-K380R, $\Delta$ aa64-84, Insert: aa66-86 of mouse TIM50	HindIII+EcoRI	this study
MSO	pQE80: WT-MSO, $\Delta$ aa1-80	SacI+Sall	this study
MSO	pQE80: MSO-R367H-K380R, $\Delta$ aa1-80	SacI+Sall	this study
MSO	pQE80: MSO-H119A-H144A, $\Delta$ aa1-80	SacI+Sall	this study
MSO	pQE80: MSO-G531D, $\Delta$ aa1-80	SacI+Sall	this study
Human <i>IMP1</i> shRNA	pJET1.2: CMV promoter fused to base pairs 91-111 of the human <i>IMMP1L</i> coding sequence, sense sequence	-	this study
Human <i>IMP1</i> shRNA	pJET1.2: CMV promoter fused to base pairs 91-111 of the human <i>IMMP1L</i> coding sequence, antisense sequence	-	this study
mARC1	pcDNA3.1: WT-mARC1	HindIII+EcoRI	this study
mARC1	pcDNA3.1: WT-mARC1, stop codon	HindIII+EcoRI	this study
mARC1	pcDNA3.1: WT-mARC1, $\Delta$ aa1-20+stop codon	HindIII+EcoRI	this study
mARC1	pcDNA3.1: WT-mARC1, $\Delta$ aa1-40+stop codon	HindIII+EcoRI	this study
mARC1	pEGFP-N1: WT-mARC1	HindIII+KpnI	this study
mARC1	pEGFP-N1: WT-mARC1, $\Delta$ aa1-20	HindIII+KpnI	this study
mARC1	pEGFP-N1: WT-mARC1, $\Delta$ aa1-40	HindIII+KpnI	this study
mARC1	pEGFP-N1: WT-mARC1, $\Delta$ aa21-40	HindIII+KpnI	this study

## 5.3 Sequences

### 5.3.1 Mouse SO:

Depicted is the peptide sequence of MSO with highlighted individual domains:

underlined: cleaved mitochondrial targeting sequence; (Kisker et al., 1997)

**fat**: predicted N-terminal MTS; <http://ihg.gsf.de/ihg/mitoprot.html>

**yellow**: predicted transmembrane domain; <http://phobius.sbc.su.se/>

**red**: heme domain; (Kisker et al., 1997)

**green**: Moco domain; (Kisker et al., 1997)

**blue**: dimerization domain; (Kisker et al., 1997)

10	20	30	40	50	60
<u>MLLQLYRSV</u>	<u>VRLPQAIRVK</u>	STPLRLCIQA	CSTNDSLEPQ	HPSLTFSDDN	SRTRR <b>WKVMG</b>
70	80	90	100	110	120
<b>TL</b> LGLGVVLV	<b>Y</b> HEHRCRASQ	<b>E</b> SPRMYSKED	<b>V</b> RSHNNPKTG	<b>V</b> WVTLGSEVF	<b>D</b> VTKFVDLHP
130	140	150	160	170	180
<b>GG</b> PSKLM <del>L</del> AA	<b>GG</b> PLEPF <del>W</del> AL	<b>Y</b> AVHNQPHVR	<b>E</b> LLAEYKIGE	<b>L</b> NPEDSMSPS	<b>V</b> EASDPYADD
190	200	210	220	230	240
<b>P</b> IRHPALRIN	<b>S</b> QRPFNAEPP	<b>P</b> ELLTEGYIT	<b>P</b> NPIFFTRNH	<b>L</b> PVFNLDPHT	<b>Y</b> RLHVVGAPG
250	260	270	280	290	300
<b>G</b> QSLSLSLDD	<b>L</b> HKFPKHEVT	<b>V</b> TLQCAGNRR	<b>S</b> EMSKVKEVK	<b>G</b> LEWRTGAIS	<b>T</b> ARWAGARLC
310	320	330	340	350	360
<b>D</b> VLAQAGHRL	<b>C</b> DSEAHVCFE	<b>G</b> LDSPTGTA	<b>Y</b> GASIP <del>L</del> ARA	<b>M</b> DPEAEVLLA	<b>Y</b> EMNGQPLPR
370	380	390	400	410	420
<b>D</b> HGF <del>P</del> RVVV	<b>P</b> GVVGARHVK	<b>W</b> LGRVSV <del>E</del> SE	<b>E</b> SYSHWQRRD	<b>Y</b> KGFSPSVDW	<b>D</b> TVNFDLAPS
430	440	450	460	470	480
<b>I</b> QELPIQSAI	<b>T</b> QPQDGAIVE	<b>S</b> GEVTIKGYA	<b>W</b> SGGGRAVIR	<b>V</b> DVSV <del>D</del> GGLT	<b>W</b> QEAELEGEE
490	500	510	520	530	540
<b>Q</b> CPRKAWAWR	<b>I</b> WQLKAQVPA	<b>E</b> QKELNIICK	<b>A</b> VDDSYNVQP	<b>D</b> TVAPIWNLR	<b>G</b> VLSNAWHRV
HVQVVP					



### 5.3.2 Human mARC1:

Depicted is the peptide sequence of mARC1 with its dual mitochondrial targeting signal:

**fat:** N-terminal MTS; according to this study

**yellow:** predicted transmembrane domain; <http://phobius.sbc.su.se/>

10	20	30	40	50	60
<b>MGAAGSSALA</b>	<b>RFVLLAQS</b>	<b>RP</b>	<b>GWLGVAALGL</b>	<b>TAVALGAVAW</b>	RRAWPTRRRR LLQQVGTVAQ
70	80	90	100	110	120
LWIYPVKSC	K GVPVSEAE	CT AMGLRSG	NLR DRFWLVIN	QE GNMVTAR	QEP RLVLISLT
130	140	150	160	170	180
GDTLTL	SAAY TKD	LLLPIKT	PTTNAVHK	CR VHGLEIE	GRD CGEATAQ
190	200	210	220	230	240
VHFEPH	MRPR RPH	QIADLFR	PKDQIAYS	DT SPFLIL	SEAS LADLNS
250	260	270	280	290	300
IVISGCD	VYA EDSW	DELLIG	DVELKRVM	AC SRCILTT	VDP DTGVMS
310	320	330			
DPSE	RKLYGK	SPLFGQY	FVL ENPGTI	KVGD	PVYLLGQ

## **6 References**

- Abe Y, Shodai T, Muto T, Mihara K, Torii H, Nishikawa S, Endo T, Kohda D (2000) Structural basis of presequence recognition by the mitochondrial protein import receptor Tom20. *Cell* 100:551-560.
- Ades IZ, Butow RA (1980) The transport of proteins into yeast mitochondria. Kinetics and pools. *The Journal of biological chemistry* 255:9925-9935.
- Ahting U, Thun C, Hegerl R, Typke D, Nargang FE, Neupert W, Nussberger S (1999) The TOM core complex: the general protein import pore of the outer membrane of mitochondria. *The Journal of cell biology* 147:959-968.
- Ahting U, Waizenegger T, Neupert W, Rapaport D (2005) Signal-anchored proteins follow a unique insertion pathway into the outer membrane of mitochondria. *The Journal of biological chemistry* 280:48-53.
- Ajioka RS, Phillips JD, Kushner JP (2006) Biosynthesis of heme in mammals. *Biochimica et biophysica acta* 1763:723-736.
- Aquila H, Misra D, Eulitz M, Klingenberg M (1982) Complete amino acid sequence of the ADP/ATP carrier from beef heart mitochondria. *Hoppe-Seyler's Zeitschrift fur physiologische Chemie* 363:345-349.
- Armstrong LC, Komiya T, Bergman BE, Mihara K, Bornstein P (1997) Metaxin is a component of a preprotein import complex in the outer membrane of the mammalian mitochondrion. *The Journal of biological chemistry* 272:6510-6518.
- Astashkin AV, Raitsimring AM, Feng C, Johnson JL, Rajagopalan KV, Enemark JH (2002) Pulsed EPR studies of nonexchangeable protons near the Mo(V) center of sulfite oxidase: direct detection of the alpha-proton of the coordinated cysteinyl residue and structural implications for the active site. *Journal of the American Chemical Society* 124:6109-6118.
- Baker MJ, Frazier AE, Gulbis JM, Ryan MT (2007) Mitochondrial protein-import machinery: correlating structure with function. *Trends in cell biology* 17:456-464.
- Baker MJ, Webb CT, Stroud DA, Palmer CS, Frazier AE, Guiard B, Chacinska A, Gulbis JM, Ryan MT (2009) Structural and functional requirements for activity of the Tim9-Tim10 complex in mitochondrial protein import. *Molecular biology of the cell* 20:769-779.
- Becker T, Wenz LS, Kruger V, Lehmann W, Muller JM, Goroncy L, Zufall N, Lithgow T, Guiard B, Chacinska A, Wagner R, Meisinger C, Pfanner N (2011) The mitochondrial import protein Mim1 promotes biogenesis of multispanning outer membrane proteins. *The Journal of cell biology* 194:387-395.
- Biederer T, Volkwein C, Sommer T (1997) Role of Cue1p in ubiquitination and degradation at the ER surface. *Science* 278:1806-1809.
- Bisaccia F, De Palma A, Palmieri F (1992) Identification and purification of the aspartate/glutamate carrier from bovine heart mitochondria. *Biochimica et biophysica acta* 1106:291-296.
- Bohnert M, Wenz LS, Zerbes RM, Horvath SE, Stroud DA, von der Malsburg K, Muller JM, Oeljeklaus S, Perschil I, Warscheid B, Chacinska A, Veenhuis M, van der Klei JJ, Daum G, Wiedemann N, Becker T, Pfanner N, van der Laan M (2012) Role of MINOS in protein biogenesis of the mitochondrial outer membrane. *Molecular biology of the cell*.
- Borgese N, Aggujaro D, Carrera P, Pietrini G, Bassetti M (1996) A role for N-myristoylation in protein targeting: NADH-cytochrome b5 reductase requires myristic acid for association with outer mitochondrial but not ER membranes. *The Journal of cell biology* 135:1501-1513.
- Borgese N, Pietrini G (1986) Distribution of the integral membrane protein NADH-cytochrome b5 reductase in rat liver cells, studied with a quantitative radioimmunoblotting assay. *The Biochemical journal* 239:393-403.
- Bottinger L, Gornicka A, Czerwik T, Bragoszewski P, Loniewska-Lwowska A, Schulze-Specking A, Truscott KN, Guiard B, Milenkovic D, Chacinska A (2012) In vivo

- evidence for cooperation of Mia40 and Erv1 in the oxidation of mitochondrial proteins. *Molecular biology of the cell*.
- Brix J, Dietmeier K, Pfanner N (1997) Differential recognition of preproteins by the purified cytosolic domains of the mitochondrial import receptors Tom20, Tom22, and Tom70. *The Journal of biological chemistry* 272:20730-20735.
- Burri L, Strahm Y, Hawkins CJ, Gentle IE, Puryer MA, Verhagen A, Callus B, Vaux D, Lithgow T (2005) Mature DIABLO/Smac is produced by the IMP protease complex on the mitochondrial inner membrane. *Molecular biology of the cell* 16:2926-2933.
- Chacinska A, Lind M, Frazier AE, Dudek J, Meisinger C, Geissler A, Sickmann A, Meyer HE, Truscott KN, Guiard B, Pfanner N, Rehling P (2005) Mitochondrial presequence translocase: switching between TOM tethering and motor recruitment involves Tim21 and Tim17. *Cell* 120:817-829.
- Chacinska A, Pfannschmidt S, Wiedemann N, Kozjak V, Sanjuan Szklarz LK, Schulze-Specking A, Truscott KN, Guiard B, Meisinger C, Pfanner N (2004) Essential role of Mia40 in import and assembly of mitochondrial intermembrane space proteins. *The EMBO journal* 23:3735-3746.
- Chamizo-Ampudia A, Galvan A, Fernandez E, Llamas A (2011) The *Chlamydomonas reinhardtii* molybdenum cofactor enzyme crARC has a Zn-dependent activity and protein partners similar to those of its human homologue. *Eukaryotic cell* 10:1270-1282.
- Chan DC (2006) Mitochondrial fusion and fission in mammals. *Annual review of cell and developmental biology* 22:79-99.
- Chen X, Van Valkenburgh C, Fang H, Green N (1999) Signal peptides having standard and nonstandard cleavage sites can be processed by Imp1p of the mitochondrial inner membrane protease. *The Journal of biological chemistry* 274:37750-37754.
- Claros MG, Vincens P (1996) Computational method to predict mitochondrially imported proteins and their targeting sequences. *European journal of biochemistry / FEBS* 241:779-786.
- Clement B (2002) Reduction of N-hydroxylated compounds: amidoximes (N-hydroxyamidines) as pro-drugs of amidines. *Drug metabolism reviews* 34:565-579.
- Clement B, Lomb R, Moller W (1997) Isolation and characterization of the protein components of the liver microsomal O<sub>2</sub>-insensitive NADH-benzamidoxime reductase. *The Journal of biological chemistry* 272:19615-19620.
- Curran SP, Leuenberger D, Oppliger W, Koehler CM (2002) The Tim9p-Tim10p complex binds to the transmembrane domains of the ADP/ATP carrier. *The EMBO journal* 21:942-953.
- Da Cruz S, Xenarios I, Langridge J, Vilbois F, Parone PA, Martinou JC (2003) Proteomic analysis of the mouse liver mitochondrial inner membrane. *The Journal of biological chemistry* 278:41566-41571.
- Deistung J, Bray RC (1989) Isolation, in the intact state, of the pterin molybdenum cofactor from xanthine oxidase. *The Biochemical journal* 263:477-483.
- Dietmeier K, Honlinger A, Bomer U, Dekker PJ, Eckerskorn C, Lottspeich F, Kubrich M, Pfanner N (1997) Tom5 functionally links mitochondrial preprotein receptors to the general import pore. *Nature* 388:195-200.
- Dimmer KS, Papic D, Schumann B, Sperl D, Krumpe K, Walther DM, Rapaport D (2012) A crucial role of Mim2 in the biogenesis of mitochondrial outer membrane proteins. *Journal of cell science*.
- Dinur-Mills M, Tal M, Pines O (2008) Dual targeted mitochondrial proteins are characterized by lower MTS parameters and total net charge. *PLoS one* 3:e2161.
- Droge W (2002) Free radicals in the physiological control of cell function. *Physiological reviews* 82:47-95.
- Dukanovic J, Rapaport D (2011) Multiple pathways in the integration of proteins into the mitochondrial outer membrane. *Biochimica et biophysica acta* 1808:971-980.
- Dumont ME, Ernst JF, Sherman F (1988) Coupling of heme attachment to import of cytochrome c into yeast mitochondria. Studies with heme lyase-deficient mitochondria and altered apocytochromes c. *The Journal of biological chemistry* 263:15928-15937.

- Eilers T, Schwarz G, Brinkmann H, Witt C, Richter T, Nieder J, Koch B, Hille R, Hansch R, Mendel RR (2001) Identification and biochemical characterization of *Arabidopsis thaliana* sulfite oxidase. A new player in plant sulfur metabolism. *The Journal of biological chemistry* 276:46989-46994.
- Esaki M, Kanamori T, Nishikawa S, Endo T (1999) Two distinct mechanisms drive protein translocation across the mitochondrial outer membrane in the late step of the cytochrome b(2) import pathway. *Proceedings of the National Academy of Sciences of the United States of America* 96:11770-11775.
- Esser K, Jan PS, Pratje E, Michaelis G (2004) The mitochondrial IMP peptidase of yeast: functional analysis of domains and identification of Gut2 as a new natural substrate. *Molecular genetics and genomics* : MGG 271:616-626.
- Ettmayer P, Amidon GL, Clement B, Testa B (2004) Lessons learned from marketed and investigational prodrugs. *Journal of medicinal chemistry* 47:2393-2404.
- Feng C, Kedia RV, Hazzard JT, Hurley JK, Tollin G, Enemark JH (2002) Effect of solution viscosity on intramolecular electron transfer in sulfite oxidase. *Biochemistry* 41:5816-5821.
- Feng C, Tollin G, Enemark JH (2007) Sulfite oxidizing enzymes. *Biochimica et biophysica acta* 1774:527-539.
- Field LS, Furukawa Y, O'Halloran TV, Culotta VC (2003) Factors controlling the uptake of yeast copper/zinc superoxide dismutase into mitochondria. *The Journal of biological chemistry* 278:28052-28059.
- Fischer K, Llamas A, Tejada-Jimenez M, Schader N, Kuper J, Ataya FS, Galvan A, Mendel RR, Fernandez E, Schwarz G (2006a) Function and structure of the molybdenum cofactor carrier protein MCP from *Chlamydomonas reinhardtii*. *J Biol Chem*.
- Fischer K, Llamas A, Tejada-Jimenez M, Schrader N, Kuper J, Ataya FS, Galvan A, Mendel RR, Fernandez E, Schwarz G (2006b) Function and structure of the molybdenum cofactor carrier protein from *Chlamydomonas reinhardtii*. *The Journal of biological chemistry* 281:30186-30194.
- Fujiki Y, Hubbard AL, Fowler S, Lazarow PB (1982) Isolation of intracellular membranes by means of sodium carbonate treatment: application to endoplasmic reticulum. *The Journal of cell biology* 93:97-102.
- Fukushima K, Ito A, Omura T, Sato R (1972) Occurrence of different types of cytochrome b 5-like hemoprotein in liver mitochondria and their intramitochondrial localization. *Journal of biochemistry* 71:447-461.
- Gakh O, Cavadini P, Isaya G (2002) Mitochondrial processing peptidases. *Biochimica et biophysica acta* 1592:63-77.
- Garattini E, Fratelli M, Terao M (2008) Mammalian aldehyde oxidases: genetics, evolution and biochemistry. *Cellular and molecular life sciences* : CMLS 65:1019-1048.
- Garrett RM, Johnson JL, Graf TN, Feigenbaum A, Rajagopalan KV (1998) Human sulfite oxidase R160Q: identification of the mutation in a sulfite oxidase-deficient patient and expression and characterization of the mutant enzyme. *Proceedings of the National Academy of Sciences of the United States of America* 95:6394-6398.
- Gasser SM, Ohashi A, Daum G, Bohni PC, Gibson J, Reid GA, Yonetani T, Schatz G (1982) Imported mitochondrial proteins cytochrome b2 and cytochrome c1 are processed in two steps. *Proceedings of the National Academy of Sciences of the United States of America* 79:267-271.
- Gebert N, Gebert M, Oeljeklaus S, von der Malsburg K, Stroud DA, Kulawiak B, Wirth C, Zahedi RP, Dolezal P, Wiese S, Simon O, Schulze-Specking A, Truscott KN, Sickmann A, Rehling P, Guiard B, Hunte C, Warscheid B, van der Laan M, Pfanner N, Wiedemann N (2011) Dual function of Sdh3 in the respiratory chain and TIM22 protein translocase of the mitochondrial inner membrane. *Molecular cell* 44:811-818.
- Glick B, Wachter C, Schatz G (1991) Protein import into mitochondria: two systems acting in tandem? *Trends in cell biology* 1:99-103.
- Glick BS, Wachter C, Reid GA, Schatz G (1993) Import of cytochrome b2 to the mitochondrial intermembrane space: the tightly folded heme-binding domain makes

- import dependent upon matrix ATP. *Protein science : a publication of the Protein Society* 2:1901-1917.
- Graham FL, Smiley J, Russell WC, Nairn R (1977) Characteristics of a human cell line transformed by DNA from human adenovirus type 5. *The Journal of general virology* 36:59-74.
- Grandchamp B, Phung N, Nordmann Y (1978) The mitochondrial localization of coproporphyrinogen III oxidase. *The Biochemical journal* 176:97-102.
- Gruenewald S, Wahl B, Bittner F, Hungeling H, Kanzow S, Kotthaus J, Schwering U, Mendel RR, Clement B (2008) The fourth molybdenum containing enzyme mARC: cloning and involvement in the activation of N-hydroxylated prodrugs. *Journal of medicinal chemistry* 51:8173-8177.
- Gutzke G, Fischer B, Mendel RR, Schwarz G (2001) Thiocarboxylation of molybdopterin synthase provides evidence for the mechanism of dithiolene formation in metal-binding pterins. *The Journal of biological chemistry* 276:36268-36274.
- Hahne K, Haucke V, Ramage L, Schatz G (1994) Incomplete arrest in the outer membrane sorts NADH-cytochrome b5 reductase to two different submitochondrial compartments. *Cell* 79:829-839.
- Hanahan D (1983) Studies on transformation of *Escherichia coli* with plasmids. *Journal of molecular biology* 166:557-580.
- Hanzelmann P, Hernandez HL, Menzel C, Garcia-Serres R, Huynh BH, Johnson MK, Mendel RR, Schindelin H (2004) Characterization of MOCS1A, an oxygen-sensitive iron-sulfur protein involved in human molybdenum cofactor biosynthesis. *The Journal of biological chemistry* 279:34721-34732.
- Hanzelmann P, Schwarz G, Mendel RR (2002) Functionality of alternative splice forms of the first enzymes involved in human molybdenum cofactor biosynthesis. *The Journal of biological chemistry* 277:18303-18312.
- Harner M, Korner C, Walther D, Mokranjac D, Kaesmacher J, Welsch U, Griffith J, Mann M, Reggiori F, Neupert W (2011) The mitochondrial contact site complex, a determinant of mitochondrial architecture. *The EMBO journal* 30:4356-4370.
- Haucke V, Ocana CS, Honlinger A, Tokatlidis K, Pfanner N, Schatz G (1997) Analysis of the sorting signals directing NADH-cytochrome b5 reductase to two locations within yeast mitochondria. *Molecular and cellular biology* 17:4024-4032.
- Havemeyer A, Bittner F, Wollers S, Mendel R, Kunze T, Clement B (2006) Identification of the missing component in the mitochondrial benzamidoxime prodrug-converting system as a novel molybdenum enzyme. *The Journal of biological chemistry* 281:34796-34802.
- Hegde RS, Keenan RJ (2011) Tail-anchored membrane protein insertion into the endoplasmic reticulum. *Nature reviews Molecular cell biology* 12:787-798.
- Hill K, Model K, Ryan MT, Dietmeier K, Martin F, Wagner R, Pfanner N (1998) Tom40 forms the hydrophilic channel of the mitochondrial import pore for preproteins [see comment]. *Nature* 395:516-521.
- Hille R (1994) The reaction mechanism of oxomolybdenum enzymes. *Biochimica et biophysica acta* 1184:143-169.
- Hille R (1996) The Mononuclear Molybdenum Enzymes. *Chemical reviews* 96:2757-2816.
- Hille R (2002) Molybdenum and tungsten in biology. *Trends in biochemical sciences* 27:360-367.
- Hille R, Nishino T (1995) Flavoprotein structure and mechanism. 4. Xanthine oxidase and xanthine dehydrogenase. *FASEB journal : official publication of the Federation of American Societies for Experimental Biology* 9:995-1003.
- Hille R, Nishino T, Bittner F (2011) Molybdenum enzymes in higher organisms. *Coordination chemistry reviews* 255:1179-1205.
- Honlinger A, Bomer U, Alconada A, Eckerskorn C, Lottspeich F, Dietmeier K, Pfanner N (1996) Tom7 modulates the dynamics of the mitochondrial outer membrane translocase and plays a pathway-related role in protein import. *The EMBO journal* 15:2125-2137.

- Hoppins S, Collins SR, Cassidy-Stone A, Hummel E, Devay RM, Lackner LL, Westermann B, Schuldiner M, Weissman JS, Nunnari J (2011) A mitochondrial-focused genetic interaction map reveals a scaffold-like complex required for inner membrane organization in mitochondria. *The Journal of cell biology* 195:323-340.
- Hoppins SC, Nargang FE (2004) The Tim8-Tim13 complex of *Neurospora crassa* functions in the assembly of proteins into both mitochondrial membranes. *The Journal of biological chemistry* 279:12396-12405.
- Horie C, Suzuki H, Sakaguchi M, Mihara K (2003) Targeting and assembly of mitochondrial tail-anchored protein Tom5 to the TOM complex depend on a signal distinct from that of tail-anchored proteins dispersed in the membrane. *The Journal of biological chemistry* 278:41462-41471.
- Humphries AD, Streimann IC, Stojanovski D, Johnston AJ, Yano M, Hoogenraad NJ, Ryan MT (2005) Dissection of the mitochondrial import and assembly pathway for human Tom40. *The Journal of biological chemistry* 280:11535-11543.
- Ichida K, Amaya Y, Kamatani N, Nishino T, Hosoya T, Sakai O (1997) Identification of two mutations in human xanthine dehydrogenase gene responsible for classical type I xanthinuria. *The Journal of clinical investigation* 99:2391-2397.
- Ichida K, Matsumura T, Sakuma R, Hosoya T, Nishino T (2001) Mutation of human molybdenum cofactor sulfurase gene is responsible for classical xanthinuria type II. *Biochemical and biophysical research communications* 282:1194-1200.
- Indiveri C, Tonazzi A, Palmieri F (1992) Identification and purification of the ornithine/citrulline carrier from rat liver mitochondria. *European journal of biochemistry / FEBS* 207:449-454.
- Ito A (1971) Hepatic sulfite oxidase identified as cytochrome b 5 -like pigment extractable from mitochondria by hypotonic treatment. *Journal of biochemistry* 70:1061-1064.
- Ito A (1980) Cytochrome b5-like hemoprotein of outer mitochondrial membrane; OM cytochrome b. I. Purification of OM cytochrome b from rat liver mitochondria and comparison of its molecular properties with those of cytochrome b5. *Journal of biochemistry* 87:63-71.
- John GB, Shang Y, Li L, Renken C, Mannella CA, Selker JM, Rangell L, Bennett MJ, Zha J (2005) The mitochondrial inner membrane protein mitofilin controls cristae morphology. *Molecular biology of the cell* 16:1543-1554.
- Johnson JL, Coyne KE, Garrett RM, Zobot MT, Dorche C, Kisker C, Rajagopalan KV (2002) Isolated sulfite oxidase deficiency: identification of 12 novel SUOX mutations in 10 patients. *Human mutation* 20:74.
- Kadlubar FF, Ziegler DM (1974) Properties of a NADH-dependent N-hydroxy amine reductase isolated from pig liver microsomes. *Archives of biochemistry and biophysics* 162:83-92.
- Kall L, Krogh A, Sonnhammer EL (2004) A combined transmembrane topology and signal peptide prediction method. *Journal of molecular biology* 338:1027-1036.
- Kanaji S, Iwahashi J, Kida Y, Sakaguchi M, Mihara K (2000) Characterization of the signal that directs Tom20 to the mitochondrial outer membrane. *The Journal of cell biology* 151:277-288.
- Kappler U, Bailey S (2005) Molecular basis of intramolecular electron transfer in sulfite-oxidizing enzymes is revealed by high resolution structure of a heterodimeric complex of the catalytic molybdopterin subunit and a c-type cytochrome subunit. *The Journal of biological chemistry* 280:24999-25007.
- Kappler U, Bennett B, Rethmeier J, Schwarz G, Deutzmann R, McEwan AG, Dahl C (2000) Sulfite: Cytochrome c oxidoreductase from *Thiobacillus novellus*. Purification, characterization, and molecular biology of a heterodimeric member of the sulfite oxidase family. *The Journal of biological chemistry* 275:13202-13212.
- Kato H, Mihara K (2008) Identification of Tom5 and Tom6 in the preprotein translocase complex of human mitochondrial outer membrane. *Biochemical and biophysical research communications* 369:958-963.

- Kellems RE, Allison VF, Butow RA (1975) Cytoplasmic type 80S ribosomes associated with yeast mitochondria. IV. Attachment of ribosomes to the outer membrane of isolated mitochondria. *The Journal of cell biology* 65:1-14.
- Kisker C, Schindelin H, Pacheco A, Wehbi WA, Garrett RM, Rajagopalan KV, Enemark JH, Rees DC (1997) Molecular basis of sulfite oxidase deficiency from the structure of sulfite oxidase. *Cell* 91:973-983.
- Knowles BB, Howe CC, Aden DP (1980) Human hepatocellular carcinoma cell lines secrete the major plasma proteins and hepatitis B surface antigen. *Science* 209:497-499.
- Knox C, Sass E, Neupert W, Pines O (1998) Import into mitochondria, folding and retrograde movement of fumarase in yeast. *The Journal of biological chemistry* 273:25587-25593.
- Kolbe HV, Costello D, Wong A, Lu RC, Wohlrab H (1984) Mitochondrial phosphate transport. Large scale isolation and characterization of the phosphate transport protein from beef heart mitochondria. *The Journal of biological chemistry* 259:9115-9120.
- Komiya T, Rospert S, Koehler C, Looser R, Schatz G, Mihara K (1998) Interaction of mitochondrial targeting signals with acidic receptor domains along the protein import pathway: evidence for the 'acid chain' hypothesis. *The EMBO journal* 17:3886-3898.
- Kornmann B, Currie E, Collins SR, Schuldiner M, Nunnari J, Weissman JS, Walter P (2009) An ER-mitochondria tethering complex revealed by a synthetic biology screen. *Science* 325:477-481.
- Kornmann B, Walter P (2010) ERMES-mediated ER-mitochondria contacts: molecular hubs for the regulation of mitochondrial biology. *Journal of cell science* 123:1389-1393.
- Kotthaus J, Wahl B, Havemeyer A, Schade D, Garbe-Schonberg D, Mendel R, Bittner F, Clement B (2011) Reduction of N(omega)-hydroxy-L-arginine by the mitochondrial amidoxime reducing component (mARC). *The Biochemical journal* 433:383-391.
- Kruse T, Gehl C, Geisler M, Lehrke M, Ringel P, Hallier S, Hansch R, Mendel RR (2010) Identification and biochemical characterization of molybdenum cofactor-binding proteins from *Arabidopsis thaliana*. *The Journal of biological chemistry* 285:6623-6635.
- Kurlemann G, Debus O, Schuierer G (1996) Dextromethorphan in molybdenum cofactor deficiency. *European journal of pediatrics* 155:422-423.
- Kyte J, Doolittle RF (1982) A simple method for displaying the hydropathic character of a protein. *Journal of molecular biology* 157:105-132.
- Lemasters JJ, Holmuhamedov E (2006) Voltage-dependent anion channel (VDAC) as mitochondrial governor--thinking outside the box. *Biochimica et biophysica acta* 1762:181-190.
- Lill R (2009) Function and biogenesis of iron-sulphur proteins. *Nature* 460:831-838.
- Llamas A, Mendel RR, Schwarz G (2004) Synthesis of adenylated molybdopterin: an essential step for molybdenum insertion. *The Journal of biological chemistry* 279:55241-55246.
- Llamas A, Otte T, Multhaup G, Mendel RR, Schwarz G (2006) The Mechanism of nucleotide-assisted molybdenum insertion into molybdopterin. A novel route toward metal cofactor assembly. *The Journal of biological chemistry* 281:18343-18350.
- Llamas A, Tejada-Jimenez M, Fernandez E, Galvan A (2011) Molybdenum metabolism in the alga *Chlamydomonas* stands at the crossroad of those in *Arabidopsis* and humans. *Metallomics : integrated biometal science* 3:578-590.
- Lutz T, Neupert W, Herrmann JM (2003) Import of small Tim proteins into the mitochondrial intermembrane space. *The EMBO journal* 22:4400-4408.
- Manders EM, Stap J, Brakenhoff GJ, van Driel R, Aten JA (1992) Dynamics of three-dimensional replication patterns during the S-phase, analysed by double labelling of DNA and confocal microscopy. *Journal of cell science* 103 ( Pt 3):857-862.
- Matthies A, Rajagopalan KV, Mendel RR, Leimkuhler S (2004) Evidence for the physiological role of a rhodanese-like protein for the biosynthesis of the molybdenum cofactor in humans. *Proceedings of the National Academy of Sciences of the United States of America* 101:5946-5951.

- Maupin-Furlow JA, Rosentel JK, Lee JH, Deppenmeier U, Gunsalus RP, Shanmugam KT (1995) Genetic analysis of the modABCD (molybdate transport) operon of *Escherichia coli*. *Journal of bacteriology* 177:4851-4856.
- McBride HM, Millar DG, Li JM, Shore GC (1992) A signal-anchor sequence selective for the mitochondrial outer membrane. *The Journal of cell biology* 119:1451-1457.
- Meineke B, Engl G, Kemper C, Vasiljev-Neumeyer A, Paulitschke H, Rapaport D (2008) The outer membrane form of the mitochondrial protein Mcr1 follows a TOM-independent membrane insertion pathway. *FEBS letters* 582:855-860.
- Meisinger C, Pfannschmidt S, Rissler M, Milenkovic D, Becker T, Stojanovski D, Youngman MJ, Jensen RE, Chacinska A, Guiard B, Pfanner N, Wiedemann N (2007) The morphology proteins Mdm12/Mmm1 function in the major beta-barrel assembly pathway of mitochondria. *The EMBO journal* 26:2229-2239.
- Meisinger C, Rissler M, Chacinska A, Szklarz LK, Milenkovic D, Kozjak V, Schonfisch B, Lohaus C, Meyer HE, Yaffe MP, Guiard B, Wiedemann N, Pfanner N (2004) The mitochondrial morphology protein Mdm10 functions in assembly of the preprotein translocase of the outer membrane. *Developmental cell* 7:61-71.
- Mendel RR (2007) Biology of the molybdenum cofactor. *Journal of experimental botany* 58:2289-2296.
- Mendel RR, Bittner F (2006) Cell biology of molybdenum. *Biochimica et biophysica acta* 1763:621-635.
- Merklinger E, Gofman Y, Kedrov A, Driessen AJ, Ben-Tal N, Shai Y, Rapaport D (2012) Membrane integration of a mitochondrial signal-anchored protein does not require additional proteinaceous factors. *The Biochemical journal* 442:381-389.
- Milenkovic D, Muller J, Stojanovski D, Pfanner N, Chacinska A (2007) Diverse mechanisms and machineries for import of mitochondrial proteins. *Biological chemistry* 388:891-897.
- Mokranjac D, Paschen SA, Kozany C, Prokisch H, Hoppins SC, Nargang FE, Neupert W, Hell K (2003) Tim50, a novel component of the TIM23 preprotein translocase of mitochondria. *The EMBO journal* 22:816-825.
- Moncada S, Palmer RM, Higgs EA (1991) Nitric oxide: physiology, pathophysiology, and pharmacology. *Pharmacological reviews* 43:109-142.
- Moriwaki Y, Yamamoto T, Higashino K (1997) Distribution and pathophysiologic role of molybdenum-containing enzymes. *Histology and histopathology* 12:513-524.
- Naamati A, Regev-Rudzki N, Galperin S, Lill R, Pines O (2009) Dual targeting of Nfs1 and discovery of its novel processing enzyme, Icp55. *The Journal of biological chemistry* 284:30200-30208.
- Nargang FE, Drygas ME, Kwong PL, Nicholson DW, Neupert W (1988) A mutant of *Neurospora crassa* deficient in cytochrome c heme lyase activity cannot import cytochrome c into mitochondria. *The Journal of biological chemistry* 263:9388-9394.
- Nason A, Lee KY, Pan SS, Ketchum PA, Lamberti A, DeVries J (1971) In vitro formation of assimilatory reduced nicotinamide adenine dinucleotide phosphate: nitrate reductase from a *Neurospora* mutant and a component of molybdenum-enzymes. *Proceedings of the National Academy of Sciences of the United States of America* 68:3242-3246.
- Neupert W (2012) SnapShot: Mitochondrial architecture. *Cell* 149:722-722 e721.
- Neupert W, Herrmann JM (2007) Translocation of proteins into mitochondria. *Annual review of biochemistry* 76:723-749.
- Neve EP, Nordling A, Andersson TB, Hellman U, Diczfalusy U, Johansson I, Ingelman-Sundberg M (2012) Amidoxime reductase system containing cytochrome b5 type B (CYB5B) and MOSC2 is of importance for lipid synthesis in adipocyte mitochondria. *The Journal of biological chemistry* 287:6307-6317.
- Nigg EA (1997) Nucleocytoplasmic transport: signals, mechanisms and regulation. *Nature* 386:779-787.
- Nunnari J, Fox TD, Walter P (1993) A mitochondrial protease with two catalytic subunits of nonoverlapping specificities. *Science* 262:1997-2004.



- Ohsato T, Ishihara N, Muta T, Umeda S, Ikeda S, Mihara K, Hamasaki N, Kang D (2002) Mammalian mitochondrial endonuclease G. Digestion of R-loops and localization in intermembrane space. *European journal of biochemistry / FEBS* 269:5765-5770.
- Olney JW, Misra CH, de Gubareff T (1975) Cysteine-S-sulfate: brain damaging metabolite in sulfite oxidase deficiency. *Journal of neuropathology and experimental neurology* 34:167-177.
- Ono H, Ito A (1982a) Biosynthesis of sulfite oxidase in rat liver - presence of a large precursor form of the enzyme in cytosol. *Journal of biochemistry* 91:117-123.
- Ono H, Ito A (1982b) Evidence for participation of the inner membrane in the import of sulfite oxidase into the intermembrane space of liver mitochondria. *Biochemical and biophysical research communications* 107:258-264.
- Ono H, Ito A (1984) Transport of the precursor for sulfite oxidase into intermembrane space of liver mitochondria: characterization of import and processing activities. *Journal of biochemistry* 95:345-352.
- Ono H, Ito A, Omura T (1982) Biosynthesis of sulfite oxidase in rat liver-determination of the site of synthesis. *Journal of biochemistry* 91:107-116.
- Osman C, Voelker DR, Langer T (2011) Making heads or tails of phospholipids in mitochondria. *The Journal of cell biology* 192:7-16.
- Ott M, Herrmann JM (2010) Co-translational membrane insertion of mitochondrially encoded proteins. *Biochimica et biophysica acta* 1803:767-775.
- Pacheco A, Hazzard JT, Tollin G, Enemark JH (1999) The pH dependence of intramolecular electron transfer rates in sulfite oxidase at high and low anion concentrations. *Journal of biological inorganic chemistry : JBIC : a publication of the Society of Biological Inorganic Chemistry* 4:390-401.
- Palmer T, Santini CL, Iobbi-Nivol C, Eaves DJ, Boxer DH, Giordano G (1996) Involvement of the narJ and mob gene products in distinct steps in the biosynthesis of the molybdoenzyme nitrate reductase in *Escherichia coli*. *Molecular microbiology* 20:875-884.
- Palmieri F (2008) Diseases caused by defects of mitochondrial carriers: a review. *Biochimica et biophysica acta* 1777:564-578.
- Papic D, Krumpke K, Dukanovic J, Dimmer KS, Rapaport D (2011) Multispan mitochondrial outer membrane protein Ugo1 follows a unique Mim1-dependent import pathway. *The Journal of cell biology* 194:397-405.
- Paschen SA, Waizenegger T, Stan T, Preuss M, Cyrklaff M, Hell K, Rapaport D, Neupert W (2003) Evolutionary conservation of biogenesis of beta-barrel membrane proteins. *Nature* 426:862-866.
- Rajagopalan KV, Johnson JL (1992) The pterin molybdenum cofactors. *The Journal of biological chemistry* 267:10199-10202.
- Rajapakshe A, Astashkin AV, Klein EL, Reichmann D, Mendel RR, Bittner F, Enemark JH (2011) Structural studies of the molybdenum center of mitochondrial amidoxime reducing component (mARC) by pulsed EPR spectroscopy and <sup>17</sup>O-labeling. *Biochemistry* 50:8813-8822.
- Rapaport D (2005) How does the TOM complex mediate insertion of precursor proteins into the mitochondrial outer membrane? *The Journal of cell biology* 171:419-423.
- Regev-Rudzki N, Karniely S, Ben-Haim NN, Pines O (2005) Yeast aconitase in two locations and two metabolic pathways: seeing small amounts is believing. *Molecular biology of the cell* 16:4163-4171.
- Rehling P, Model K, Brandner K, Kovermann P, Sickmann A, Meyer HE, Kuhlbrandt W, Wagner R, Truscott KN, Pfanner N (2003) Protein insertion into the mitochondrial inner membrane by a twin-pore translocase. *Science* 299:1747-1751.
- Rosenblum WI (1968) Neuropathologic changes in a case of sulfite oxidase deficiency. *Neurology* 18:1187-1196.
- Ross K, Rudel T, Kozjak-Pavlovic V (2009) TOM-independent complex formation of Bax and Bak in mammalian mitochondria during TNFalpha-induced apoptosis. *Cell death and differentiation* 16:697-707.

- Salman MS, Ackerley C, Senger C, Becker L (2002) New insights into the neuropathogenesis of molybdenum cofactor deficiency. *The Canadian journal of neurological sciences / Le journal canadien des sciences neurologiques* 29:91-96.
- Santamaria-Araujo JA, Wray V, Schwarz G (2012) Structure and stability of the molybdenum cofactor intermediate cyclic pyranopterin monophosphate. *Journal of biological inorganic chemistry : JBIC : a publication of the Society of Biological Inorganic Chemistry* 17:113-122.
- Sass E, Blachinsky E, Karniely S, Pines O (2001) Mitochondrial and cytosolic isoforms of yeast fumarase are derivatives of a single translation product and have identical amino termini. *The Journal of biological chemistry* 276:46111-46117.
- Scherer WF, Syverton JT, Gey GO (1953) Studies on the propagation in vitro of poliomyelitis viruses. IV. Viral multiplication in a stable strain of human malignant epithelial cells (strain HeLa) derived from an epidermoid carcinoma of the cervix. *The Journal of experimental medicine* 97:695-710.
- Schmidt O, Pfanner N, Meisinger C (2010) Mitochondrial protein import: from proteomics to functional mechanisms. *Nature reviews Molecular cell biology* 11:655-667.
- Schrader N, Fischer K, Theis K, Mendel RR, Schwarz G, Kisker C (2003) The crystal structure of plant sulfite oxidase provides insights into sulfite oxidation in plants and animals. *Structure* 11:1251-1263.
- Schulz C, Lytovchenko O, Melin J, Chacinska A, Guiard B, Neumann P, Ficner R, Jahn O, Schmidt B, Rehling P (2011) Tim50's presequence receptor domain is essential for signal driven transport across the TIM23 complex. *The Journal of cell biology* 195:643-656.
- Schwarz G (2005) Molybdenum cofactor biosynthesis and deficiency. *Cellular and molecular life sciences : CMLS* 62:2792-2810.
- Schwarz G, Mendel RR (2006) Molybdenum cofactor biosynthesis and molybdenum enzymes. *Annual review of plant biology* 57:623-647.
- Schwarz G, Mendel RR, Ribbe MW (2009) Molybdenum cofactors, enzymes and pathways. *Nature* 460:839-847.
- Shirihai OS, Gregory T, Yu C, Orkin SH, Weiss MJ (2000) ABC-me: a novel mitochondrial transporter induced by GATA-1 during erythroid differentiation. *The EMBO journal* 19:2492-2502.
- Shore GC, McBride HM, Millar DG, Steenaart NA, Nguyen M (1995) Import and insertion of proteins into the mitochondrial outer membrane. *European journal of biochemistry / FEBS* 227:9-18.
- Smolinsky B, Eichler SA, Buchmeier S, Meier JC, Schwarz G (2008) Splice-specific functions of gephyrin in molybdenum cofactor biosynthesis. *The Journal of biological chemistry* 283:17370-17379.
- Stojanovski D, Guiard B, Kozjak-Pavlovic V, Pfanner N, Meisinger C (2007) Alternative function for the mitochondrial SAM complex in biogenesis of alpha-helical TOM proteins. *The Journal of cell biology* 179:881-893.
- Suzuki H, Maeda M, Mihara K (2002) Characterization of rat TOM70 as a receptor of the preprotein translocase of the mitochondrial outer membrane. *Journal of cell science* 115:1895-1905.
- Taketani S, Adachi Y, Kohno H, Ikehara S, Tokunaga R, Ishii T (1998) Molecular characterization of a newly identified heme-binding protein induced during differentiation of urine erythroleukemia cells. *The Journal of biological chemistry* 273:31388-31394.
- Tan WH, Eichler FS, Hoda S, Lee MS, Baris H, Hanley CA, Grant PE, Krishnamoorthy KS, Shih VE (2005) Isolated sulfite oxidase deficiency: a case report with a novel mutation and review of the literature. *Pediatrics* 116:757-766.
- Tejada-Jimenez M, Galvan A, Fernandez E (2011) Algae and humans share a molybdate transporter. *Proceedings of the National Academy of Sciences of the United States of America* 108:6420-6425.

- Tejada-Jimenez M, Llamas A, Sanz-Luque E, Galvan A, Fernandez E (2007) A high-affinity molybdate transporter in eukaryotes. *Proceedings of the National Academy of Sciences of the United States of America* 104:20126-20130.
- Terao M, Kurosaki M, Barzago MM, Fratelli M, Bagnati R, Bastone A, Giudice C, Scanziani E, Mancuso A, Tiveron C, Garattini E (2009) Role of the molybdoflavoenzyme aldehyde oxidase homolog 2 in the biosynthesis of retinoic acid: generation and characterization of a knockout mouse. *Molecular and cellular biology* 29:357-377.
- Teschner J, Lachmann N, Schulze J, Geisler M, Selbach K, Santamaria-Araujo J, Balk J, Mendel RR, Bittner F (2010) A novel role for Arabidopsis mitochondrial ABC transporter ATM3 in molybdenum cofactor biosynthesis. *The Plant cell* 22:468-480.
- Tossi A, Sandri L, Giangaspero A (2002) New consensus hydrophobicity scale extended to non-proteinogenic amino acids. In *Peptides 2002: Proceedings of the twenty-seventh European peptide symposium*. Edizioni Ziino, Napoli, Italy. pp. 416-417
- Touati G, Rusthoven E, Depondt E, Dorche C, Duran M, Heron B, Rabier D, Russo M, Saudubray JM (2000) Dietary therapy in two patients with a mild form of sulphite oxidase deficiency. Evidence for clinical and biological improvement. *Journal of inherited metabolic disease* 23:45-53.
- Ungermann C, Neupert W, Cyr DM (1994) The role of Hsp70 in conferring unidirectionality on protein translocation into mitochondria. *Science* 266:1250-1253.
- van der Laan M, Bohnert M, Wiedemann N, Pfanner N (2012) Role of MINOS in mitochondrial membrane architecture and biogenesis. *Trends in cell biology* 22:185-192.
- Veldman A, Santamaria-Araujo JA, Sollazzo S, Pitt J, Gianello R, Yapliito-Lee J, Wong F, Ramsden CA, Reiss J, Cook I, Fairweather J, Schwarz G (2010) Successful treatment of molybdenum cofactor deficiency type A with cPMP. *Pediatrics* 125:e1249-1254.
- Vial S, Lu H, Allen S, Savory P, Thornton D, Sheehan J, Tokatlidis K (2002) Assembly of Tim9 and Tim10 into a functional chaperone. *The Journal of biological chemistry* 277:36100-36108.
- Vogel RO, Janssen RJ, van den Brand MA, Dieteren CE, Verkaart S, Koopman WJ, Willems PH, Pluk W, van den Heuvel LP, Smeitink JA, Nijtmans LG (2007) Cytosolic signaling protein Ecsit also localizes to mitochondria where it interacts with chaperone NDUFAF1 and functions in complex I assembly. *Genes & development* 21:615-624.
- von der Malsburg K, Muller JM, Bohnert M, Oeljeklaus S, Kwiatkowska P, Becker T, Loniewska-Lwowska A, Wiese S, Rao S, Milenkovic D, Hutu DP, Zerbes RM, Schulze-Specking A, Meyer HE, Martinou JC, Rospert S, Rehling P, Meisinger C, Veenhuis M, Warscheid B, van der Klei IJ, Pfanner N, Chacinska A, van der Laan M (2011) Dual role of mitofilin in mitochondrial membrane organization and protein biogenesis. *Developmental cell* 21:694-707.
- Vorbach C, Harrison R, Capecchi MR (2003) Xanthine oxidoreductase is central to the evolution and function of the innate immune system. *Trends in immunology* 24:512-517.
- Wachter C, Schatz G, Glick BS (1994) Protein import into mitochondria: the requirement for external ATP is precursor-specific whereas intramitochondrial ATP is universally needed for translocation into the matrix. *Molecular biology of the cell* 5:465-474.
- Wahl B, Reichmann D, Niks D, Krompholz N, Havemeyer A, Clement B, Messerschmidt T, Rothkegel M, Biester H, Hille R, Mendel RR, Bittner F (2010) Biochemical and spectroscopic characterization of the human mitochondrial amidoxime reducing components hmARC-1 and hmARC-2 suggests the existence of a new molybdenum enzyme family in eukaryotes. *The Journal of biological chemistry* 285:37847-37859.
- Waizenegger T, Stan T, Neupert W, Rapaport D (2003) Signal-anchor domains of proteins of the outer membrane of mitochondria: structural and functional characteristics. *The Journal of biological chemistry* 278:42064-42071.
- Walther DM, Rapaport D (2009) Biogenesis of mitochondrial outer membrane proteins. *Biochimica et biophysica acta* 1793:42-51.

- Wang C, Youle RJ (2009) The role of mitochondria in apoptosis\*. *Annual review of genetics* 43:95-118.
- Wiedemann N, Frazier AE, Pfanner N (2004a) The protein import machinery of mitochondria. *The Journal of biological chemistry* 279:14473-14476.
- Wiedemann N, Kozjak V, Chacinska A, Schonfisch B, Rospert S, Ryan MT, Pfanner N, Meisinger C (2003) Machinery for protein sorting and assembly in the mitochondrial outer membrane. *Nature* 424:565-571.
- Wiedemann N, Truscott KN, Pfannschmidt S, Guiard B, Meisinger C, Pfanner N (2004b) Biogenesis of the protein import channel Tom40 of the mitochondrial outer membrane: intermembrane space components are involved in an early stage of the assembly pathway. *The Journal of biological chemistry* 279:18188-18194.
- Wilson HL, Wilkinson SR, Rajagopalan KV (2006) The G473D mutation impairs dimerization and catalysis in human sulfite oxidase. *Biochemistry* 45:2149-2160.
- Young JC, Hoogenraad NJ, Hartl FU (2003) Molecular chaperones Hsp90 and Hsp70 deliver preproteins to the mitochondrial import receptor Tom70. *Cell* 112:41-50.
- Zeviani M (2004) Mitochondrial disorders. *Supplements to Clinical neurophysiology* 57:304-312.
- Zhang X, Vincent AS, Halliwell B, Wong KP (2004) A mechanism of sulfite neurotoxicity: direct inhibition of glutamate dehydrogenase. *The Journal of biological chemistry* 279:43035-43045.
- Zhao J, Lendahl U, Nister M (2012) Regulation of mitochondrial dynamics: convergences and divergences between yeast and vertebrates. *Cellular and molecular life sciences* : CMLS.

## **Acknowledgment**

I want to thank Prof. Dr. Günter Schwarz for the opportunity to pursue my PhD in his lab. Thank you for finding a great balance between guiding me with my projects and supporting me in following my own ideas. It was great to work in the multidisciplinary environment of your lab and your curiosity, your unbiased way of thinking and also your disposition to enter new fields of research were highly motivating and essential for my PhD. Thank you for many scientific discussions, they were always focusing and extremely helpful for my projects. Also, I want to thank you for giving me the opportunity to visit a number of exciting conferences. I always enjoyed working in your lab and I thank you for the great atmosphere you were always providing. Thank you for everything!

I acknowledge Prof. Dr. Thomas Langer for being the co-referee of my thesis and for your support in the final phases of my both projects which were crucial for their publication. Thank you also for a great collaboration and for giving me the opportunity to perform some experiments in your lab.

I thank Prof. Dr. Jürgen Dohmen for his disposition to preside my defense.

I want to thank Natalie for a fantastic time we spend together and for her support in and out of the lab. It was a very good decision to join Günters lab for many reasons, but meeting Natalie was by far the best.

I appreciate everybody in the lab of Prof. Schwarz for a great atmosphere in the lab and your friendly help whenever needed.

I thank Borislav Dejanovic for a great and often hilarious time. It was a pleasure to work with you and I thank you for an unlimited number of extensive and very helpful scientific discussions.

I would like to thank Jakob Busch for his great and essential work in the beginning of my second project and for many matches on the cologne basketball courts.

Special thanks to Dr. Michael Baker, Dr. Takashi Tatsuta and Dr. Christoph Potting for many scientific discussions and a great collaboration.

Ich danke meiner Familie und meinen Freunden für den großartigen Rückhalt und die Unterstützung, ohne die ich nie so weit gekommen wäre.

I am very thankful to the “Studienstiftung des deutschen Volkes” for excellent financial and non-financial support during my PhD and to the Graduate School for Biological sciences for financial support.

## **Erklärung**

Ich versichere, dass ich die von mir vorgelegte Dissertation selbstständig angefertigt, die benutzten Quellen und Hilfsmittel vollständig angegeben und die Stellen der Arbeit – einschließlich Tabellen, Karten und Abbildungen –, die anderen Werken im Wortlaut oder dem Sinn nach entnommen sind, in jedem Einzelfall als Entlehnung kenntlich gemacht habe; dass diese Dissertation noch keiner anderen Fakultät oder Universität zur Prüfung vorgelegen hat; dass sie – abgesehen von unten angegebenen Teilpublikationen – noch nicht veröffentlicht worden ist sowie, dass ich eine solche Veröffentlichung vor Abschluss des Promotionsverfahrens nicht vornehmen werde.

Die Bestimmungen dieser Promotionsordnung sind mir bekannt. Die von mir vorgelegte Dissertation ist von Prof. Dr. G. Schwarz am Institut für Biochemie der Mathematisch-Naturwissenschaftlichen Fakultät der Universität zu Köln betreut worden.

Köln, 17.09. 2012

## **Curriculum vitae**

### **Personal details**

Name: Julian Klein  
Date and place of birth: 01.04. 1985 in Köln  
Nationality: German

### **Education**

10/2007-09/2009: Studies of Biology at the University of Cologne. Degree "Master of Science in Biology" 2009. Thesis title: „Assembly and maturation of sulfite oxidase“, Group Prof. Dr. Günter Schwarz.

since 11/2008: PhD student at the Institute of Biochemistry, University of Cologne, Group Prof. Dr. Günter Schwarz.

09/2007: Uptake into the „Fast/Track Masters/Doctoral programme“ of the Graduate School for Biological Sciences, University of Cologne.

10/2004-09/2007: Studies of Biology at the University of Cologne. Degree „Bachelor of Science in Biology“ 2007. Thesis title: „Peptide aptamer inhibition of selective proteolysis“, Group Prof. Dr. Jürgen Dohmen

09/1995-06/2004: Stadtgymnasium Köln-Porz, Abitur 2004

08/1991-07/1995: Peter-Petersen Grundschule Köln-Grengel

### **Awards and fellowships**

since 04/2012: Research fellowship of the „Graduate School for Biological Sciences“ (University of Cologne)

06/2011: „Best Presentation Award“, University of Cologne

08/2009-03/2012: Fellowship of the „German National Merit Foundation“

04/2008-10/2008: Research fellowship of the „Graduate School for Biological Sciences“ (University of Cologne)